

Quantitative study of coherent pairing modes with two neutron transfer: Sn-isotopes

G. Potel*

Dipartimento di Fisica, Università di Milano, Via Celoria 16, 20133 Milano, Italy.

INFN, Sezione di Milano Via Celoria 16, 20133 Milano, Italy. and

Departamento de Fisica Atomica, Molecular y Nuclear,

Universidad de Sevilla, Facultad de Fisica,

Avenida Reina Mercedes s/n, Sevilla, Spain

A. Idini[†]

Dipartimento di Fisica, Università di Milano,

Via Celoria 16, 20133 Milano, Italy. and

INFN, Sezione di Milano Via Celoria 16, 20133 Milano, Italy.

F. Barranco[‡]

Departamento de Fisica Aplicada III, Universidad de Sevilla,

Escuela Superior de Ingenieros, Sevilla, 41092 Camino de los Descubrimientos s/n, Spain.

E. Vigezzi[§]

INFN, Sezione di Milano Via Celoria 16, 20133 Milano, Italy.

R. A. Broglia[¶]

Dipartimento di Fisica, Università di Milano, Via Celoria 16, 20133 Milano, Italy.

INFN, Sezione di Milano Via Celoria 16, 20133 Milano, Italy. and

The Niels Bohr Institute, University of Copenhagen,

Blegdamsvej 17, 2100 Copenhagen Ø, Denmark.

Pairing rotations and pairing vibrations are collective modes associated with a field, the pair field, which changes the number of particles by two. Consequently, they can be studied at profit with the help of two-particle transfer reactions on superfluid and in normal nuclei, respectively. The advent of exotic beams has opened, for the first time, the possibility to carry out such studies in medium heavy nuclei, within the same isotopic chain. In the case

studied in the present paper that of the Sn-isotopes (essentially from closed ($Z = N = 50$) to closed ($Z = 50, N = 82$) shells). The static and dynamic off-diagonal, long range order phase coherence in gauge space displayed by pairing rotations and vibrations respectively, leads to coherent states which behave almost classically. Consequently, these modes are amenable to an accurate nuclear structure description in terms of simple models containing the right physics, in particular BCS plus QRPA and HF mean field plus RPA respectively. The associated two- nucleon transfer spectroscopic amplitudes predicted by such model calculations can thus be viewed as essentially “exact”. This fact, together with the availability of optical potentials for the different real and virtual channels involved in the reactions considered, namely $^{A+2}\text{Sn}+p$, $^{A+1}\text{Sn}+d$ and $^A\text{Sn}+t$, allows for the calculation of the associated absolute cross sections without, arguably, free parameters. The numerical predictions of the absolute differential cross sections, obtained making use of the above mentioned nuclear structure and optical potential inputs, within the framework of second order DWBA, taking into account simultaneous, successive and non-orthogonality contributions provide, within experimental errors in general, and below 10% uncertainty in particular, an overall account of the experimental findings for all of the measured $^{A+2}\text{Sn}(p, t)^A\text{Sn}(gs)$ reactions, for which absolute cross sections have been reported to date.

* gregory.potel@gmail.com

† andrea.idini@mi.infn.it

‡ barranco@us.es

§ enrico.vigezzi@mi.infn.it

¶ broglia@mi.infn.it; Corresponding author. Tel:(+39)3388959875

I. INTRODUCTION

Customarily, the fingerprint of shell closure in nuclei is associated with a sharp, step function–like distinction between occupied and empty single–particle states, in correspondence with magic numbers [1] (for a recent example concerning ^{132}Sn , see [2] and [3]). At variance with the case of infinite, fermionic systems, in which there essentially exists a continuum of states at the Fermi energy, in finite–many-body (FMB) systems, like e.g. the atomic nucleus, ε_F is not, in principle, well defined, at least not in closed shell nuclei. This is because a sizable energy gap is observed between the last occupied ($j_<$) and the first unoccupied ($j_>$) orbitals. This is also the case for other FMB fermionic systems, e.g. C_{60} fullerene, which displays a relatively large HOMO–LUMO gap, of the order of 1.6 eV as compared to $\varepsilon_F \approx 15$ eV [4]. In such cases, one can use as a working definition of ε_F [5], $(\varepsilon_{j_>} - \varepsilon_{j_<})/2$ ($(\varepsilon_{HOMO} - \varepsilon_{LUMO})/2$ in the case of C_{60}). Away from closed shells, medium-heavy nuclei become, as a rule, superfluid, the distinction between occupied and empty states being blurred around ε_F . The Fermi energy is, in such situation, well defined and equal to the energy for which the occupancy probability attains the value of one half. In keeping with this result, in the case of closed shell nuclei, ε_F can be properly defined as the minimum of the dispersion relation associated with pair addition and pair removal modes.

II. PAIR–SPIN FORMALISM

The mixing taking place in superfluid nuclei between particle and holes is economically embodied in the Bogoliubov–Valatin [6, 7] quasiparticle transformation

$$\alpha_\nu = U_\nu a_\nu - V_\nu a_{\bar{\nu}}^\dagger = U'_\nu a'_\nu - V'_\nu a'_{\bar{\nu}}{}^\dagger, \quad (1a)$$

$$\alpha_\nu^\dagger = U_\nu^* a_\nu^\dagger - V_\nu^* a_{\bar{\nu}} = U'_\nu a'_\nu{}^\dagger - V'_\nu a'_{\bar{\nu}}, \quad (1b)$$

where

$$U_\nu = U'_\nu e^{i\phi} \quad , \quad V_\nu = V'_\nu e^{-i\phi}, \quad (2)$$

are the BCS occupation amplitudes, U'_ν and V'_ν being real quantities, while $a'_{\bar{\nu}}{}^\dagger = \mathcal{G}(\phi) a_{\bar{\nu}}^\dagger \mathcal{G}^{-1}(\phi) = e^{-i\phi} a_{\bar{\nu}}^\dagger$ and $a'_\nu = \mathcal{G}(\phi) a_\nu \mathcal{G}^{-1}(\phi) = e^{i\phi} a_\nu$ are creation and annihilation operators referred to the intrinsic system of reference in gauge space (i.e. body fixed BCS deformed state), $\mathcal{G} = \exp(-iN\phi)$ inducing a rotation of the angle ϕ in this (2-D) space (gauge transformation), N being the number of particle operator (see Apps. A, B and C). The states $|\nu\rangle$ and $|\bar{\nu}\rangle$, connected by the time reversal

operator, have the same energy (Kramers degeneracy). In keeping with the fact that (1) is a unitary transformation,

$$U_\nu U_\nu^* + V_\nu V_\nu^* = U_\nu'^2 + V_\nu'^2 = 1 \quad (3)$$

The transformation (1) provides the rotation in Hilbert space of the creation and annihilation fermion operators, which diagonalizes the mean field, BCS pairing Hamiltonian (angle θ_ν , see Figs. A.1(b) and (c)),

$$(H_p - \lambda N)_{MF} = \sum_{\nu>0} \epsilon_\nu N_\nu - G\alpha'_0(P'^\dagger + P') + G\alpha_0'^2 = \sum_{\nu>0} E_\nu \tilde{N}_\nu + E_{gs}, \quad (4)$$

where, $\epsilon_\nu = \varepsilon_\nu - \lambda$ and

$$E_{gs} = \sum_{\nu>0} (\epsilon_\nu - E_\nu) + \frac{\Delta'^2}{G}, \quad (5)$$

is the ground state energy (see Appendix A), while $\lambda = \varepsilon_F$. In the above expression we find the particle number operators

$$N_\nu = a_\nu^\dagger a_\nu + a_{\bar{\nu}}^\dagger a_{\bar{\nu}}, \quad (6)$$

the pair creation and annihilation operators,

$$P_\nu^\dagger = a_\nu^\dagger a_{\bar{\nu}}^\dagger, \quad P_\nu = a_{\bar{\nu}} a_\nu, \quad (7)$$

the complex (ϕ indicating the gauge angle) condensed (superfluid) Cooper field (see Appendix B)

$$\alpha_0 = \langle BCS | P | BCS \rangle = \langle BCS | P^\dagger | BCS \rangle^* = e^{-2i\phi} \alpha'_0 = e^{-2i\phi} \sum_{\nu>0} U'_\nu V'_\nu = \sum_{\nu>0} U_\nu^* V_\nu, \quad (8)$$

the quasiparticle energy

$$E_\nu = (\epsilon_\nu^2 + \Delta'^2)^{1/2}, \quad (9)$$

the absolute value (modulus) of the pairing gap

$$\Delta' = G\alpha'_0 = G \sum_{\nu>0} U'_\nu V'_\nu = G e^{2i\phi} \sum_{\nu>0} U_\nu^* V_\nu = \Delta e^{2i\phi}, \quad (10)$$

and the quasiparticle number operators,

$$\tilde{N}_\nu = a_\nu^\dagger \alpha_\nu + a_{\bar{\nu}}^\dagger \alpha_{\bar{\nu}}. \quad (11)$$

For the case of ^{120}Sn , the quantities ϵ_ν , E_ν , U'_ν , V'_ν and $U_\nu^* V_\nu$ introduced above are given in Tables 1 and 2.

The ground state of the system referred to the laboratory system of reference \mathcal{K} as well as to the intrinsic (body-fixed) frame \mathcal{K}' (see Appendices A and B), can be written as

$$\begin{aligned} |BCS(\phi)\rangle_{\mathcal{K}} &= \frac{1}{\text{Norm}} \prod_{\nu>0} \alpha_{\nu} \alpha_{\bar{\nu}} |0\rangle = \prod_{\nu>0} (U_{\nu} + V_{\nu} a_{\nu}^{\dagger} a_{\bar{\nu}}^{\dagger}) |0\rangle \\ &= \prod_{\nu>0} e^{i\phi} (U'_{\nu} + V'_{\nu} e^{-2i\phi} a_{\nu}^{\dagger} a_{\bar{\nu}}^{\dagger}) |0\rangle = e^{i\Omega\phi} \prod_{\nu>0} (U'_{\nu} + V'_{\nu} a'_{\nu}{}^{\dagger} a'_{\bar{\nu}}{}^{\dagger}) |0\rangle \\ &= |BCS(\phi=0)\rangle_{\mathcal{K}'}, \end{aligned} \quad (12)$$

where Ω is the pair degeneracy of the single-particle subspace, leading to an overall (trivial) phase.

The central feature of the $|BCS\rangle$ wavefunction, that is condensation of largely overlapping Cooper pairs, is captured by the pairspin (quasispin) formulation of superconductivity (see [8, 9] and refs. therein), which ascribes values (see Fig. 1(a) and Appendix A)

$$s_x(\nu) = s_y(\nu) = 0, \quad s_z(\nu) = -1/2, \quad (13)$$

to empty states, and

$$s_x(\nu) = s_y(\nu) = 0, \quad s_z(\nu) = +1/2, \quad (14)$$

to occupied states of the non-interacting (normal) system. The symmetry axis in pairspin space (the z -axis) is referred to as the gauge axis (see Appendix A, Fig. A.1(a)). A superfluid system (see Fig. 1(b), see also Fig. A.3 Appendix A) is characterized by a collective pairspin $\vec{S}_{\perp} \equiv \{S_x, S_y\}$, which points in a direction perpendicular to z , associated with the azimuthal angle 2ϕ . This direction defines an intrinsic reference frame \mathcal{K}' (see Fig. B1, Appendix B), in which the components of the average total pairspin $\langle \vec{S} \rangle = \sum_{\nu>0} \langle \vec{S}(\nu) \rangle$ in the mean field ground state, take the values (see Fig. A.1(b) and Appendix A, see also (B28a) and B29a)

$$\langle S_{y'} \rangle = 0, \quad (15a)$$

$$\langle S_{x'} \rangle = \alpha'_0 = \sum_{\nu>0} U'_{\nu} V'_{\nu}, \quad (15b)$$

$$\langle S_z \rangle \equiv \langle S_{z'} \rangle = \frac{1}{2} \sum_{\nu>0} (V'^2_{\nu} - U'^2_{\nu}). \quad (15c)$$

Thus, S_{\perp} gives a measure of the mixing of empty and occupied states of the BCS solution (see Eqs. (13,14). This is tantamount to saying that S_{\perp} defines a privileged orientation in gauge space (see Appendix A), in keeping with the fact that (12) is a wavepacket in the number of pairs of particles. An emergent property of the associated symmetry breaking phase transition is generalized rigidity in gauge space (see Appendix D). That is, the system can be set into rotation

(or change its rotational frequency) in gauge space in terms of two-particle transfer reactions. The pairspin polarization may rotate collectively around the gauge axis, and the azimuthal angle 2ϕ of S_\perp (see Appendix A and Fig. A.1, see also (B28a) and (B29a)) is therefore a dynamical variable associated with pairing rotational bands.

A. Order Parameter

The modulus of the order parameter (8), that is, of the quantity $\alpha'_0 \approx \sum_{\nu>0} U'_\nu V'_\nu = \Delta'/G$, is, for medium heavy nuclei ($A \approx 120$) of the order of $1.4 \text{ MeV}/G \approx 7$, in keeping with the fact that $G \approx 25 \text{ MeV}/A$ (major j-shell approximation, see [10] Chapters 2 and 3 and refs. therein). In other words, roughly of the order of ten ($\nu, \bar{\nu}$) Cooper pairs contribute to the nuclear condensate in superfluid nuclei. Consequently, large fluctuations are expected for α'_0 .

These fluctuations are generated by the residual interaction acting between the quasiparticles (cf. [8], cf. also [10] in particular Ch. 4 and Appendices I and J of this reference). In the harmonic (QRPA) approximation the two associated pair fields are: 1) $(U_\nu^2 - V_\nu^2)(\Gamma_\nu^\dagger + \Gamma_\nu)$ leading essentially to a bound two-quasiparticle like state (pairing vibration mixed to β -vibrations, in deformed nuclei, cf. [11] and refs. therein) lying on top of the pairing gap, $\Gamma_\nu^\dagger = \alpha_\nu^\dagger \alpha_{\bar{\nu}}^\dagger$ being the two-quasiparticle creation quasiboson operator; 2) $(U_\nu^2 + V_\nu^2)(\Gamma_\nu^\dagger - \Gamma_\nu)$ which sets the $|BCS\rangle_{\mathcal{K}}$ intrinsic state into rotation in gauge space, and whose fluctuations diverge in the long-wavelength limit, in just such a way that the resulting ground state

$$|N_0\rangle \sim \int d\phi e^{iN_0\phi} |BCS(\phi)\rangle_{\mathcal{K}} \sim \left(\sum_{\nu>0} c(\nu) a_\nu^\dagger a_{\bar{\nu}}^\dagger \right)^{N_0/2} |0\rangle, \quad (16)$$

transforms irreducibly under gauge transformation

$$\mathcal{G}(\phi) = e^{-iN\phi}. \quad (17)$$

The states (16) are the members of a pairing rotational band build out of a condensation of $N/2$ Cooper pairs each described by $|\tilde{0}\rangle = \sum_{\nu>0} c(\nu) a_\nu^\dagger a_{\bar{\nu}}^\dagger |0\rangle$ (see Appendix B, in particular Eq. (B16),(B17) and (B23)). It is of notice that the presence of rotational bands in the spectra of many-body systems is the fingerprint of deformation both in real (3D) and abstract (e.g. gauge) spaces (see Fig. 2, see also Table XI in ref. [12]).

Fluctuations of the pair field are, of course, already present in the normal (correlated) ground state $|0\rangle = |gs(A_0)\rangle$ of closed shell nuclei (mass number A_0). That is in systems in which, while

$\alpha'_0 = 0$, the (dynamical) value of the order parameter, i.e. the zero-point fluctuation of α'_0 around its zero value,

$$\begin{aligned}\alpha_{dyn} &= \langle (\alpha - \alpha'_0)^2 \rangle = 1/2 \left(\langle 0|P^\dagger P|0 \rangle + \langle 0|PP^\dagger|0 \rangle \right) = \\ &= \frac{1}{2} \left(\sum_{int} |\langle int(A_0 - 2)|P|0 \rangle|^2 + |\langle int(A_0 + 2)|P^\dagger|0 \rangle|^2 \right) \\ &\approx \frac{1}{2} \left(\langle gs(A_0 - 2)|P|0 \rangle + \langle gs(A_0 + 2)|P^\dagger|0 \rangle \right),\end{aligned}\quad (18)$$

displays finite values (see [11, 13–15] and refs. therein), directly related to the quantity E_{corr}/G , where E_{corr} is the average correlation energy of the pair addition ($|gs(A_0 + 2) \rangle$ state) and of the pair removal ($|gs(A_0 - 2) \rangle$ state) modes. In other words, the binding energy of the two-nucleon Cooper pair moving on top of the A_0 closed shell system, and of the two-hole Cooper pair moving in the A_0 Fermi sea.

In the case of ^{132}Sn ($A_0 = 132$), we obtain (see Table III and Fig. 3)

$$E_{corr}(A + 2) = 2|\varepsilon_{j>} - \lambda| - W(A + 2) = 1.17\text{MeV}, \quad (19a)$$

$$E_{corr}(A - 2) = 2|\varepsilon_{j<} - \lambda| - W(A - 2) = 2.14\text{MeV}, \quad (19b)$$

and thus $\bar{E}_{corr} = 1.66$ MeV. It is of notice that in the case in which the energies $W \rightarrow 0$, the system becomes superfluid, the BCS λ parameter coinciding with the minimum value of the dispersion relation shown in Fig. 3(a). Consequently $E_{corr}/G \approx \frac{1}{2} \left[\frac{E_{corr}(A_0+2)}{G(A_0+2)} + \frac{E_{corr}(A_0-2)}{G(A_0-2)} \right] \approx \frac{1}{2}(8.9+13.6) \approx 11$, a value which is not very different from that of Δ'/G associated with the superfluid nucleus ^{120}Sn .

The quantity (18) can be also estimated from the ratio (Λ/G) between the (two-particle)-(two-hole) (pairing) vibration coupling strength (see e.g. [11]) and the pairing coupling constant. In the two-level model [10], this quantity is given by $(\Lambda/G) = 2\sqrt{\Omega}$, Ω being the pair degeneracy of the single-particle space in which the two nucleons (two nucleon holes) participating in the pair addition and removal modes are allowed to correlate. As a rule, these are the valence shells of the closed shell system A_0 .

In the case of the newly discovered ^{132}Sn , doubly magic nucleus, $\Omega \approx 30$ and $\alpha_{dyn} \approx (\Lambda/G) \approx 2\sqrt{30} \approx 11$. Making use of the actual values of Λ (see Table III) one obtains $\frac{1}{2} \left[\frac{1.08}{0.131} + \frac{1.60}{0.157} \right] \approx 9$. Summing up, $\alpha_{dyn}(^{132}\text{Sn}) \geq \alpha(^{120}\text{Sn})$.

This result embodies the very difference between gauge spontaneous symmetry breaking in atomic nuclei and in condensed matter. In a chunk of e.g. Pb, of which more than 50% is the

atom built on the isotope ^{208}Pb , (or of Sn, of which none is the atom built on the isotope ^{132}Sn , the corresponding nucleus being highly unstable), at a temperature below the critical temperature $T_c = 7.2\text{K}$ (3.72K) at which the metal becomes superconducting but in the presence of a magnetic field stronger than the critical value $H_c = 0.08\text{ T}$ (0.03 T), of the order of 10^3 times the earth magnetic field, Cooper pairs break as soon as they are formed, leading to a hardly observable effect, in particular concerning the structure and stability of the crystal.

On the other hand, in the case of their ground state and thus at absolute zero temperature – as it is the case for all natural occurring nuclear species on earth – the Cooper pairs associated with the normal (non superfluid) system displaying two nucleons above or two holes below closed shell, like e.g. $|gs(^{210}_{82}\text{Pb}_{128})\rangle$ and $|gs(^{206}_{82}\text{Pb}_{124})\rangle$ respectively, these fermions are strongly correlated, as evidenced by the large two-nucleon transfer cross sections with which they are excited (see e.g. [12] and refs. therein). In keeping with the fact that a consistent fraction of this cross section arises, e.g. in the case of $^{208}\text{Pb}(t, p)^{210}\text{Pb}(gs)$ by the transfer of two particles to levels below the Fermi energy of ^{208}Pb (ground state correlations), Cooper pair correlations blur dynamically the difference between occupied and empty single-particle states thought to be a trademark of closed shell systems.

The same arguments presented above, can be used for $^{132}_{50}\text{Sn}_{82}$, in which case the summed backwardsgoing amplitudes amount to $\sum_i Y_i \approx 0.5$, as reported in Table III. Arguably, one can posit, that in the nuclear case it is not, or at least not only, the condensed (superfluid) state which is peculiar, but the normal state[16], in which pair addition and pair removal Cooper are virtually poised in the ground state of the closed shell system A_0 , ready to condense (i.e. $W(A_0 + 2), W(A_0 - 2) \rightarrow 0$, see Fig. 3). inducing a (fluctuating) alignment of pairspins perpendicular to the gauge (z -axis), and thus to a domain wall and associated generalized rigidity (see Fig. A.3). This can also be seen from the pairspin states in normal systems (see Figs. 4 and 5), defined as,

$$\begin{aligned} |0\rangle_\nu &= \frac{1}{\text{Norm.}} (Y_{add}(\nu)|s_z(\nu) = -1/2\rangle + X_{rem}(\nu)|s_z(\nu) = 1/2\rangle) \\ &= \frac{1}{\text{Norm.}} (Y_{add}(\nu)|2\rangle_\nu + X_{rem}(\nu)|1\rangle_\nu), \quad \text{for } \epsilon_\nu < \epsilon_F, \end{aligned} \quad (20a)$$

and

$$\begin{aligned} |0\rangle_\nu &= \frac{1}{\text{Norm.}} (Y_{rem}(\nu)|s_z(\nu) = +1/2\rangle + X_{add}(\nu)|s_z(\nu) = -1/2\rangle) \\ &= \frac{1}{\text{Norm.}} (Y_{rem}(\nu)|1\rangle_\nu + X_{add}(\nu)|2\rangle_\nu), \quad \text{for } \epsilon_\nu > \epsilon_F, \end{aligned} \quad (20b)$$

where X, Y are the forwardgoing and backwardgoing RPA pair vibration amplitudes (see insets of Fig.3)

$$\left. \begin{array}{l} X_n(\nu; \beta) \\ Y_n(\nu; \beta) \end{array} \right\} = \frac{(\sqrt{\Omega_\nu}/2)\Lambda_n(\beta)}{2\epsilon_\nu \mp W_n(\beta)}. \quad (21)$$

The quantity $\Omega_\nu = (2j_\nu + 1)/2$ is the pair degeneracy of orbital ν , $\beta = -2$ and $\beta = +2$ label the pair addition and pair removal modes respectively, while $n (= 1, 2, \dots)$ numbers the solutions of the RPA dispersion relation in subsequent order of excitation energy (we deal here only with the $n = 1$, lowest energy pairing vibrations). Consequently, as soon as the single-particle field H_{sp} – field which acts on the nuclear pairspin along the gauge (z)-axis in a similar way in which a magnetic field acts in the case of a metallic superconductor (see App. A, discussion after Eq. (A27); see also discussion after Eq. (A35)) – is decreased, a fact that takes place moving away from magic numbers (in the case of e.g. ^{132}Sn this implies reducing the single-particle gap $|\epsilon_{j<} - \epsilon_{j>}|$ from about ≈ 5 MeV to few hundreds of keV, see Tables II and III), nuclear Cooper pairs condense, the ground state of the corresponding nucleus becoming amenable to a BCS-type description, a fact which already takes place with the presence of two removal modes in A_0 .

It is of notice the presence of strong fluctuations in pairspin observed in Fig. 5, as compared to the smooth variations shown in Fig. 1, idealization of the situation representative of a high purity, metallic crystal (within this context see Fig. A.3 of Appendix A). In fact, finite nuclei display orbitals which contribute very differently to pairing correlations, in particular hot orbitals (see e.g. [12, 17, 18]), related to the different pair degeneracy Ω_ν and with the relative amount of s -component of the different $j_\nu^2(0)$ pure two-particle configurations. One can view such an imperfect pairspin alignment as a limitation of its applicability to finite many-body systems. Conversely, one can interpret it as a reflection of the richness with which these systems in general, and finite nuclei in particular, embody symmetry breaking phase transitions. Namely, among other things, in terms of very non-conventional normal phases. Normal phases which display (virtually) traces of e.g. domain walls with varied degree of stability, dynamically violating the symmetry in question (gauge symmetry in the present case). These properties are precisely those which render the study of pairing correlations in nuclei central, in the quest for the mechanism which are at the basis of the stability of nuclear species, in particular along the drip lines [19].

In keeping with the fact that the P^\dagger and P are the basic operators entering both the pairing interaction ($H_p = -GP^\dagger P$) and the pair mean field ($-G\alpha'_0(P^\dagger + P) + G(\alpha'_0)^2$), two-nucleon transfer can be viewed as the specific probe of pairing correlations in nuclei, in a similar way as Coulomb exci-

tation, inelastic scattering and γ -decay are specific tools to probe (quadrupole) surface vibrations and rotations (see Fig. 2). In other words, specific information on α'_0 and α_{dyn} can be obtained through two-nucleon transfer reactions.

Because the correlation length associated with the nuclear Cooper pairs is

$$\xi = \begin{cases} \frac{\hbar v_F}{2\Delta'}, & (\alpha'_0 \neq 0), \\ \frac{\hbar v_F}{2E_{corr}}, & (\alpha'_0 = 0), \end{cases} \quad (22)$$

Cooper pair partners are correlated over distances considerably larger than nuclear dimensions ($\xi \approx 20 - 30$ fm, as compared to $R \approx 5$ fm). Consequently, from a nuclear structure point of view, Cooper pair transfer involves also regions in which the pairing interaction $G(x)$, x representing e.g. the surface-surface distance between target and projectile (see e.g. [20] Ch. III), vanishes, a situation already known in condensed matter in connection with the Josephson effect [21–23]. This result, together with the fact that the depth of the single-particle potential $|V_0|(\approx 50$ MeV) is much larger than $G(\approx 25/A$ MeV), implies that, exception made for Q -value effects, successive transfer induced by the mean field single-particle (Saxon-Woods-like) potential, is expected to be, as a rule, the largest contribution to the two-nucleon transfer cross sections [24–35][36]. The difficulties to absorb this simple result by nuclear structure practitioners partially stems from the fact that, neglecting reaction details, the two-particle transfer cross sections $gs \rightarrow gs$ can be schematically written as

$$\sigma(gs \rightarrow gs) \sim \begin{cases} |\alpha'_0|^2 & (\alpha'_0 \neq 0), \\ |\alpha_{dyn}|^2 & (\alpha'_0 = 0), \end{cases} \quad (23)$$

corresponding to the square modules of matrix elements of P^\dagger and P , the associated spectroscopic amplitudes in the intrinsic coordinate system in gauge space \mathcal{K}' being (see e.g. [12], and Appendix B)

$$B(\nu\bar{\nu}; J=0) \sim {}_{\mathcal{K}'}\langle BCS(A+2)|P_\nu^\dagger|BCS(A)\rangle_{\mathcal{K}'}, \quad (24a)$$

where

$${}_{\mathcal{K}'}\langle BCS(A+2)|P_\nu^\dagger|BCS(A)\rangle_{\mathcal{K}'} = U'_\nu(A)V'_\nu(A+2) (= {}_{\mathcal{K}'}\langle BCS(A)|P'_\nu|BCS(A+2)\rangle_{\mathcal{K}'}). \quad (24b)$$

Now, thinking in terms of the transfer of a nucleon at a time, e.g. in the case of the reaction

$$(A+2) + p \rightarrow F(\equiv A+1) + d \rightarrow A + t \quad (25)$$

one can write, in connection with the first step $((A + 2) + p \rightarrow F + d)$,

$$a_{\nu_d}^{\dagger} a_{\nu}^{\prime} |BCS(A + 2)\rangle |p\rangle \sim V_{\nu}^{\prime}(A + 2) \alpha_{\bar{\nu}}^{\dagger} |BCS(F)\rangle |d\rangle, \quad (26)$$

and

$$a_{\nu_t}^{\dagger} a_{\bar{\nu}}^{\prime} |BCS(F)\rangle |d\rangle \sim U_{\nu}^{\prime}(A) V_{\nu}^{\prime}(A + 2) |BCS(F)\rangle |d\rangle, \quad (27)$$

in connection with the second step $(F + d \rightarrow A + t)$, in keeping with the fact that

$$a_{\nu}^{\dagger} = U_{\nu}^{\prime} \alpha_{\nu}^{\dagger} + V_{\nu} \alpha_{\bar{\nu}},$$

$$a_{\nu}^{\prime} = U_{\nu}^{\prime} \alpha_{\nu} + V_{\nu}^{\prime} \alpha_{\bar{\nu}}^{\dagger},$$

$$a_{\bar{\nu}}^{\dagger} = U_{\nu}^{\prime} \alpha_{\bar{\nu}}^{\dagger} - V_{\nu} \alpha_{\nu},$$

$$a_{\bar{\nu}}^{\prime} = U_{\nu}^{\prime} \alpha_{\bar{\nu}} - V_{\nu}^{\prime} \alpha_{\nu}^{\dagger},$$

and that $|BCS\rangle$ is the quasiparticle vacuum. The primed quantities are referred to the intrinsic, body-fixed frame (see App. A and B).

Consequently, the associated (successive) two-nucleon transfer spectroscopic amplitude

$$B(\nu^2(0)) = U_{\nu}(A) V_{\nu}(A + 2) (= c_{\nu}), \quad (28)$$

has the same dependence on the BCS occupation numbers as that displayed by the amplitudes associated with simultaneous transfer (order parameter) [12], and with the $c(\nu)$ amplitude entering in the Cooper pair wavefunction. This last result is closely related to the smooth behavior of the BCS occupation parameters with mass number (see Appendix B). Summing up, pair coherence is maintained both in successive as well as in simultaneous transfer.

It is of notice that all the above results, which constitute the very essence of nuclear BCS, are not only inescapable, they are also almost tautological, at least for well bound nuclei. In fact, pairing in nuclei does not affect neither the single-particle energies ε_{ν} (see in any case Eq. (A27) and following discussion), nor the corresponding wavefunctions $\phi_{\nu}(\vec{r})$, but only the single-particle occupation probabilities. And this takes place in a small $(\Delta/\varepsilon_F \approx 5 \times 10^{-2})$ region around the Fermi energy. In this region, and in keeping with the structure of the BCS wavefunction, which takes into account the variety of excitations of pairs of particles $(\nu, \bar{\nu}')$, so as to produce the most efficient mixing of empty and occupied states leading to Cooper pairs, the only possible excitation mechanism of the nuclear superfluid, is that of breaking a Cooper pair, individual two-particle $(\nu \bar{\nu})$ excitations being already taken into account in the BCS ground state. It is then

neither surprising that the amplitudes of the Cooper pair wavefunction are $c(\nu) \sim U'_\nu V'_\nu$, nor that the absolute cross section for Cooper pair transfer are proportional to $(\sum_{\nu>0} U'_\nu V'_\nu)^2$. And least of all, it is not surprising the fact these amplitudes and two-nucleon transfer processes involve not only $(nljm, nlj-m)$ configurations, but also $(nljm, n'lj-m)$ as well as $[(J(A) + n_1 l_1 j_1)_{J_1} \otimes (J'(a) + n_2 l_2 j_2)_{J_2}]_{J_0}$. This is in keeping with the non-orthogonality of the single-particle wavefunctions describing the target and projectile in the different channels ($a + A \rightarrow f + F \rightarrow b + B$). Within this context, not only n and n' are possible, due to the fact that partners of a Cooper pair feel different mean fields ($\phi_{n'ljm}^f, \phi_{nljm}^F$), but also because a general nuclear structure treatment of pairing, will include Cooper-like correlations associated with multipole pairing (see e.g. [10] Sect. 5.3 and refs. therein), correlations which, in the present case, have not a dynamical origin (one works with $H_p = -GP^\dagger P$), but only a trivial kinematical one.

III. REACTION MECHANISM

In what follows we present the elements which enter the calculation of the absolute two-particle transfer differential cross section in terms of the reaction

$$A + t \rightarrow B(\equiv A + 2) + p, \quad (29)$$

in which $A + 2$ and A denotes the mass number of even nuclei in their ground state. In other words, one concentrates on $L = 0$ transfer. The wavefunction of nucleus $A + 2$ is written as,

$$\Psi_{A+2}(\xi_A, \mathbf{r}_{A1}, \sigma_1, \mathbf{r}_{A2}, \sigma_2) = \psi_A(\xi_A) \sum_{l_i, j_i} [\phi_{l_i, j_i}^{A+2}(\mathbf{r}_{A1}, \sigma_1, \mathbf{r}_{A2}, \sigma_2)]_0^0, \quad (30)$$

product of the wavefunction describing the ground state of the nucleus A , the corresponding relative (intrinsic) $3A - 3$ radial coordinates being denoted ξ_A , and of the wavefunction of two-correlated nucleons

$$\phi_{l_i, j_i}^{A+2}(\mathbf{r}_{A1}, \sigma_1, \mathbf{r}_{A2}, \sigma_2)_0^0 = \sum_{nm} a_{nm} [\varphi_{n, l_i, j_i}^{A+2}(\mathbf{r}_{A1}, \sigma_1) \varphi_{m, l_i, j_i}^{A+2}(\mathbf{r}_{A2}, \sigma_2)]_0^0 \quad (31)$$

the wavefunctions $\varphi_{n, l_i, j_i}^{A+2}(\mathbf{r}, \sigma)$ describing the single-particle motion of a nucleon in a mean field potential, e.g. a Saxon-Woods potential. The spatial part of the two-neutron wavefunction in the triton can be written as, $\phi_t(\mathbf{r}_{p1}, \mathbf{r}_{p2}) = \rho(r_{p1})\rho(r_{p2})\rho(r_{12})$, r_{p1} and r_{p2} denoting the modulus of the relative coordinate of each of the two neutrons involved in the transfer process, measured with respect to the proton, while r_{12} denotes the modulus of the relative coordinate of the two

neutrons in the triton. The functions $\rho(r)$, as depicted in Fig. 6(a), are generated with the $p - n$ Tang–Herndon interaction [37]

$$v(r) = -v_0 \exp(-k(r - r_c)) \quad r > r_c \quad (32)$$

$$v(r) = \infty \quad r < r_c, \quad (33)$$

where $k = 2.5\text{fm}^{-1}$ and $r_c = 0.45\text{fm}$ denotes the radius of the hard core. The depth v_0 is adjusted so as to reproduce the binding energy of the triton and of the deuteron respectively. This hard-core potential is also used in the above expressions as the $n - p$ interaction potential responsible for neutron transfer.

The two-particle transfer differential cross section is written as

$$\frac{d\sigma}{d\Omega} = \frac{\mu_i \mu_f}{(4\pi\hbar^2)^2} \frac{k_f}{k_i} |T^{(1)} + T_{succ}^{(2)} - T_{NO}^{(2)}|^2. \quad (34)$$

The amplitudes appearing in it describe the simultaneous,

$$T^{(1)} = 2 \sum_{l_i, j_i} \sum_{\sigma_1 \sigma_2} \int d\mathbf{r}_{tA} d\mathbf{r}_{p1} d\mathbf{r}_{A2} [\phi_{l_i, j_i}^{A+2}(\mathbf{r}_{A1}, \sigma_1, \mathbf{r}_{A2}, \sigma_2)]_0^{0*} \chi_{pB}^{(-)*}(\mathbf{r}_{pB}) \\ \times v(\mathbf{r}_{p1}) \phi_t(\mathbf{r}_{p1}, \mathbf{r}_{p2}) \chi_{tA}^{(+)}(\mathbf{r}_{tA}), \quad (35a)$$

successive

$$T_{succ}^{(2)} = 2 \sum_{l_i, j_i} \sum_{l_f, j_f, m_f} \sum_{\sigma_1' \sigma_2'} \int d\mathbf{r}_{dF} d\mathbf{r}_{p1} d\mathbf{r}_{A2} [\phi_{l_i, j_i}^{A+2}(\mathbf{r}_{A1}, \sigma_1, \mathbf{r}_{A2}, \sigma_2)]_0^{0*} \chi_{pB}^{(-)*}(\mathbf{r}_{pB}) v(\mathbf{r}_{p1}) \\ \times \phi_d(\mathbf{r}_{p1}) \varphi_{l_f, j_f, m_f}^{A+1}(\mathbf{r}_{A2}) \int d\mathbf{r}'_{dF} d\mathbf{r}'_{p1} d\mathbf{r}'_{A2} G(\mathbf{r}_{dF}, \mathbf{r}'_{dF}) \\ \times \phi_d(\mathbf{r}'_{p1})^* \varphi_{l_f, j_f, m_f}^{A+1*}(\mathbf{r}'_{A2}) \frac{2\mu_{dF}}{\hbar^2} v(\mathbf{r}'_{p2}) \phi_d(\mathbf{r}'_{p1}) \phi_d(\mathbf{r}'_{p2}) \chi_{tA}^{(+)}(\mathbf{r}'_{tA}), \quad (35b)$$

and non-orthogonality

$$T_{NO}^{(2)} = 2 \sum_{l_i, j_i} \sum_{l_f, j_f, m_f} \sum_{\sigma_1' \sigma_2'} \int d\mathbf{r}_{dF} d\mathbf{r}_{p1} d\mathbf{r}_{A2} [\phi_{l_i, j_i}^{A+2}(\mathbf{r}_{A1}, \sigma_1, \mathbf{r}_{A2}, \sigma_2)]_0^{0*} \chi_{pB}^{(-)*}(\mathbf{r}_{pB}) v(\mathbf{r}_{p1}) \\ \times \phi_d(\mathbf{r}_{p1}) \varphi_{l_f, j_f, m_f}^{A+1}(\mathbf{r}_{A2}) \int d\mathbf{r}'_{p1} d\mathbf{r}'_{A2} d\mathbf{r}'_{dF} \\ \times \phi_d(\mathbf{r}'_{p1})^* \varphi_{l_f, j_f, m_f}^{A+1*}(\mathbf{r}'_{A2}) \phi_d(\mathbf{r}'_{p1}) \phi_d(\mathbf{r}'_{p2}) \chi_{tA}^{(+)}(\mathbf{r}'_{tA}), \quad (35c)$$

contributions to the transfer process. In these expressions, $\varphi_{l_f, j_f, m_f}^{A+1}(\mathbf{r}_{A1})$ are the wavefunctions describing the intermediate states of the nucleus $F \equiv A + 1$, generated as solutions of a Saxon-Woods

potential, while $\phi_d(\mathbf{r}_{p2})$ is the wavefunction describing the deuteron bound state (see Fig. 6(b)). We have chosen the so called post-post representation [20], in which the $p - n$ interaction appears twice in the successive amplitude. The Green function $G(\mathbf{r}_{dF}, \mathbf{r}'_{dF})$ propagates the intermediate channel d, F , and can be expanded in partial waves

$$G(\mathbf{r}_{dF}, \mathbf{r}'_{dF}) = i \sum_l \sqrt{2l+1} \frac{f_l(k_{dF}, r_<) P_l(k_{dF}, r_>)}{k_{dF} r_{dF} r'_{dF}} \left[Y^l(\hat{r}_{dF}) Y^l(\hat{r}'_{dF}) \right]_0^0. \quad (36)$$

The functions $f_l(k_{dF}, r)$ and $P_l(k_{dF}, r)$ are the regular and the irregular solutions of a Schrödinger equation associated with a suitable optical potential and an energy equal to the kinetic energy in the intermediate state. In most cases of interest, the result is hardly altered if one uses the same energy of relative motion for all the intermediate states. This representative energy is calculated when both nuclei appearing in the intermediate state are in their ground states. The validity of this approximation can break down in particular cases. For example, in the case in which some relevant intermediate states are strongly off shell, in which case their contribution is significantly quenched. An interesting situation can develop when this situation becomes operative for all possible intermediate states, in which case they can only be virtually populated, thus emphasizing the role of simultaneous transfer.

IV. THE ISOTOPIC CHAIN $^{100}_{50}\text{Sn}$ – $^{132}_{50}\text{Sn}_{82}$

A collective mode is characterized by: 1) an enhanced cross section of transition probability; 2) a simple expression of its energy as a function of the quantum number characterizing the states connected by the transition. This quantum number is related to restoration of the symmetry violation (static or dynamical, e.g. particle number in the case of pairing rotations and vibrations, angular momentum in the case of e.g. quadrupole rotations and vibrations).

For example, in the case of a quadrupole rotational band of a 3D-deformed nucleus like, e.g. ^{152}Dy , 1) corresponds to the $B(E2)$ transition probability, measured e.g. in the terms of single-particle Weisskopf units (of the order of 10^3 in the example chosen), while 2) corresponds to $E_I = (\hbar^2/2\mathcal{J})I(I+1)$, I being the angular momentum of the system ($I = 0, 2, 4, \dots$). In the case of pairing rotational bands 1) corresponds to the absolute value of the two-nucleon differential cross section, measured in terms of the average pure two-particle units [12, 17, 18] (typical value of the enhancement factor being, in the case of Sn-isotopes, of the order of 10^2), while 2) corresponds to $E_N = (\hbar^2/2I)(N - N_0)^2$, N being the number of particles associated with the condensate, namely

with the neutrons in the case of ${}^A_{50}\text{Sn}_N$, while N_0 is the mean number of neutrons representative of the particle number wavepacket describing the superfluid Sn-isotopes ($N_0 \approx 68$, see discussion below). Of these two quantities, 1) is arguably the most representative one. This is because accidental degeneracies or residual interactions may modify the energies without much altering the long-range correlation of the coherent state.[38] This is also the reason why, in what follows, use is made of the single j-shell model to discuss the basic features of the pairing rotational modes.

In this Section we present evidence of the accuracy with which the model of pairing rotations discussed in Section 2, together with the two-nucleon transfer reaction scheme summarized in the last section allows for an overall quantitative description of the absolute value of the two-nucleon transfer cross sections, when use is made of global optical parameters to describe the (three) elastic channels involved in the process. Consequently, the predictions given in Sect. IV B concerning the pairing vibrational spectrum expected in connection with the two unstable closed shell systems ${}^{132}\text{Sn}$ and the most exotic one ${}^{100}\text{Sn}$ can be considered potentially important and likely quantitative.

A. Pairing rotations

In Fig. 7 we display the value of the absolute differential cross sections associated with the reactions ${}^{A+2}_{50}\text{Sn}(p, t){}^A_{50}\text{Sn}(gs)$ for which absolute measurements have been reported in the literature, in comparison with the experimental data [39–45] (see also [46, 47]). The corresponding integrated cross section are collected in Table IV. In all cases the contribution of the successive process is the dominant one. Examples of two-nucleon spectroscopic amplitudes obtained from BCS calculations are displayed in Table 2 (U, V for ${}^{120}\text{Sn}(p, t){}^{118}\text{Sn}$). They have been computed solving the gap and number equations with a monopole interaction acting on the bound orbitals, calculated as the eigenfunctions of a standard parametrized Saxon-Woods potential, and imposing that the gap reproduces the value obtained from the empirical odd-even mass differences for the various isotopes. The BCS spectroscopic amplitudes are in good agreement with those predicted by extended shell model calculation (see refs. [43, 44] and refs. therein). The optical parameters in the entrance, intermediate, and final channel were taken from refs. in [39–44] and from [48] for the deuteron channel.

From the above results one can posit that theory provides an account of the experimental absolute differential cross section well within the experimental errors and, arguably, without free parameters.

Let us now concentrate our attention on the value and on the structure of the probability amplitude for two nucleon, at \vec{r} and \vec{r}' to belong to a Cooper pair, namely $\alpha'_0(\vec{r}, \vec{r}') = \sum_{\nu>0} c_\nu \phi_\nu(\vec{r}) \phi_\nu(\vec{r}')$ (see (16) and (28)). That is, the nuclear structure component of the two-particle transfer cross section amplitude. To clarify the physics at the basis of the BCS description of pairing rotational bands, we discuss two scenarios for the case of the $^{120}\text{Sn}(p, t)^{118}\text{Sn}$ reaction. In the first one, we consider all bound single-particle states, the cutoff energy being $E_{\text{cutoff}} = 0$ MeV. In the second case one sets $E_{\text{cutoff}} = 60$ MeV, discretizing the continuum inside a spherical box of 15 fm of radius. The BCS gap ($\Delta = 1.47$ MeV; experimental value) and number ($N = 70$) equations lead to $G = 0.18$ MeV and $\lambda = -6.72$ MeV in the first case and $G = 0.05$ MeV and $\lambda = -6.9$ MeV in the second one. The associated Cooper pair probability distributions in r -space are essentially identical (see Fig. 8 and Tables I and II). It is then not surprising that they lead to essentially the same absolute value of the two-particle transfer cross section associated with the reaction $^{120}\text{Sn}(p, t)^{118}\text{Sn}(\text{gs})$.

Let us now repeat the argument, but this time in terms of $\sigma(gs \rightarrow gs) \sim (\Delta/G)^2$, as it customary done since the first publication which introduced it [49]. Because the pairing gap has been fixed to reproduce the experimental value (1.47 MeV), one obtains in the case of $E_{\text{cutoff}} = 0$ MeV $(\Delta/G)^2 \sim 70$ and $(\Delta/G)^2 \sim 889$ in the case of $E_{\text{cutoff}} = 60$ MeV. This result emphasizes the problem of working with an expression which contains explicitly the pairing coupling constant.

One could argue that such an objection could also be leveled off against the relation $\sigma \sim |\alpha_0|^2$. Note however, that a (p, t) reaction would hardly feel the effect of contributions far removed from the Fermi surface λ . This is in keeping with the fact that transfer to levels lying far away from λ will be unfavorable due to Q -value effects. If one argues in terms of the relative distance r between target and projectile ($r \gg R_0$ for continuum-like contributions; $r < R_0$ for deeply bound-like contributions), the outcome is similar. In fact, for large distances the two-particle transfer form factor vanishes while at small distances the outgoing tritium will experience strong absorption (see Appendix E).

In fact, considering only the contribution to α'_0 arising from the valence orbitals, that is, essentially those contributing to the “naked” vision of the Cooper pair wavefunctions, one obtains $\alpha'_0 = 2.12$ and $\alpha'_0 = 2.08$ respectively, and thus, a negligible squared relative difference between the two predicted cross sections, namely $(0.04/2.1)^2 \approx 2 \times 10^{-3}$.

Summing up, because the pair condensed state can be viewed as a coherent state which behaves essentially classically when viewed in terms of its building block (Cooper pair) the description of

pairing rotational bands provided by the BCS model in terms of a coupling constant and an energy cutoff can be considered essentially “exact” when probed with two-nucleon transfer processes, reactions which filter the inaccuracies of each individual $U_\nu V_\nu$ component, emphasizing the off-diagonal long range order provided by the phase coherence (cf. ref. [50]). In fact, studying nuclear Cooper pair condensation in terms of e.g. single-nucleon transfer (see e.g. [51, 52], the individual inaccuracies of the BCS occupation numbers cannot be averaged out. As a consequence, the overall agreement between theory and experiment is much poorer than that reflected by e.g. the results collected in Table IV. The above arguments provide further evidence of why two-nucleon transfer is the specific probe of pairing superfluidity.

In Fig. 9 a quantity closely related to the Sn-isotopes binding energy is reported as a function of the number of neutrons. Also displayed is the best parabolic fit to these energies, a quantity to be compared with

$$E_N = \frac{\hbar^2}{2I}(N - N_0)^2, \quad (37)$$

namely the energy associated with the members of the pairing rotational band.

A simple estimate of the pairing rotational band moment of inertia is given by the single j -shell model (see e.g. [10] App. H $\hbar^2/2I = G/4 \approx 25/(4N_0)$ MeV).

This estimate turns out to be rather accurate, even beyond expectation. Of notice that to the extent that one is discussing properties of a coherent state like that described by (12), for which H_{sp} plays a secondary role (see discussion following Eq. (A27) in Appendix A) this is not a surprising results. As can be seen from Fig. 9, the estimate (37) is rather accurate except close to $N=50$ and $N=82$, in keeping with the fact that, as discussed before, the pairing deformed picture ($\alpha_0 \neq 0$) breaks down around closed shell ($\alpha'_0 = 0$), where a vibrational regime (associated with the dynamic distortion α_{dyn} , see Eq. (18)) is expected to be valid.

Also reported in Fig. 9, are the integrated values of the measured absolute two-particle transfer cross sections. Naively, one would expect a marked constancy of these transitions, in keeping with the fact that the (pairing) rotational model implies a common intrinsic (deformed) state (Cooper pair condensate, see Eq. (12)). On the other hand, due to the fact that the number of Cooper pairs contributing to the pairing distortion α'_0 is rather small (less than 10), one expect strong fluctuations in this quantity ($\alpha'_0 \approx \sqrt{7}/7 \approx 0.4$) and consequently in the two-particle transfer cross section ($\sigma \sim \alpha'^2_0$, i.e. fluctuation in σ of the order of 100 %).

In keeping with the analogy presented in Fig. 2, in the case of electromagnetic transition between members of a quadrupole rotational band one expects in heavy nuclei fluctuations of the

order of $(\sqrt{250}/250)^2$, i.e. less than 1%. Within this context the average value of the absolute experimental cross section reported in Table IV is $1551 \mu\text{b}$, while the average difference between experimental and predicted values is $81 \mu\text{b}$. Thus the discrepancies between theory and experiment are bound in the interval $0 \leq |\sigma_{exp}(i \rightarrow f) - \sigma_{th}(i \rightarrow f)|/\sigma_{exp}(i \rightarrow f) \leq 0.09$, the average discrepancy being 5%.

In Fig. 10 the excited, pairing rotational band associated with the average value of the 0^+ pairing vibrational states with energy $\leq 3 \text{ MeV}$, is displayed together with the best parabolic fit. Also given is the relative (p, t) integrated cross section normalized with respect to the $gs \rightarrow gs$ transitions, a value which is in all cases $\leq 8\%$, in overall agreement with the single j-shell estimate (see ref. [10] App. H), given in the inset to the figure. The result testifies to the weak cross talk between pairing rotational bands and thus of the robust off-diagonal, long range order coherence of these modes.

B. Pairing vibrational band in closed shell nuclei

In Fig. 11 we display the expected pairing vibrational spectrum (harmonic approximation, see refs. [10–12] and refs. therein) associated with the closed shell exotic nucleus ^{132}Sn [2, 3], up to two-phonon states. Within this approximation, the one-phonon states are the pair addition $|a\rangle = |gs(^{134}\text{Sn})\rangle$ and pair removal $|r\rangle = |gs(^{130}\text{Sn})\rangle$ modes. The two-phonon 0^+ ($|pv(^{132}\text{Sn})\rangle = |r\rangle \otimes |a\rangle = |0^+(^{132}\text{Sn}); 6.5 \text{ MeV}\rangle$) pairing vibrational ($(2p - 2h)$ -like) state of ^{132}Sn , is predicted at an excitation energy of 6.5 MeV (see Fig. 3). The absolute two-particle transfer differential cross sections associated with $|a\rangle$ and $|r\rangle$, namely

$$^{132}\text{Sn}(t, p)^{134}\text{Sn}(gs), \quad (E_{CM} = 20\text{MeV}), \quad (38)$$

$$^{132}\text{Sn}(p, t)^{130}\text{Sn}(gs), \quad (E_{CM} = 26\text{MeV}), \quad (39)$$

are reported in the insets. Using detailed balance the reactions above

$$^{130}\text{Sn}(t, p)^{132}\text{Sn}(0^+; 6.5\text{MeV}), \quad (E_{CM} = 20\text{MeV}), \quad (40)$$

$$^{134}\text{Sn}(p, t)^{132}\text{Sn}(0^+; 6.5\text{MeV}), \quad (E_{CM} = 26\text{MeV}), \quad (41)$$

are, within the harmonic approximation, equivalent to (38) and (39), except for the relative flux which is determined by the ratio k_f/k_i .

Similar calculations to the ones discussed above have been carried out for the closed shell nucleus ^{100}Sn , the results being collected in Fig. 12. In this case the two-phonon 0^+ , pairing vibrational mode of ^{100}Sn is expected, again within the harmonic approximation, at an excitation energy of 7.1 MeV. As it emerges from Figs. 11 and 12, and at variance with the pairing rotational scheme, the two-particle transfer cross section associated with the excited pairing vibrational state is of the same order of magnitude than that connecting the ground states.

Within this context, it could be intriguing to check whether the reaction $^{106}\text{Sn}(p,t)^{104}\text{Sn}$ populates a 0^+ state at an excitation energy of the order of 7 MeV. This state, can be written within the (pairing vibration) harmonic approximation, as $|^{104}\text{Sn}(0^+; 7.1\text{MeV})\rangle = |a\rangle \otimes |a\rangle \otimes |a\rangle \otimes |r\rangle$. Namely a four-phonon pairing vibrational state, where

$$|a\rangle = |gs(^{102}\text{Sn})\rangle \quad ; \quad |r\rangle = |gs(^{98}\text{Sn})\rangle. \quad (42)$$

In other words, the reaction $^{106}\text{Sn}(p,t)^{104}\text{Sn}(0^+, 7.1 \text{ MeV})$ is, within the harmonic picture of pairing vibrations, equivalent to the reaction $^{100}\text{Sn}(p,t)^{98}\text{Sn}(gs)$. It is of notice that a three-phonon pairing vibrational states has been observed [53] in the reaction $^{204}\text{Pb}(t, p)^{206}\text{Pb}$ at an excitation energy of about 6 MeV, with Q -values and absolute differential cross sections compatible with the excitation of the ^{208}Pb pair addition mode, namely $^{208}\text{Pb}(t,p)^{210}\text{Pb}(gs)$. While in this case deviations from the harmonic prediction are modest (essentially, most of them arising from the presence of the valence orbital $p_{1/2}$ lying just below $\epsilon_F(^{208}\text{Pb})$ [54]), in the case of pairing vibrations based on ^{100}Sn , anharmonicities are expected to be much stronger. This is in keeping with the fact that $N = Z$ nuclei display, as a rule, coexistence phenomena. That is, a strong competition between spherical and deformed 0^+ states (cf. e.g. [55–57] and refs. therein, see also [58]).

V. CONCLUSIONS

The microscopic nuclear structure (BCS) description of pairing rotational bands, together with the second order DWBA description of two-nucleon transfer reactions which include successive, simultaneous and non-orthogonality channels provide, arguably without free parameters, an overall account of Cooper pair transfer to superfluid nuclei. Inarguably, theory not only reproduces all reported $^{A+2}\text{Sn}(p, t)^A\text{Sn}(gs)$ absolute cross section data within experimental errors, but it does so with uncertainties below the 10% level.

The study of the pairing vibrational scheme around the starting and end points of the pairing

rotational spectrum promises to provide new insight on pairing fluctuations and their anharmonicities, in situations of large neutron excess and of $N \sim Z$, i.e. around closed shell system ^{132}Sn and of the, likely deformation coexistent ^{100}Sn , respectively.

	ε_v	ϵ_v	E_v	U'_v	V'_v	$U'_v V'_v$	$\Omega_v U'_v V'_v$
$d_{5/2}$	-9.21	-2.31	2.72	0.28	0.96	0.27	0.81
$g_{7/2}$	-8.70	-1.80	2.31	0.34	0.94	0.32	1.28
$s_{1/2}$	-7.42	-0.52	1.55	0.58	0.81	0.47	0.47
$d_{3/2}$	-6.98	-0.08	1.47	0.69	0.72	0.50	1.00
$h_{11/2}$	-5.97	1.07	1.75	0.88	0.48	0.42	2.52
$f_{7/2}$	-1.87	5.03	5.26	0.99	0.14	0.14	0.56
$p_{3/2}$	-0.78	6.12	6.32	0.99	0.12	0.12	0.24

TABLE I: Results for the valence shell lying closer to Fermi energy, of a BCS calculation, for ^{120}Sn . The mean field used corresponds to a Saxon-Woods potential, in a 15 fm spherical box (continuum discretization). The pairing coupling constant used, $G = 0.05$ MeV leads to the value of pairing gap obtained from the three point formula ($\Delta = 1.47$ MeV), summing the contributions of states from the $1s_{1/2}$ at -39 MeV to +60 MeV. The resulting Fermi energy computed by solving the BCS number equation is $\lambda = -6.9$ MeV. The quantity $\alpha'_0 = \sum_{v>0} U'_v V'_v (= \sum_j \sum_{m>0} U'_j V'_j = \sum_j \Omega_j U'_j V'_j) \approx 6.1$ for the valence-shell space and $\alpha'_0 \approx 29.4$ for the whole single-particle space used in the calculation.

	ε_v	ϵ_v	E_v	U'_v	V'_v	$U'_v V'_v$	$\Omega_v U'_v V'_v$
$d_{5/2}$	-9.21	-2.45	2.90	0.26	0.96	0.25	0.75
$g_{7/2}$	-8.70	-1.98	2.48	0.32	0.95	0.30	1.20
$s_{1/2}$	-7.42	-0.70	1.63	0.54	0.84	0.45	0.45
$d_{3/2}$	-6.98	-0.26	1.49	0.64	0.77	0.49	0.98
$h_{11/2}$	-5.97	0.75	1.64	0.85	0.53	0.45	2.70
$f_{7/2}$	-1.88	4.84	5.04	0.99	0.15	0.15	0.60
$p_{3/2}$	-0.78	5.94	6.10	0.99	0.12	0.12	0.24

TABLE II: Results for the valence shell lying closer to Fermi energy, of a BCS calculation, for ^{120}Sn . The mean field used corresponds to a Saxon-Woods potential, in a 15 fm spherical box (continuum discretization). The pairing coupling constant used, $G = 0.18$ MeV leads to the value of pairing gap obtained from the three point formula ($\Delta = 1.47$ MeV), summing the contributions of states from the $1s_{1/2}$ at -39 MeV to +0 MeV. The resulting Fermi energy computed by solving the BCS number equation is $\lambda = -6.72$ MeV. The quantity $\alpha'_0 \approx 6.1$ (see caption to Table I) for the valence-shell space and $\alpha'_0 \approx 8.2$ for the whole single-particle space.

¹³² Sn							
Ω_j	ε_j	X_{rem}	Y_{add}	$X_{rem}Y_{add}$	$\sqrt{\Omega_j}\Lambda_{rem}$	$\sqrt{\Omega_j}\Lambda_{add}$	
$g_{7/2}$	4	-9.78	0.229	0.080	0.018	3.20	2.16
$d_{5/2}$	3	-9.01	0.255	0.078	0.020	2.78	1.88
$s_{1/2}$	1	-7.68	0.286	0.058	0.017	1.60	1.08
$h_{11/2}$	6	-7.52	0.791	0.147	0.116	3.92	2.64
$d_{3/2}$	2	-7.35	0.529	0.088	0.047	2.26	1.52
		Y_{rem}		X_{add}			
$f_{7/2}$	4	-2.44	0.922	0.209	0.192	3.20	2.16
$p_{3/2}$	2	-1.59	0.265	0.121	0.032	2.26	1.52
$h_{9/2}$	5	-0.88	0.281	0.166	0.046	3.58	2.42
$p_{1/2}$	1	-0.78	0.120	0.073	0.009	1.60	1.08
$f_{5/2}$	3	-0.44	0.180	0.119	0.021	2.78	1.88
¹⁰⁰ Sn							
Ω_j	ε_j	X_{rem}	Y_{add}	$X_{rem}Y_{add}$	$\sqrt{\Omega_j}\Lambda_{rem}$	$\sqrt{\Omega_j}\Lambda_{add}$	
$f_{5/2}$	3	-22.02	0.353	0.116	0.041	9.22	4.72
$p_{3/2}$	2	-21.75	0.300	0.098	0.029	7.52	3.84
$p_{1/2}$	1	-20.20	0.282	0.082	0.023	5.32	2.72
$g_{9/2}$	4	-18.05	1.156	0.248	0.286	11.90	6.08
		Y_{rem}		X_{add}			
$d_{5/2}$	3	-10.47	0.461	0.803	0.370	9.22	4.72
$g_{7/2}$	4	-9.23	0.427	0.502	0.214	10.64	5.44
$s_{1/2}$	1	-8.41	0.188	0.192	0.036	5.32	2.72
$d_{3/2}$	2	-7.70	0.242	0.226	0.055	7.52	3.84
$h_{11/2}$	6	-6.83	0.377	0.325	0.123	13.04	6.66

TABLE III: RPA wavefunctions of pair addition and removal mode of ¹³²Sn (above) and ¹⁰⁰Sn (below). Single particle energies have been taken from experimental values referenced in the National Nuclear Data Center. The energy of the lowest pairing addition and removal phonons in ¹³²Sn are respectively $W(A + 2) = 3.45$ MeV with $G(A + 2) = 0.131$ MeV and $W(A - 2) = 3.06$ MeV with $G(A - 2) = 0.157$ MeV, the associated particle-pair vibration coupling strength (see Eq.(21)) being $\Lambda_{add} = \Lambda(A + 2) = 1.08$ MeV and $\Lambda_{rem} = \Lambda(A - 2) = 1.60$ MeV respectively. The minimum of the dispersion relation, and thus the Fermi energy, are equal to $\lambda = -4.75$ MeV (see Fig. 3(a)). The pair degeneracy of the single-particle space associated with ¹³²Sn and ¹⁰⁰Sn is $\Omega = 31$ and $\Omega = 27$ respectively. The energy of the lowest pairing addition and removal phonons in ¹⁰⁰Sn are respectively $W(A + 2) = 5.13$ MeV with $G(A + 2) = 0.290$ MeV and $W(A - 2) = 1.96$ MeV with $G(A - 2) = 0.380$ MeV, the Fermi energy being $\lambda = -14.5$ MeV (see Fig. 3(b)). The associated Λ values being $\Lambda_{add} = 2.72$ MeV and $\Lambda_{rem} = 5.32$ MeV. The binding energy of ⁹⁸Sn was assumed to be $B(^{98}\text{Sn}) = 794.24$ MeV, from the polinomial (4th grade) fit of the binding energies of tin isotopic chain.

	$\sigma(\text{gs} \rightarrow \text{gs})$	
	Theory	Experiment ^{c,d)}
$^{112}\text{Sn}(p, t)^{110}\text{Sn}, E_p = 26 \text{ MeV}$	1301 ^{a)}	$1309 \pm 200(\pm 14)$ ^{a)} $[6^\circ \leq \theta \leq 62.7^\circ]$
$^{114}\text{Sn}(p, t)^{112}\text{Sn}, E_p = 22 \text{ MeV}$	1508 ^{a)}	$1519.3 \pm 228(\pm 16.2)$ ^{a)} $[7.64^\circ \leq \theta \leq 62.24^\circ]$
$^{116}\text{Sn}(p, t)^{114}\text{Sn}, E_p = 26 \text{ MeV}$	2078 ^{a)}	$2492 \pm 374(\pm 32)$ ^{a)} $[4^\circ \leq \theta \leq 70^\circ]$
$^{118}\text{Sn}(p, t)^{116}\text{Sn}, E_p = 24.6 \text{ MeV}$	1304 ^{a)}	$1345 \pm 202(\pm 24)$ ^{a)} $[7.63^\circ \leq \theta \leq 59.6^\circ]$
$^{120}\text{Sn}(p, t)^{118}\text{Sn}, E_p = 21 \text{ MeV}$	2190 ^{a)}	$2250 \pm 338(\pm 14)$ ^{a)} $[7.6^\circ \leq \theta \leq 69.7^\circ]$
$^{122}\text{Sn}(p, t)^{120}\text{Sn}, E_p = 26 \text{ MeV}$	2466 ^{a)}	$2505 \pm 376(\pm 18)$ ^{a)} $[2.5^\circ \leq \theta \leq 78.5^\circ]$
$^{124}\text{Sn}(p, t)^{122}\text{Sn}, E_p = 25 \text{ MeV}$	838 ^{a)}	$958 \pm 144(\pm 15)$ ^{a)} $[4^\circ \leq \theta \leq 57^\circ]$
$^{112}\text{Sn}(p, t)^{110}\text{Sn}, E_p = 40 \text{ MeV}$	3349 ^{b)}	3715 ± 1114 ^{b)}
$^{114}\text{Sn}(p, t)^{112}\text{Sn}, E_p = 40 \text{ MeV}$	3790 ^{b)}	3776 ± 1132 ^{b)}
$^{116}\text{Sn}(p, t)^{114}\text{Sn}, E_p = 40 \text{ MeV}$	3085 ^{b)}	3135 ± 940 ^{b)}
$^{118}\text{Sn}(p, t)^{116}\text{Sn}, E_p = 40 \text{ MeV}$	2563 ^{b)}	2294 ± 668 ^{b)}
$^{120}\text{Sn}(p, t)^{118}\text{Sn}, E_p = 40 \text{ MeV}$	3224 ^{b)}	3024 ± 907 ^{b)}
$^{122}\text{Sn}(p, t)^{120}\text{Sn}, E_p = 40 \text{ MeV}$	2339 ^{b)}	2907 ± 872 ^{b)}
$^{124}\text{Sn}(p, t)^{122}\text{Sn}, E_p = 40 \text{ MeV}$	1954 ^{b)}	2558 ± 767 ^{b)}

TABLE IV: Absolute cross section associated with the $^{A+2}\text{Sn}(p, t)^A\text{Sn}(\text{gs})$ cross sections (i.e. between the members of the Sn-ground state pairing rotational band) calculated as described in the text, in comparison with the experimental findings.

^{a)} μb ; the number in parenthesis corresponds to the statistical errors; the numbers in square brackets provide the angular range of integration of the absolute two-particle differential cross sections.

^{b)} $\mu\text{b/sr}$ ($\sum_{i=1}^N (d\sigma/d\Omega)$; differential cross section summed over the few, $N = 3 - 7$ experimental points)

^{c)} P. Guazzoni, L. Zetta, et al., Phys. Rev. **C 60**, 054603 (1999).

P. Guazzoni, L. Zetta, et al., Phys. Rev. **C 85**, 054609 (2012),

P. Guazzoni, L. Zetta, et al., Phys. Rev. **C 69**, 024619 (2004).

P. Guazzoni, L. Zetta, et al., Phys. Rev. **C 74**, 054605 (2006).

P. Guazzoni, L. Zetta, et al., Phys. Rev. **C 83**, 044614 (2011).

P. Guazzoni, L. Zetta, et al., Phys. Rev. **C 78**, 064608 (2008).

^{d)} G. Bassani et al., Phys. Rev. **139**, (1965)B830.

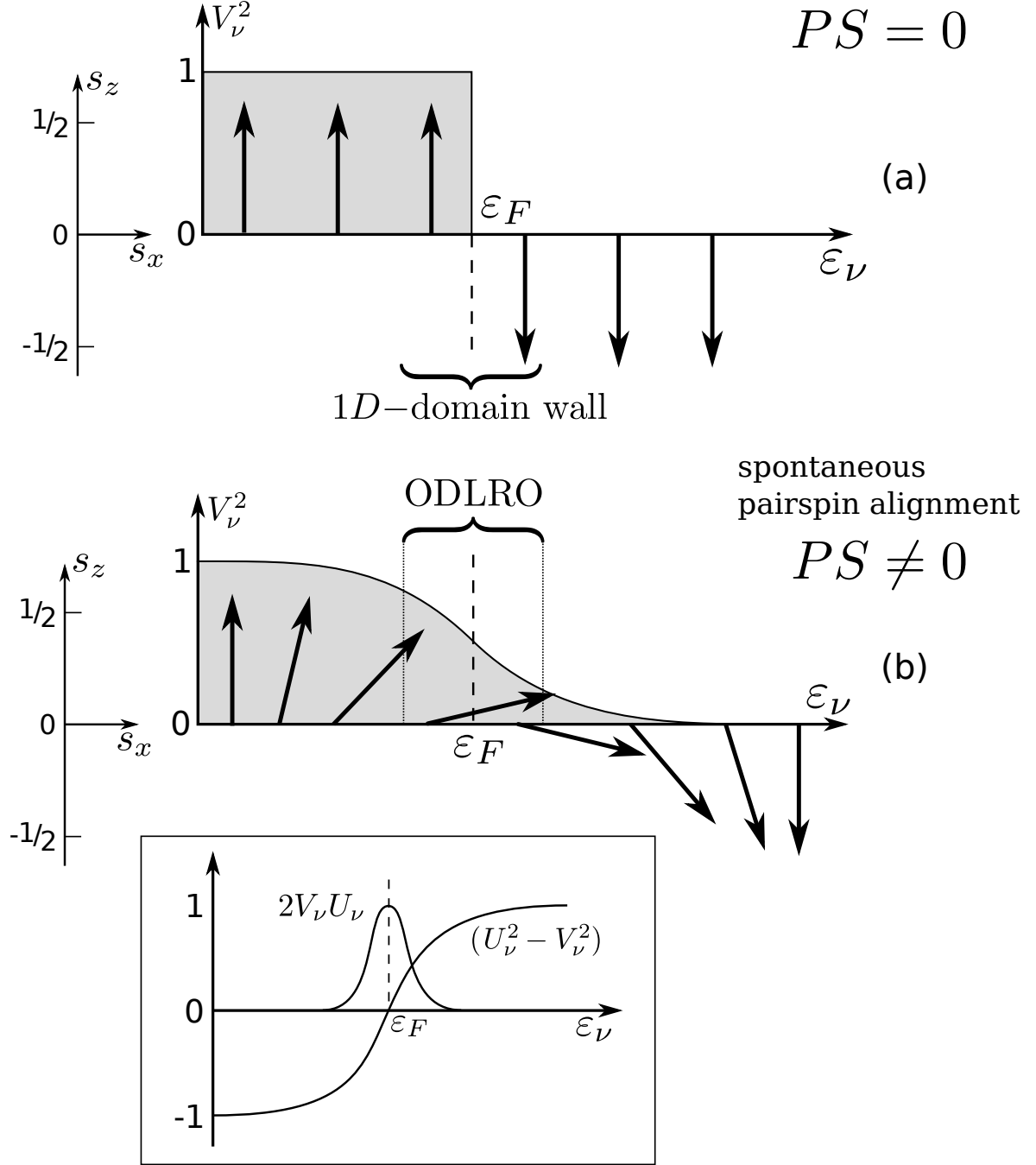


FIG. 1: (a) The occupancy $\langle N_\nu \rangle \sim V_\nu'^2$ of the single-particle states of the unperturbed system, in which the individual pairspins are aligned along the gauge (z -)axis (see Fig. A.1). This non-correlated system ($\alpha'_0 = 0$), displays zero pairspin alignment ($PS = 0$), that is $\langle S_x \rangle = 0$. (b) The superconducting (nucleon superfluid) ground state displays Off-Diagonal Long Range Order (ODLRO, see Eq. (A32)) and a finite value of the total pairspin ($PS \neq 0$; $\alpha'_0 = \sum_{\nu>0} U'_\nu V'_\nu$), i.e. $\langle s_x(\nu) \rangle \neq 0$, can be viewed as a one-dimensional domain wall (see also Fig. A.3 of Appendix A). The quantities in the inset, are the amplitudes with which z - and x -components of the pairspin mix, leading to a privileged orientation in gauge space perpendicular to the gauge (z -)axis (see Fig. A.1 (b)).

Spontaneous Symmetry Breaking

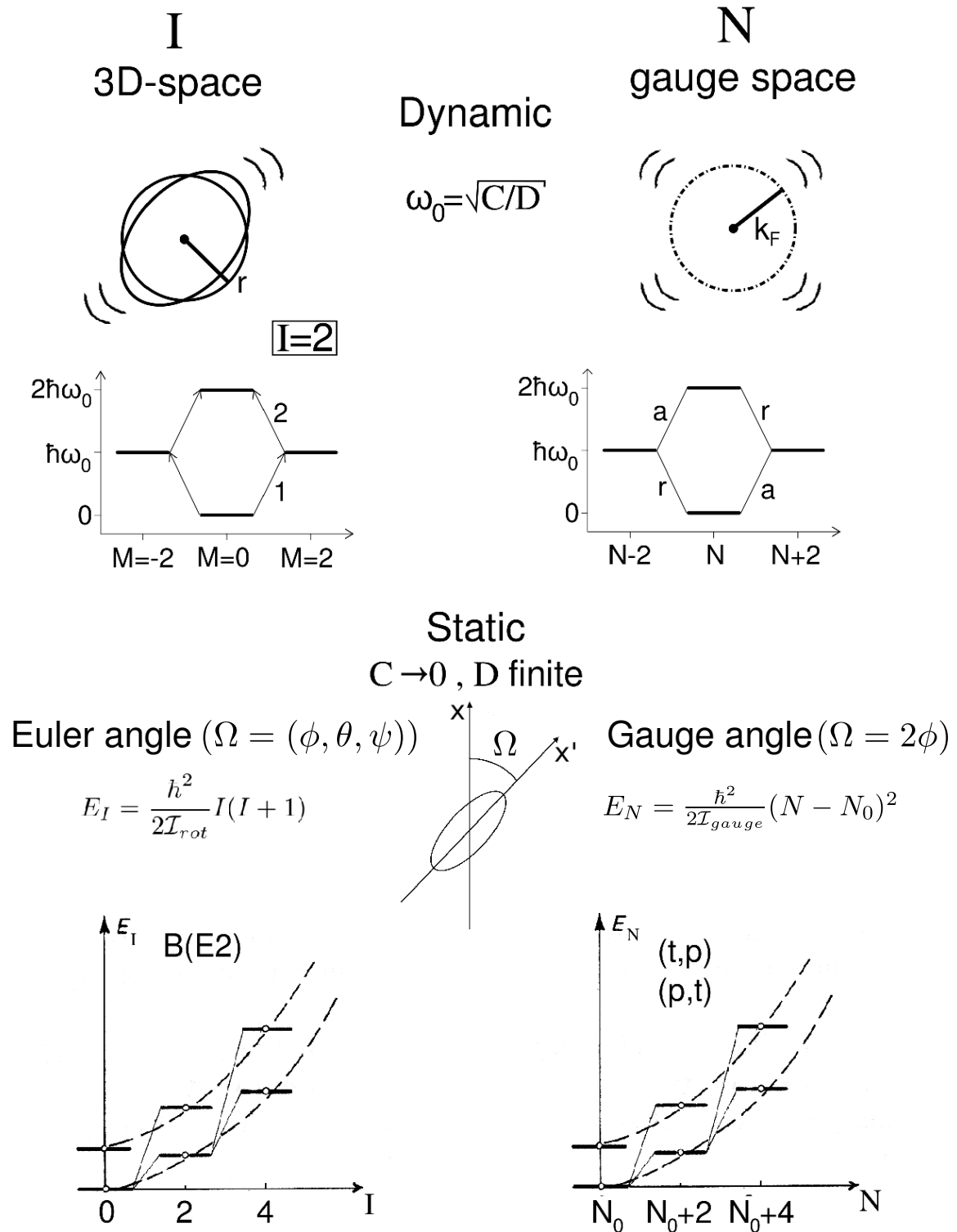


FIG. 2: Schematic representation of the nuclear structure consequences of spontaneous symmetry breaking of rotational and of gauge invariance (see also Table XI of ref. [12]).

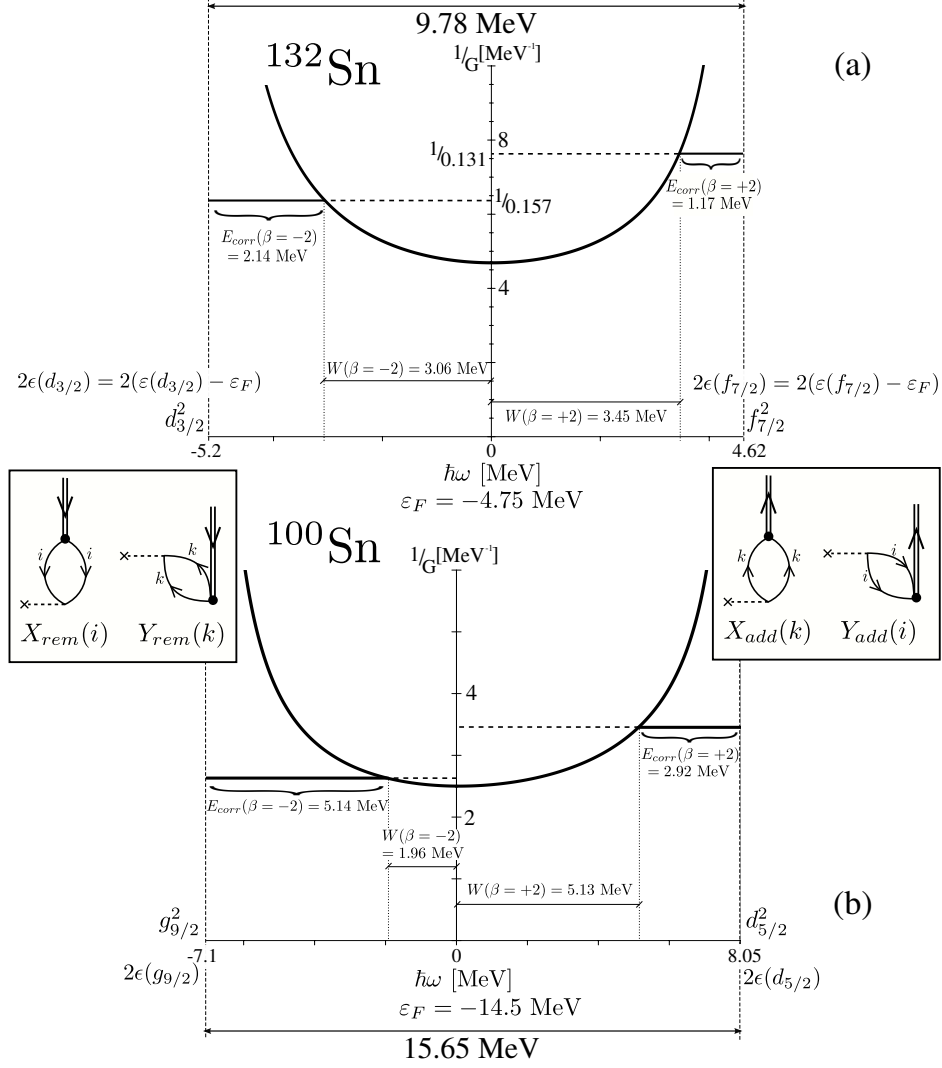


FIG. 3: Dispersion relation (see [11]; see also [10] Eq.(5.50)) associated with the pairing vibration of ^{132}Sn (a) and of ^{100}Sn (b). (a) The part of the curve to the left of the minimum corresponds to the pair removal mode ($|gs(^{130}\text{Sn})\rangle$) while that to the right is associated with the pair addition mode ($|gs(^{134}\text{Sn})\rangle$). The energy of the modes $W(A \pm 2)$ are measured from the minimum of the dispersion relation, its values being explicitly indicated (see also caption to Table 2). The coupling constants $G(A \pm 2)$ used in the calculations are given in the caption of Table 2, where the X and Y amplitudes of the corresponding wavefunctions are displayed. As seen from the insets, the pairing vibrational modes blur the sharp distinction between occupied and empty states. In fact, the pair addition mode can be excited not only by transferring two neutrons to levels lying above the Fermi energy, a process proportional to the $X_{add}(k) = \frac{(\sqrt{\Omega_v}/2)\Lambda_{add}}{2\epsilon_k - W_{add}}$ amplitude (inset to the right), but also to states lying below the Fermi energy, a process proportional to $Y_{add}(i) = \frac{(\sqrt{\Omega_v}/2)\Lambda_{add}}{2\epsilon_i + W_{add}}$. The associated values of the particle-pairing vibration coupling strength are $\Lambda_{add} = \Lambda(\beta = +2) = 1.08$ MeV and $\Lambda_{rem} = \Lambda(\beta = -2) = 1.6$ MeV . (b) The same as above, but for the closed shell system ^{100}Sn . In this case $\Lambda_{add} = 2.72$ MeV and $\Lambda_{rem} = 5.32$ MeV .

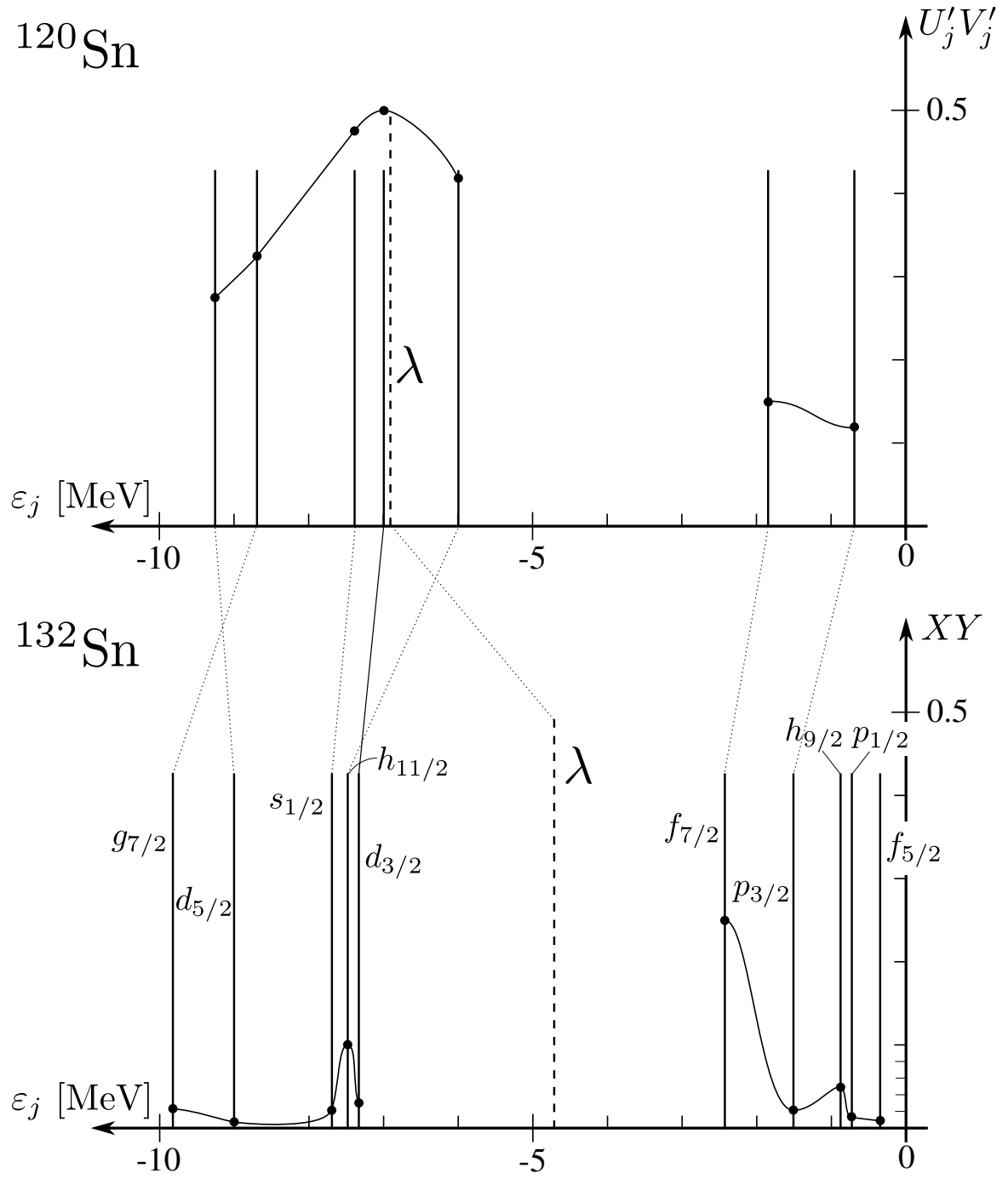


FIG. 4: (a) Value of the $U'V'$ products associated with ^{120}Sn (see Table II). (b) Value of the XY products associated with the pair addition and removal modes of ^{132}Sn (see Table III).

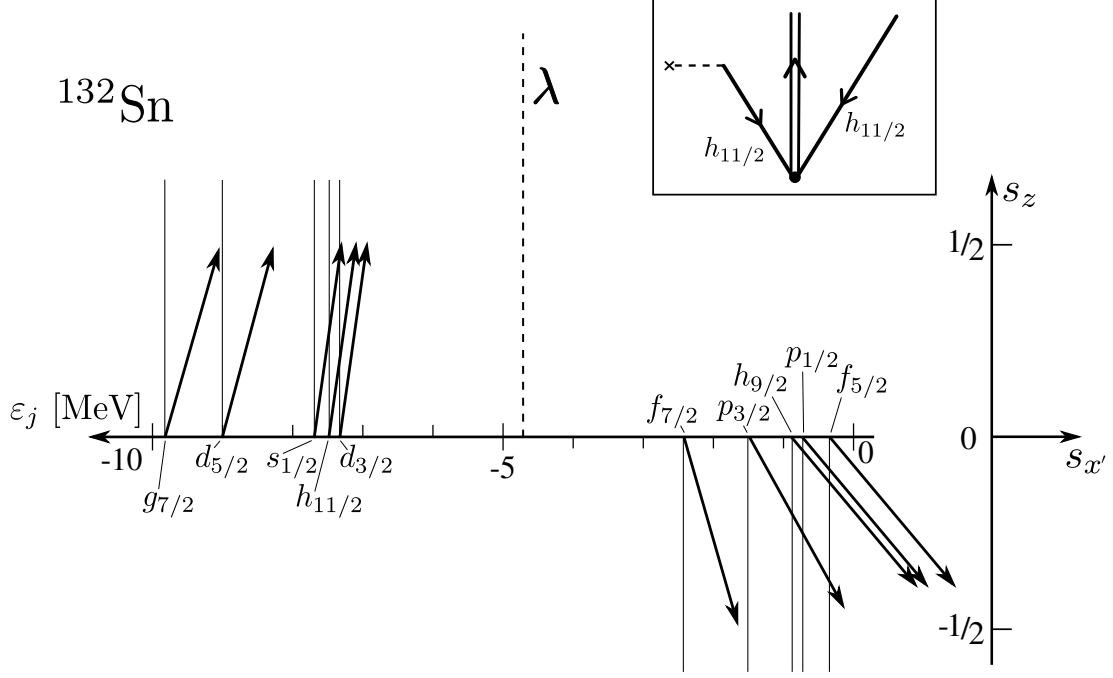


FIG. 5: Schematic representation, in terms of pairspin alignment, of the dynamical ODLRO induced in the ground state of the doubly magic nucleus ^{132}Sn , by the zero-point fluctuations (ground state correlations) associated with pair addition and pair removal of the closed shell system (for comparison with the superfluid system ^{120}Sn see Fig. A.3 of Appendix A). The pairspin states are defined in Eq. (20a) ($\epsilon_\nu < \epsilon_F$) and in Eq. (20b) ($\epsilon_\nu > \epsilon_F$), the X and Y amplitudes corresponding to Eq. (21) (see Table 3). The mean square root value of the angle of the pairspin measured from the gauge (z -)axis is fixed by the relation $\cos\tilde{\theta}_\nu = \langle s_z(\nu) \rangle / |s|$, which for occupied states is $\cos\tilde{\theta}_\nu = (1/2)/(3/4)^{1/2}$, i.e. $\tilde{\theta}_\nu = 54.5^\circ$, the average angle of the precession cone of pairspins centered around the z -axis. Pairspin states (20a) and (20b), have been calculated making use of the X, Y values reported in Table III and of $\tilde{\theta}_\nu$ similar to the above one, but which for simplicity was chosen equal to be 45° . In the orientation of the pairspin reported in the figure, this fixed angle has been subtracted. In other words, the z -axis has been rotated by 45° into the z' -axis. Within the present scenario, it is expected that one-particle transfer reactions on ^{132}Sn may e.g. excite the $h_{11/2}^{-1} \otimes gs(^{134}\text{Sn})$ $2p - 1h$ state of ^{133}Sn (see inset) with a weak, but likely observable cross section.

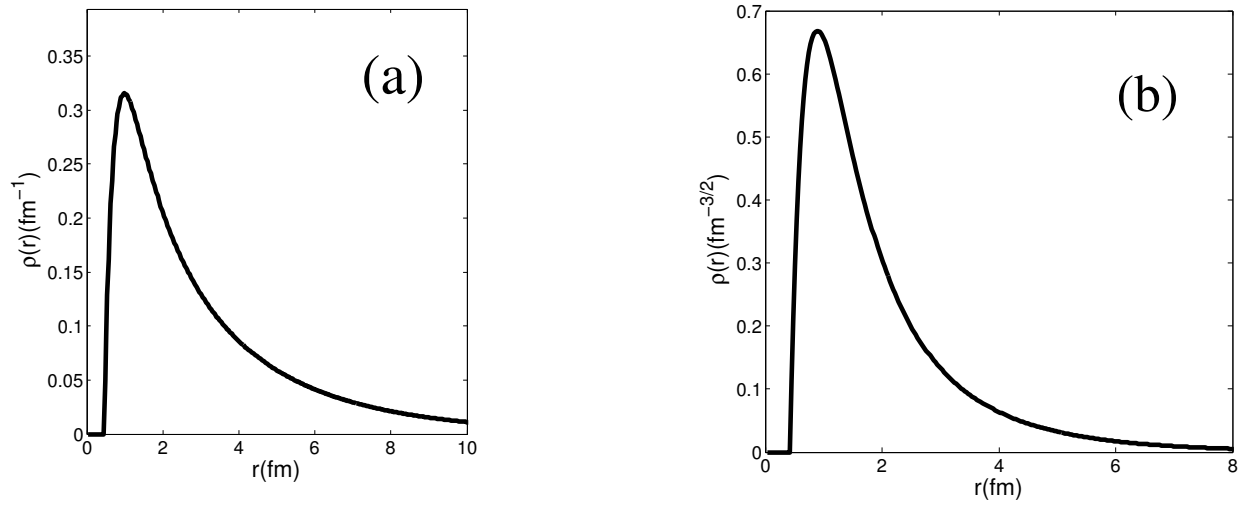


FIG. 6: (a) Radial function $\rho(r)$ (hard core 0.45 fm) entering the triton wavefunction. (b) Radial function $\rho(r)$ entering the deuteron wavefunction.

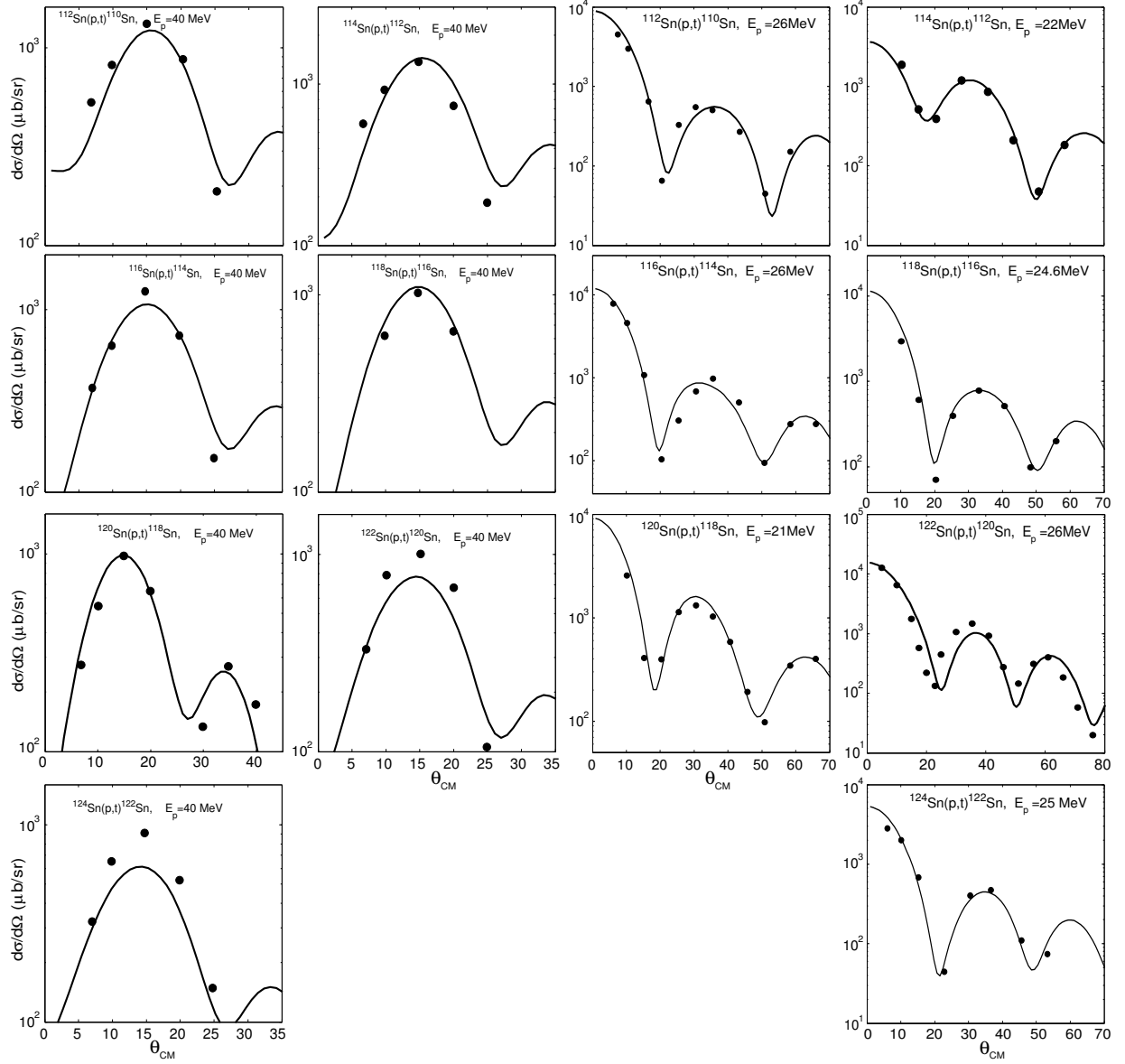


FIG. 7: Predicted absolute differential $A+^2\text{Sn}(p,t)^A\text{Sn}(gs)$ cross sections for bombarding energies $21 \text{ MeV} \leq E_p \leq 26 \text{ MeV}$, and $E_p = 40 \text{ MeV}$ in comparison with the experimental data (see [39–44] and [45] respectively).

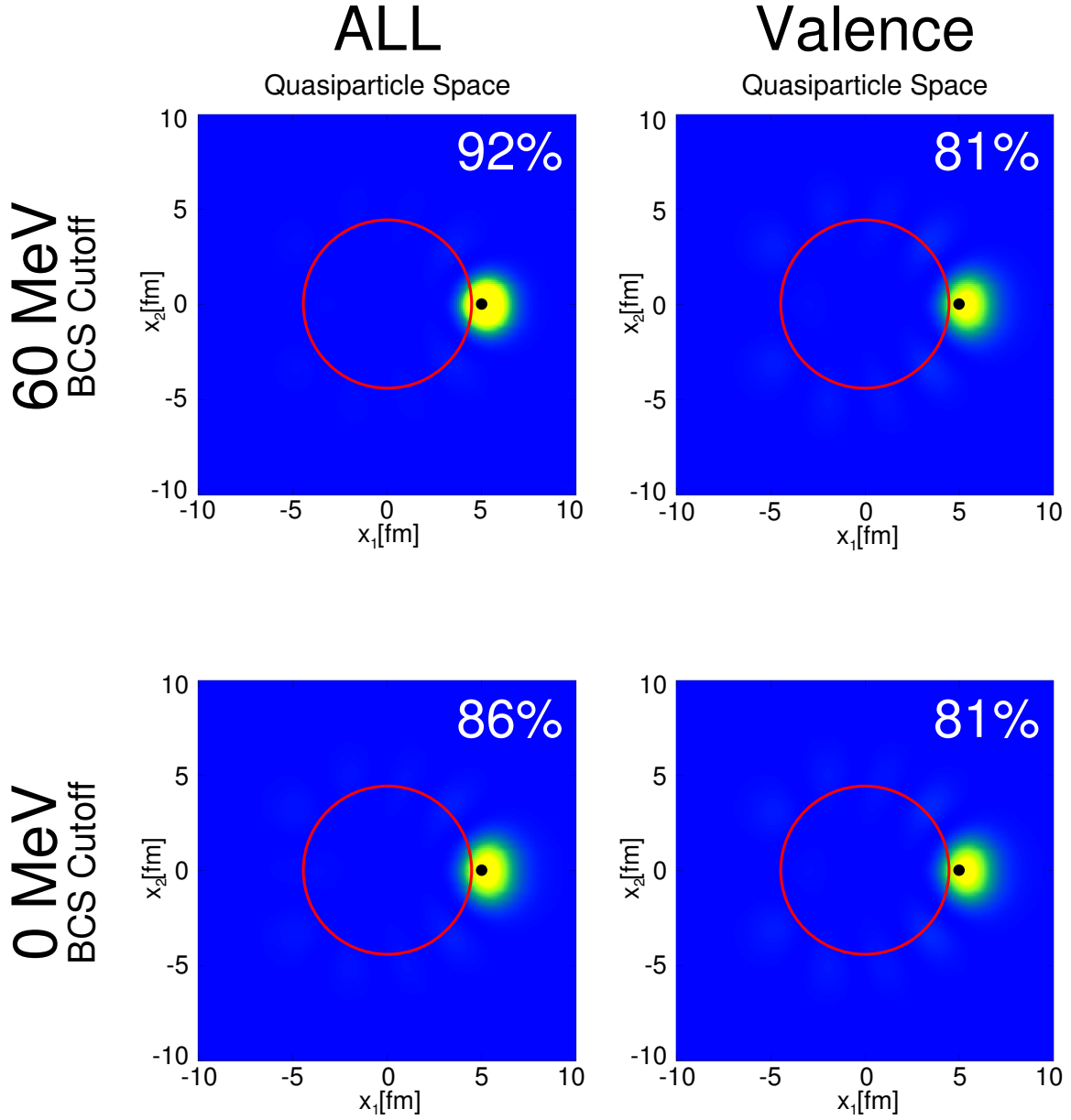


FIG. 8: (Color online) Spatial structure of a two-neutron Cooper pair of ^{120}Sn (see (B16),(B17) and (B23)). The modulus squared wavefunction $|\Psi_0(\vec{r}_1, \vec{r}_2)|^2 = |\tilde{\mathcal{O}}|\vec{r}_1, \vec{r}_2\rangle|^2$ (see Tables I and II), multiplied by $16\pi^2 r_1^2 r_2^2$ and normalized to unity, is displayed as a function of the cartesian coordinates $x_1 = r_2 \cos \theta_{12}$ and $x_2 = r_2 \sin \theta_{12}$ of particle 2, for a fixed value of $r_1 = x_1 = 5$ fm (black dot) of particle 1, close to the surface of the nucleus (red circle). The numerical percentages correspond to the two-nucleon integrated density in a spherical box of radius 4 fm centered at the coordinates of the fixed particle.

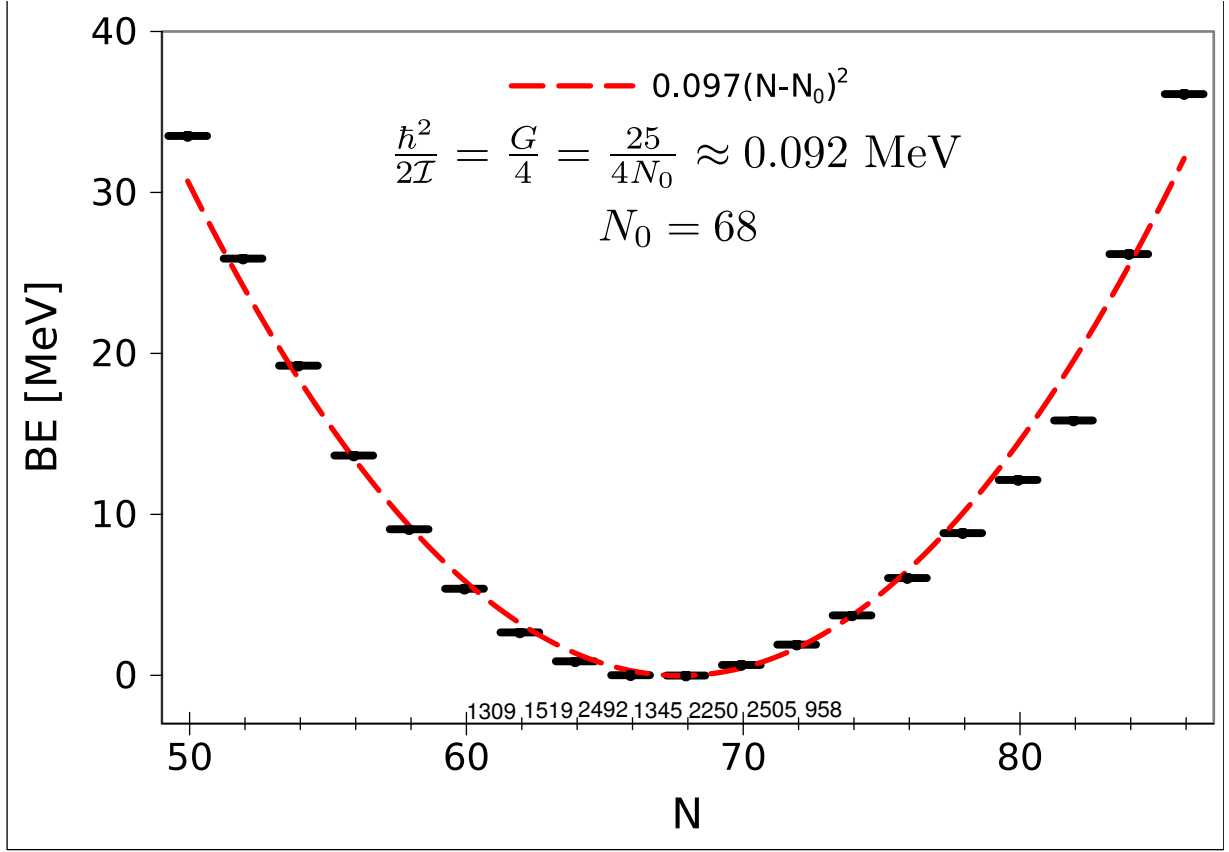


FIG. 9: (Color online) Pairing rotational band along the tin isotopes. The lines represent the energies calculated according to the expression $\Delta B = B(^{50+N}\text{Sn}_N) - 8.124N + 46.33$ [10], subtracting the contribution of the single nucleon addition to the nuclear binding energy obtained by a linear fitting of the binding energies of the whole Sn-chain. The estimate of $\hbar^2/2I$ was obtained using the single j -shell model (see e.g. [10] App. H). The numbers given on the abscissa are the absolute values of the experimental $gs \rightarrow gs$ (in units of μb ; see Table 4).

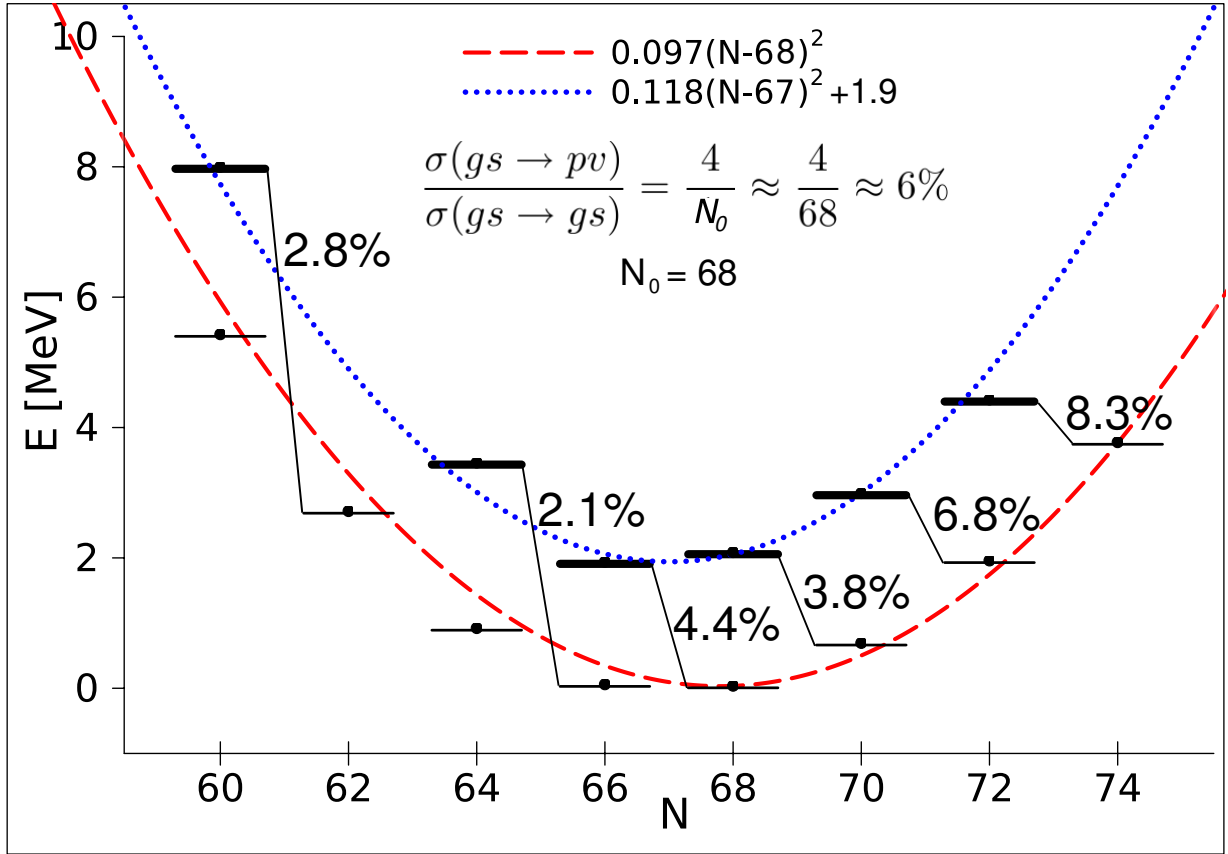


FIG. 10: (Color online) The weighted average energies ($E_{exc} = \sum_i E_i \sigma_i / \sum_i \sigma_i$) of the excited 0^+ states below 3 MeV in the Sn isotopic chain are shown on top of the pairing rotational band, already displayed in

Fig. 9. Also indicated is the percentage of cross section for two-neutron transfer to excited states, normalized to the cross sections populating the ground states. The estimate of the ratio of cross sections displayed on top of the figure was obtained making use of the single j -shell model (see e.g. [10] App. H).

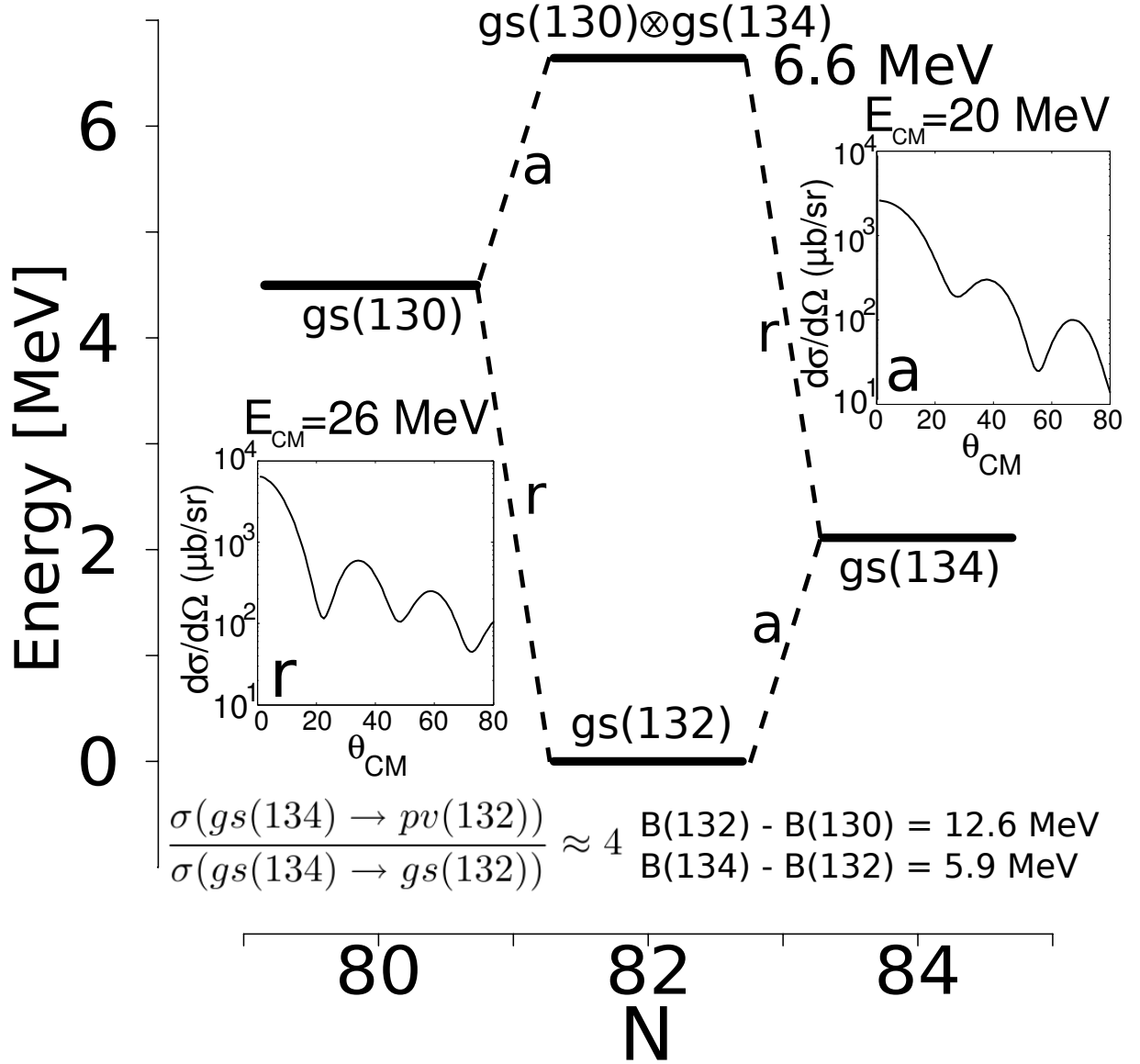


FIG. 11: Pairing vibrational scheme around ^{132}Sn and calculated absolute reaction cross sections associated with the pairing addition and removal modes. The two-nucleon transfer spectroscopic amplitudes, used in the calculation are collected in Table III. The optical model potential for the three channels, (namely $A + t \rightarrow (A + 1) + d \rightarrow (A + 2) + p$ or reversed) were taken from refs. [41] and [48].

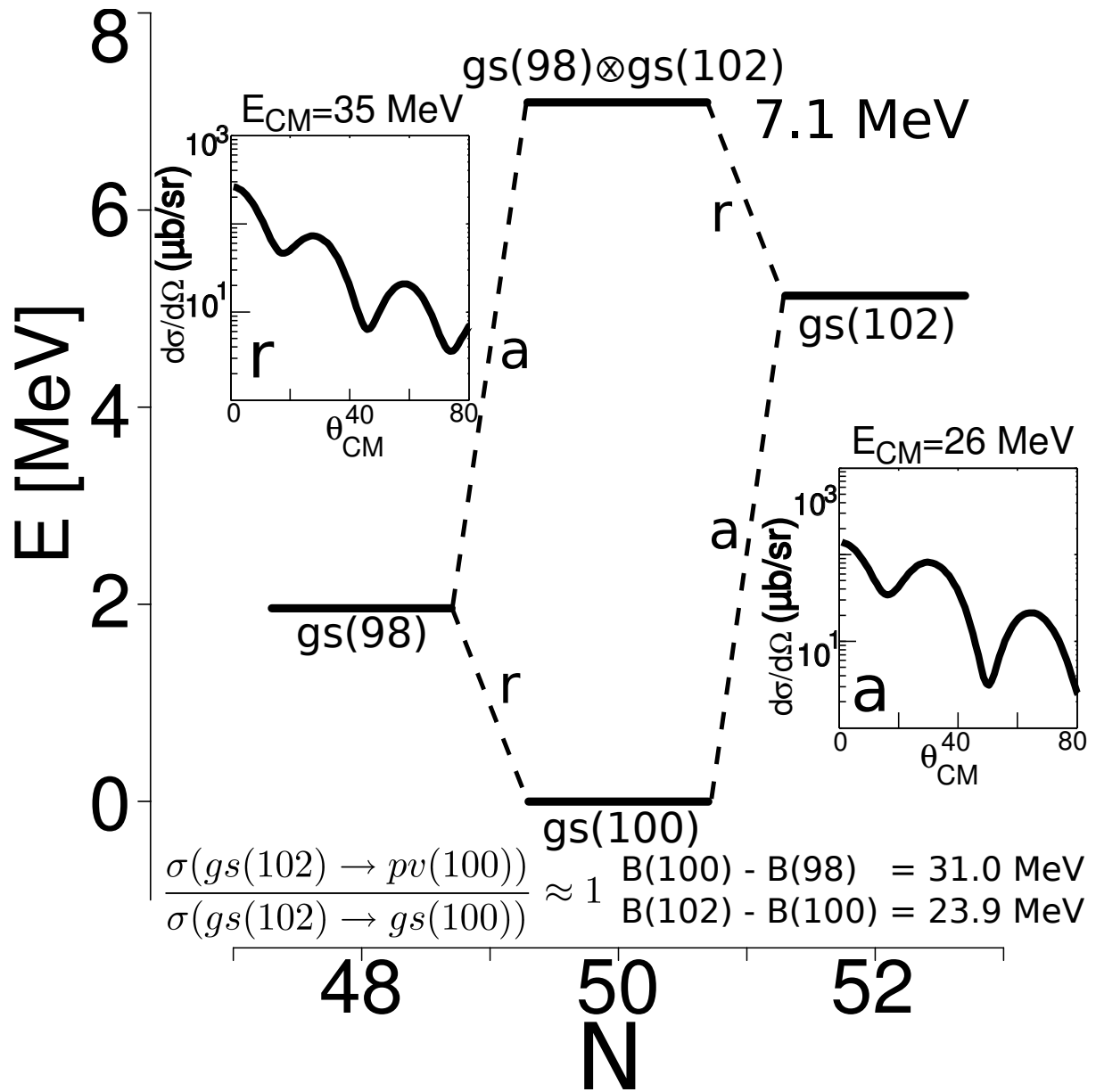


FIG. 12: Pairing vibrational scheme around ^{100}Sn and calculated absolute reaction cross sections associated with the pairing addition and removal modes. Concerning the spectroscopic amplitudes and optical parameters used in the calculations see caption to Fig.11.

Appendix A: Pair spin and domain wall

In what follows we will discuss the mean field properties of the Hamiltonian

$$H_p - \lambda N = H'_{sp} + V_p, \quad (\text{A1})$$

where

$$H'_{sp} = \sum_{\nu>0} \epsilon_\nu N_\nu, \quad (\text{A2})$$

with

$$\epsilon_\nu \equiv \varepsilon_\nu - \lambda \quad (\text{A3})$$

and

$$N_\nu = a_\nu^+ a_\nu + a_{\bar{\nu}}^+ a_{\bar{\nu}}. \quad (\text{A4})$$

The pairing interaction is defined as

$$V_p = -GP^+P, \quad (\text{A5})$$

where

$$P^+ = \sum_{\nu>0} P_\nu^+, \quad (\text{A6})$$

and

$$P_\nu^+ = a_\nu^+ a_{\bar{\nu}}^+. \quad (\text{A7})$$

The single-particle Hamiltonian H'_{sp} is invariant under time reversal operations. As a consequence, orbitals are twofold degenerate, the corresponding states being denoted $|\nu\rangle$ and $|\bar{\nu}\rangle$.

Because the operators N_ν , P_ν^+ and P_ν satisfy the commutation relations (cf. Appendix C)

$$[P_\nu^+, P_\nu] = N_\nu - 1, \quad (\text{A8})$$

$$[N_\nu - 1, P_\nu^+] = 2P_\nu^+, \quad (\text{A9})$$

and

$$[N_\nu - 1, P_\nu] = -2P_\nu, \quad (\text{A10})$$

one can define the x , y and z components of the pairspin operator $\vec{s}(\nu)$ according to the relations,

$$s_x(\nu) = \frac{1}{2} (P_\nu^+ + P_\nu) = \frac{1}{2} \begin{pmatrix} 0 & 1 \\ 1 & 0 \end{pmatrix}, \quad s_y(\nu) = \frac{1}{2i} (P_\nu^+ - P_\nu) = \frac{1}{2} \begin{pmatrix} 0 & -i \\ i & 0 \end{pmatrix}, \quad (\text{A11})$$

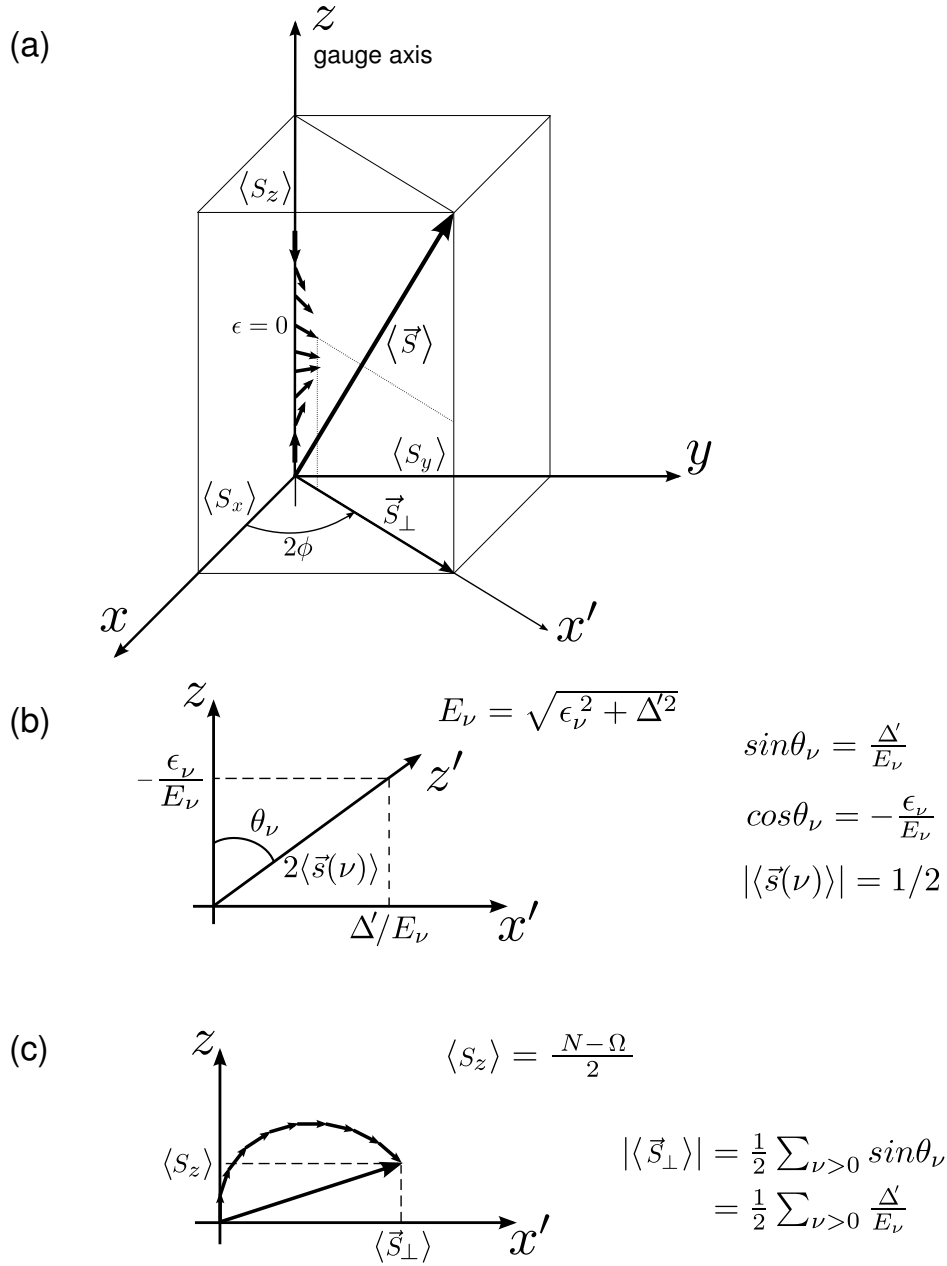


FIG. A.1: (a) In the presence of the pairing interaction, the pairspin vector $\langle \vec{S} \rangle$ acquires a component in the x, y plane. It is then possible to define an intrinsic system \mathcal{K}' , which is obtained rotating the laboratory system \mathcal{K} by the gauge angle 2ϕ around the z - (gauge) axis (positive angles correspond to counter clockwise rotations). The contributions from the individual pairspins (all lying in the (z, x') plane) are schematically shown. The perpendicular component dominates for states close to the Fermi energy ($\epsilon \approx 0$), while the pairspins associated with states far from ϵ_F are aligned along the z -axis. (b) Contribution of a pairspin associated with single-particle states of energy ϵ_ν . The pairspin vector makes an angle θ_ν with the gauge z -axis such that $\sin\theta_\nu = \Delta'/E_\nu$ and $\cos\theta_\nu = -\epsilon_\nu/E_\nu$. (c) The total pairspin vector is the sum of many individual contributions. The value of its projection on the z -axis is equal to $(N - \Omega)/2$, where N is the number of particles and Ω is the total pair degeneracy of the single-particle subspace considered to describe the system (see Eq. (B18)).

and

$$s_z(\nu) = \frac{1}{2}(N_\nu - 1) = \frac{1}{2} \begin{pmatrix} 1 & 0 \\ 0 & -1 \end{pmatrix}. \quad (\text{A12})$$

In fact, using the commutation relations (A8)-(A10) stated above one obtains (cf. Appendix C),

$$[s_x(\nu), s_y(\nu)] = i s_z(\nu), \quad (\text{A13})$$

$$[s_y(\nu), s_z(\nu)] = i s_x(\nu), \quad (\text{A14})$$

$$[s_z(\nu), s_x(\nu)] = i s_y(\nu). \quad (\text{A15})$$

Of notice that these $\vec{s} \equiv (s_x, s_y, s_z)$ operators although acting in an abstract, gauge space, are as real as the standard spin of electrons and nucleons. The z -component of pairspin pointing up means “occupied” two-fold degenerate orbitals, pairspin pointing down means ”empty”, while a pairspin pointing sidewise implies a certain phased linear combination of up and down (see Fig. 1 as well as Fig. A.1). In keeping with this scenario, the BCS ground state displays a gradual rotation, like a domain wall, of the pairspin vectors across the Fermi surface.

The eigenvectors of $s_z(\nu)$ in pairspin space are

$$|1\rangle_\nu = \begin{pmatrix} 1 \\ 0 \end{pmatrix}_\nu \equiv a_\nu^+ a_{\bar{\nu}}^+ |0\rangle_\nu \quad (\text{A16a})$$

and

$$|2\rangle_\nu = \begin{pmatrix} 0 \\ 1 \end{pmatrix}_\nu \equiv |0\rangle_\nu. \quad (\text{A16b})$$

To better clarify the meaning of state $|1\rangle_\nu$ and $|2\rangle_\nu$, let us assume to be working with a set of two-fold degenerate states ν_1, ν_2, \dots , each pair of levels connected by time reversal, e.g. $(\nu_1, \bar{\nu}_1)$. In the uncorrelated case ($G = 0$), $|1\rangle$ and $|2\rangle$ can be viewed as fully occupied or fully empty states (see Fig. A.2). That is, a two-particle (filled) and a two-hole state (empty) respectively (see. Eqs. (A.17) and (A.18) below; see also (A.22) and (A.23)). The same argumentation can be applied to each pair of $(m, -m)$ states connected by time reversal, of a general set of $(2j + 1)$ degenerate single-particle states. In other words, the system under consideration displays its pair addition and pair removal modes, at the level of individual pairs of time reversal states $(\nu, \bar{\nu})$, building blocks of which Cooper pairs are built. Within this context, it is of notice that Cooper’s model works

equally well if one thinks of it in terms of a correlated two-hole state in the Fermi sea, BCS being an extension and, in a way, a natural melting of the two views, as required by quantum mechanics (zero point fluctuations (ZPF) which, within the present context can be interpreted in terms of ground state correlations (gsc)). The quantal nature of these correlations is further evidenced by the fact that the different components enter the correlated Cooper pair in terms of probability amplitudes (see in particular (B17)).

In the basis (A.16), the operators s_x , s_y and s_z have the same matrix representation as the Pauli matrices except for a factor 1/2, that is, $\vec{\sigma} = 2\vec{s}$. The action of s_z and N on the states (A.16) is given by

$$\begin{aligned}
 s_z(\nu) \begin{pmatrix} 1 \\ 0 \end{pmatrix}_\nu &= \frac{1}{2} \begin{pmatrix} 1 & 0 \\ 0 & -1 \end{pmatrix} \begin{pmatrix} 1 \\ 0 \end{pmatrix}_\nu = 1/2 \begin{pmatrix} 1 \\ 0 \end{pmatrix}_\nu ; \\
 s_z(\nu) \begin{pmatrix} 0 \\ 1 \end{pmatrix}_\nu &= \frac{1}{2} \begin{pmatrix} 1 & 0 \\ 0 & -1 \end{pmatrix} \begin{pmatrix} 0 \\ 1 \end{pmatrix}_\nu = -1/2 \begin{pmatrix} 0 \\ 1 \end{pmatrix}_\nu ; \\
 N_\nu \begin{pmatrix} 1 \\ 0 \end{pmatrix}_\nu &= \begin{pmatrix} 2 & 0 \\ 0 & 0 \end{pmatrix} \begin{pmatrix} 1 \\ 0 \end{pmatrix}_\nu = 2 \begin{pmatrix} 1 \\ 0 \end{pmatrix}_\nu \\
 N_\nu \begin{pmatrix} 0 \\ 1 \end{pmatrix}_\nu &= \begin{pmatrix} 2 & 0 \\ 0 & 0 \end{pmatrix} \begin{pmatrix} 0 \\ 1 \end{pmatrix}_\nu = 0.
 \end{aligned} \tag{A17}$$

Inverting the relations (A11), the pair operators P^+ and P can be identified with the raising and lowering operator in pairspace. In fact,

$$P^+ = \sum_{\nu>0} (s_x(\nu) + i s_y(\nu)) = S_x + i S_y \equiv S_+, \tag{A18}$$

and

$$P = \sum_{\nu>0} (s_x(\nu) - i s_y(\nu)) = S_x - i S_y \equiv S_-. \tag{A19}$$

In this space, i.e. the space subtended by the states $|1\rangle_\nu$ and $|2\rangle_\nu$, the operators $S_+(\nu)$ and $S_-(\nu)$ are represented by the matrices

$$\langle i | S_+(\nu) | j \rangle = \begin{pmatrix} \langle 1 | P_\nu^+ | 1 \rangle & \langle 1 | P_\nu^+ | 2 \rangle \\ \langle 2 | P_\nu^+ | 1 \rangle & \langle 2 | P_\nu^+ | 2 \rangle \end{pmatrix} = \begin{pmatrix} 0 & 1 \\ 0 & 0 \end{pmatrix}, \tag{A20}$$

$$(\langle i|S_-(\nu)|j\rangle) = \begin{pmatrix} \langle 1|P_\nu|1\rangle & \langle 1|P_\nu|2\rangle \\ \langle 2|P_\nu|1\rangle & \langle 2|P_\nu|2\rangle \end{pmatrix} = \begin{pmatrix} 0 & 0 \\ 1 & 0 \end{pmatrix}, \quad (\text{A21})$$

while

$$(\langle i|N(\nu) - 1|j\rangle) = \begin{pmatrix} \langle \nu\bar{\nu}|(N_\nu - 1)|\nu\bar{\nu}\rangle & \langle \nu\bar{\nu}|(N_\nu - 1)|0\rangle \\ \langle 0|(N_\nu - 1)|\nu\bar{\nu}\rangle & \langle 0|(N_\nu - 1)|0\rangle \end{pmatrix} = \begin{pmatrix} 1 & 0 \\ 0 & -1 \end{pmatrix}. \quad (\text{A22})$$

Consequently

$$P_\nu^+ \begin{pmatrix} 0 \\ 1 \end{pmatrix}_\nu = \begin{pmatrix} 0 & 1 \\ 0 & 0 \end{pmatrix} \begin{pmatrix} 0 \\ 1 \end{pmatrix}_\nu = \begin{pmatrix} 1 \\ 0 \end{pmatrix}_\nu \quad ; \quad P_\nu^+ \begin{pmatrix} 1 \\ 0 \end{pmatrix}_\nu = \begin{pmatrix} 0 & 1 \\ 0 & 0 \end{pmatrix} \begin{pmatrix} 1 \\ 0 \end{pmatrix}_\nu = 0, \quad (\text{A23})$$

while

$$P_\nu \begin{pmatrix} 0 \\ 1 \end{pmatrix}_\nu = \begin{pmatrix} 0 & 0 \\ 1 & 0 \end{pmatrix} \begin{pmatrix} 0 \\ 1 \end{pmatrix}_\nu = 0 \quad , \quad P_\nu \begin{pmatrix} 1 \\ 0 \end{pmatrix}_\nu = \begin{pmatrix} 0 & 0 \\ 1 & 0 \end{pmatrix} \begin{pmatrix} 1 \\ 0 \end{pmatrix}_\nu = \begin{pmatrix} 0 \\ 1 \end{pmatrix}_\nu. \quad (\text{A24})$$

The total pairspin in the z -direction is closely related to the number operator

$$S_z = \sum_{\nu>0} s_z(\nu) = \frac{1}{2}(N - \Omega), \quad (\text{A25})$$

where $N = \sum_{\nu>0} N_\nu$, and Ω is the total number of two-fold degenerated single-particle orbitals, associated with the single-particle space considered. Within this context, see Eq. (B18).

The two terms of the pairing Hamiltonian can now be rewritten, as

$$H'_{sp} = \sum_{\nu>0} \epsilon_\nu N_\nu = \sum_{\nu>0} \epsilon_\nu (1 + 2s_z(\nu)), \quad (\text{A26})$$

and

$$\begin{aligned} V_p &= - \sum_{\nu_1, \nu_2>0} G P_{\nu_1}^+ P_{\nu_2} \\ &= -G \left[\sum_{\nu_1>0} s_x(\nu_1) \sum_{\nu_2>0} s_x(\nu_2) + \sum_{\nu_1>0} s_y(\nu_1) \sum_{\nu_2>0} s_y(\nu_2) \right] - G \sum_{\nu_1>0} s_z(\nu_1) \\ &= -G \sum_{\nu_1, \nu_2>0} (\vec{s}_\perp(\nu_1) \cdot \vec{s}_\perp(\nu_2)) - G \sum_{\nu_1>0} s_z(\nu_1), \end{aligned} \quad (\text{A27})$$

where $s_\perp(\nu) = s_x(\nu)\hat{i} + s_y(\nu)\hat{j}$, \hat{i} and \hat{j} being unit vectors along the x - and y - directions. The last term is the contribution of the pairing interaction to the single-particle mean field H_{sp} . Although it can easily be incorporated in this term, it is customary to neglect it, in keeping with the

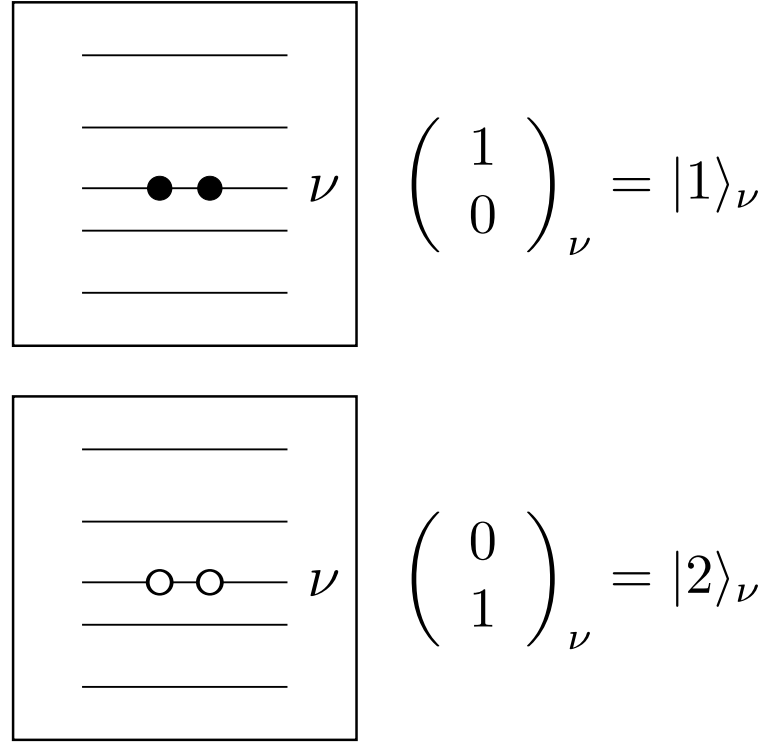


FIG. A.2: Schematic representation of the eigenvectors of $s_z(\nu)$ in pairspin space: states $|1\rangle_\nu$ and $|2\rangle_\nu$ can be viewed as a pair addition and a pair removal mode, at the level of individual pairs of time reversal states $(\nu, \bar{\nu})$.

schematic nature of V_p , tailored to act on the pair space. On the other hand, this contribution is to be considered when comparing the solution of schematic models with exact solutions (see e.g. [59],[60]).

The interaction V_p is a spin-spin coupling, which seeks to align the transverse components of the pairspins. Was it not for H_{sp} , which depends on S_z , all pairspins would line up in the same direction (strong coupling limit), perpendicular to the z -axis, in keeping with the fact that V_p is a function of only the S_x and S_y pairspin operator. In the opposite limit, that is, for $V_p = 0$, pairspin alignment is zero, that is, there is no component of the pairspin in the (x, y) plane perpendicular to the z -axis (see Fig. 1(a)). From this figure it is clear that H_{sp} counteracts pair spin alignment. Indeed H_{sp} plays, in the nucleus, the role of a magnetic field in a solid, which tends to align the spins in the z -direction, or opposite to it, with a strength (as measured by ε_ν) that increases in absolute value as a function of the energy of the twofold degenerate levels $(\nu, \bar{\nu})$ away from the Fermi energy $\varepsilon_F = \lambda$. Thus, for sufficiently large values of $|\varepsilon_\nu - \varepsilon_F|$, of the order of 2Δ (2-3

MeV), the single-particle energy as measured by H_{sp} dominates (see Fig. 1 as well as Fig. A.1(a) and A.3). This is also the reason why calculations of pairing correlations in nuclei, which depend on small contributions arising from orbitals distant from the Fermi energy are to be handled with care, in particular when comparing the calculated results with the experimental findings. Within this context see Sect. IV A, discussion connected with $\alpha'_0(\vec{r}_1, \vec{r}_2)$. Close to the Fermi energy, V_p is the overriding effect, and a large transverse pairspin is expected, as testified by the coherent sums in Eq. (A27). While any single pairspin in these sums displays large quantal fluctuations, the total pairspin has a well defined magnitude and orientation, since the fluctuations of the constituent pairspins add quadratically.

The pairing Hamiltonian can be diagonalized in the mean field approximation, substituting one of the sums in Eq. (A27) with its average value in the mean field ground state. Let us assume that the average value of the pairspin polarization vector $|\langle \vec{S}_\perp \rangle| = \mathcal{K}' \langle BCS | S_\perp | BCS \rangle \mathcal{K}'$ (see. Eq. A51 below) is non-zero, and choose a definite orientation for it in the $x - y$ plane (denoted x'), subtending an angle 2ϕ with the x - axis (definition of the body-fixed, intrinsic frame, see Fig. A.1). The pair interaction is then replaced by a mean field, namely the pair field of strength $\Delta' \equiv G|\langle \vec{S}_\perp \rangle|$. One can then write,

$$\begin{aligned} U_p &= -2G|\langle \vec{S}_\perp \rangle| \sum_{\nu>0} [s_x(\nu)\cos 2\phi + s_y(\nu)\sin 2\phi] \\ &= -2\Delta' \sum_{\nu>0} [s_x(\nu)\cos 2\phi + s_y(\nu)\sin 2\phi]. \end{aligned} \quad (\text{A28})$$

Making use of the relation given in (A11) one finds,

$$\Delta'(s_x(\nu)\cos 2\phi + s_y(\nu)\sin 2\phi) = \frac{1}{2} (P_\nu^\dagger \Delta' e^{-2i\phi} + P_\nu \Delta' e^{2i\phi}) = \frac{1}{2} (P_\nu^\dagger \Delta + P_\nu \Delta^*), \quad (\text{A29})$$

where we have introduced $\Delta = e^{-2i\phi} \Delta'$. Consequently,

$$U_p = -\Delta' \sum_{\nu>0} (P_\nu^{\dagger'} + P_\nu') = - \sum_{\nu>0} (P_\nu^\dagger \Delta + P_\nu \Delta^*), \quad (\text{A30})$$

P'^\dagger, P' denoting the operators in the body-fixed frame of axis (x', y') (cf. Fig. A.1(a) and Appendix B) in which by definition $\phi = 0$, that is $\langle S'_y \rangle = 0$ and $\langle S'_x \rangle = \langle S'_\perp \rangle = \alpha'_0$.

The total Hamiltonian then becomes a sum over individual pairspins,

$$(H_p)_{MF} = \sum_{\nu>0} h_\nu, \quad (\text{A31})$$

where

$$h_\nu = \epsilon_\nu + \epsilon_\nu \begin{pmatrix} 1 & 0 \\ 0 & -1 \end{pmatrix} - \Delta' \begin{pmatrix} 0 & \cos 2\phi - i \sin 2\phi \\ \cos 2\phi + i \sin 2\phi & 0 \end{pmatrix}. \quad (\text{A32})$$

It is of notice that thinking in terms of the independent (quasiparticle) densities the first term is connected with the normal and the second with the so called abnormal density respectively, leading to ODLRO.

Within this context, in the mean field associated with the (diagonal) first term of the above equation (see also Eq. (A.2)), the particles which move independently of each other, are nucleons. In order that this can happen, all the nucleons must participate in a highly coherent ballet following a refined coreography, in such a way that each dancer moves as if he was alone in the scene, being fenced-in through a dancers-like wall, only when approaching the edges of the scene. As it has been stated in the literature [61], it is a "rather unfortunate perversity" which views independent particle motion as antithetic to nuclear collective motion.

In the case of the mean field described by the second term of Eq. (A32), the entities which play the role of nucleons in the case above, are now pairspins (pair addition and pair removal ($\nu, \bar{\nu}$ modes)). The only circumstance in which pairspins feel the pushings and pullings of the other pairspins, is when they try to adopt a different orientation but that defined by S_\perp (i.e. x' -direction, see Fig. A.1), being forced to align back by a domain wall. In the present case, the ballet is not performed by single dancers in a scene, but by couples in a crowded dancing hall. In spite of such a less cultured setup, the coreography is even more refined than previously described. This is because the partners of each dancing couple can, not only when close to each other, but also when finding themselves at opposite extremes of the dancing hall (coherence length), follow the other partners moves without missing a single step. Such a coreography of strongly overlapping pairs translates, in the gauge (pairspin) space, into the definition of a privileged orientation.

This can be better seen by expressing the diagonalization condition (4), namely

$$\sum_{\nu>0} \epsilon_\nu N_\nu - \Delta' (P'^\dagger + P') + \frac{\Delta'^2}{G} = \sum_{\nu>0} E_\nu \tilde{N}_\nu + \text{const} \quad (\text{A33a})$$

in terms of the quasispin operators (A11) (A12) and

$$s_{z'}(\nu) = -\frac{1}{2}(\tilde{N}_\nu - 1). \quad (\text{A33b})$$

That is,

$$\sum_{\nu>0} [\epsilon_\nu 2s_{z'}(\nu) - \Delta' 2s_x(\nu)] + \sum_{\nu>0} (\epsilon_\nu - E_\nu) + \frac{\Delta'^2}{G} = - \sum_{\nu>0} E_\nu 2s_{z'}(\nu) + \text{const}. \quad (\text{A33c})$$

In a similar way in which $s_z(\nu)$ is diagonal in the independent (pair) particle situation, $s_{z'}(\nu)$ is diagonal in the quasiparticle representation, with eigenvalues $1/2$ when acting on the corresponding occupied states ($|HF\rangle$ and $|BCS\rangle$ states respectively), and $-1/2$ when acting on the corresponding unoccupied states (levels above ϵ_F and two quasiparticle states respectively). Equating the (quasispin) operator terms and the c-number terms one obtains

$$const = \sum_{\nu>0} (\epsilon_\nu - E_\nu) + \frac{\Delta'^2}{G}, \quad (\text{A34a})$$

and

$$-\frac{\epsilon_\nu}{E_\nu} s_z(\nu) + \frac{\Delta'}{E_\nu} s_x(\nu) = s_{z'}(\nu). \quad (\text{A34b})$$

The above equation determines the angle θ_ν in the $z-x$ plane, which leads to independent quasispin motion. In the strong coupling limit ($|\Delta'| \gg |\epsilon_\nu - \lambda|$), "magnetization" is total, all pairspins (pair addition and removal $(\nu, \bar{\nu})$ pairs) pointing along the x - direction.

As already stated in connection with Eq. (4) of the text, the c-number $const$ is equal to the ground state energy, also known as the U term of $(H_p)_{MF}$ (see e.g. [10] Eq. (G.11) of App. G; see also below, subsection on ground state energy and pairing correlation energy).

In keeping with the fact that the quasispin states are normalized, and that one has chosen a representation in which $s_y(\nu) = 0$, the quasispin prefactors of Eq. (A34b) must fulfill the relation,

$$\left(-\frac{\epsilon_\nu}{E_\nu}\right)^2 + \frac{\Delta'^2}{E_\nu^2} = 1. \quad (\text{A35})$$

It is of notice that the eigenvalue equation (A32),

$$\epsilon_\nu - \begin{pmatrix} -\epsilon_\nu & \Delta' e^{-2i\phi} \\ \Delta' e^{2i\phi} & \epsilon_\nu \end{pmatrix} \begin{pmatrix} V_\nu \\ U_\nu \end{pmatrix} = (\epsilon_\nu - E) \begin{pmatrix} V_\nu \\ U_\nu \end{pmatrix}, \quad (\text{A36})$$

has the solutions $\pm E_\nu$, where (see also (A35))

$$E_\nu = \sqrt{\epsilon_\nu^2 + \Delta'^2}. \quad (\text{A37})$$

The positive sign corresponds to the lowest total pairspin energy ($\epsilon_\nu - E_\nu$), while the negative sign corresponds to the excited states (2-quasiparticle states, cf. subsection below on excited states). The relation between the U_ν and the V_ν components of the eigenvector can be deduced from equation (A36),

$$-\epsilon_\nu V_\nu + \Delta' e^{-2i\phi} U_\nu = E_\nu V_\nu \quad (\text{A38})$$

$$\Delta' e^{-2i\phi} V_\nu + \epsilon_\nu U_\nu = E_\nu U_\nu. \quad (\text{A39})$$

Eq.(A38) leads to $(E_\nu + \epsilon_\nu)V_\nu = \Delta' e^{-2i\phi} U_\nu$, implying a phase difference -2ϕ between the V_ν and the U_ν occupation amplitudes, This allows one to write the following relations

$$U_\nu = U'_\nu e^{i\phi}, \quad (\text{A40})$$

$$V_\nu = V'_\nu e^{-i\phi}, \quad (\text{A41})$$

with U'_ν and V'_ν being the moduli of U_ν and V_ν respectively. These quantities can be calculated from the square modulus of Eq. (A38)

$$(\epsilon_\nu + E_\nu)^2 |V_\nu|^2 = \Delta'^2 |U_\nu|^2. \quad (\text{A42})$$

Making use of the normalization relation $|V_\nu|^2 = 1 - |U_\nu|^2$, one obtains

$$\begin{aligned} U_\nu'^2 &= \frac{1}{2} \left(1 + \frac{\epsilon_\nu}{E_\nu} \right), \\ V_\nu'^2 &= \frac{1}{2} \left(1 - \frac{\epsilon_\nu}{E_\nu} \right). \end{aligned} \quad (\text{A43})$$

Defining the angle θ_ν according to

$$\cos\theta_\nu = -\frac{\epsilon_\nu}{E_\nu}, \quad \sin\theta_\nu = \frac{\Delta'}{E_\nu}, \quad (\text{A44})$$

one can rewrite the quasiparticle amplitudes as

$$U'_\nu = \sin(\theta_\nu/2), \quad V'_\nu = \cos(\theta_\nu/2), \quad (\text{A45})$$

where the angle θ_ν represents the angle between the direction of $\vec{s}(\nu)$ (z' -axis in Fig. A.1(b)) and the z -axis. The average value of $s_x(\nu)$, $s_y(\nu)$ calculated with these eigenfunctions, generalizations of the eigenvectors introduced before (see Eqs. (A16a) and (A16b)), are given by

$$\begin{aligned} \langle s_x(\nu) \rangle &= (V_\nu^*, U_\nu^*) s_x(\nu) \begin{pmatrix} V_\nu \\ U_\nu \end{pmatrix} = \frac{1}{2} (U_\nu V_\nu^* + V_\nu U_\nu^*) \\ &= \sin \frac{\theta_\nu}{2} \cos \frac{\theta_\nu}{2} \cos 2\phi = U'_\nu V'_\nu \cos 2\phi = \frac{\Delta'}{2E_\nu} \cos 2\phi, \end{aligned} \quad (\text{A46})$$

$$\begin{aligned} \langle s_y(\nu) \rangle &= (V_\nu^*, U_\nu^*) s_y(\nu) \begin{pmatrix} V_\nu \\ U_\nu \end{pmatrix} = \frac{i}{2} (U_\nu V_\nu^* - V_\nu^* U_\nu) \\ &= \sin \frac{\theta_\nu}{2} \cos \frac{\theta_\nu}{2} \sin 2\phi = U'_\nu V'_\nu \sin 2\phi = \frac{\Delta'}{2E_\nu} \sin 2\phi, \end{aligned} \quad (\text{A47})$$

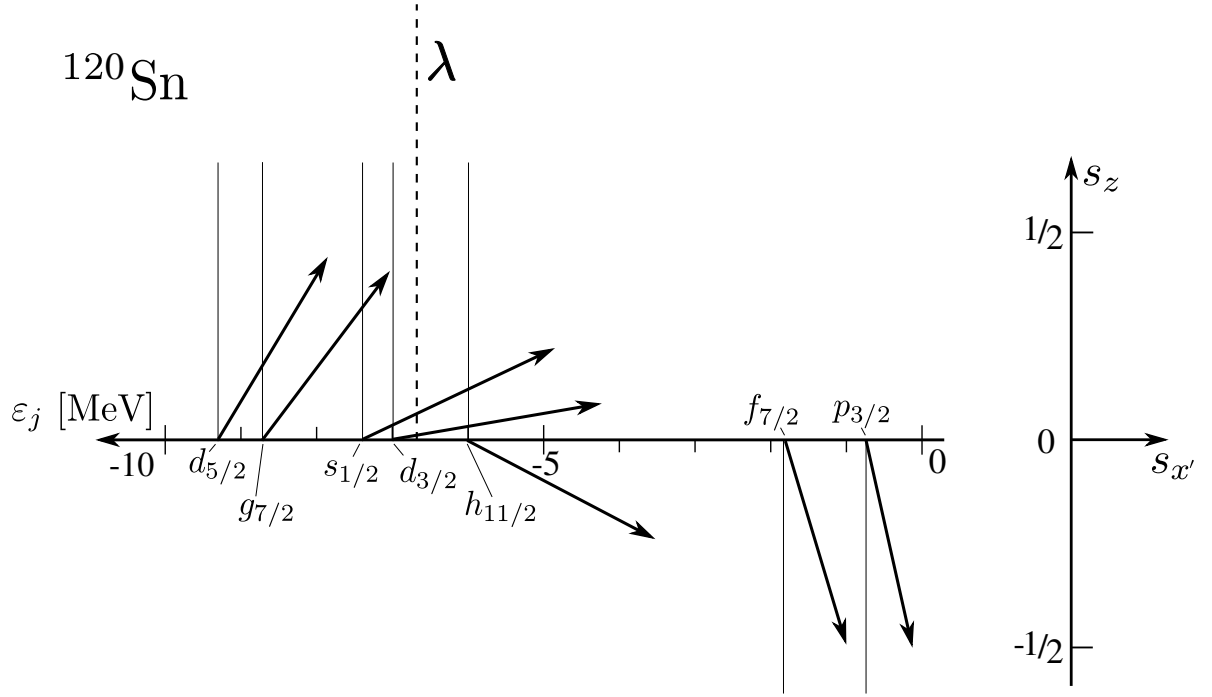


FIG. A.3: Pairspin distribution associated with the seven valence single-particle orbitals lying around the Fermi energy of ^{120}Sn . The calculations were carried out making use of the results displayed in Table II, in particular the values $U'_\nu V'_\nu$, following the prescription discussed in the caption to Fig. 5.

and

$$\begin{aligned} \langle s_z(\nu) \rangle &= (V_\nu^*, U_\nu^*) s_z(\nu) \begin{pmatrix} V_\nu \\ U_\nu \end{pmatrix} = \frac{1}{2} (V_\nu V_\nu^* - U_\nu^* U_\nu) \\ &= \frac{1}{2} \left(\cos^2 \frac{\theta_\nu}{2} - \sin^2 \frac{\theta_\nu}{2} \right) = -\frac{1}{2} (U_\nu'^2 - V_\nu'^2) = -\frac{\varepsilon_\nu}{2E_\nu}. \end{aligned} \quad (\text{A48})$$

The dependence of $\langle s_x(\nu) \rangle$ and $\langle s_y(\nu) \rangle$ on the the angle ϕ is consistent with the ansatz (A28). Furthermore, making use of Eq. (A47), one can determine the modulus of S_\perp selfconsistently

$$|\sum_{\nu>0} \langle \vec{s}_\perp(\nu) \rangle| = |\langle \vec{S}_\perp \rangle| = \sum_{\nu>0} \left[\cos \frac{\theta_\nu}{2} \sin \frac{\theta_\nu}{2} \right] = \sum_{\nu>0} U'_\nu V'_\nu = \alpha'_0, \quad (\text{A49})$$

a relation which is closely connected with the BCS gap equation. In Fig. A.3 the pairspin distribution associated with the valence orbitals of ^{120}Sn , calculated making use of the results collected in Table II and the scheme discussed in the caption to Fig. 5, is displayed.

The wavefunction describing the ground state of the system is the product of all pairspins,

each of which is a linear combination of the pair addition and removal $(\nu, \bar{\nu})$ modes with the corresponding weights V_ν and U_ν respectively, amplitudes which define their alignment in gauge space. That is,

$$\begin{aligned} \prod_{\nu>0} (U_\nu |2\rangle_\nu + V_\nu |1\rangle_\nu) &= \prod_{\nu>0} \left(U_\nu \begin{pmatrix} 0 \\ 1 \end{pmatrix} + V_\nu \begin{pmatrix} 1 \\ 0 \end{pmatrix} \right) = \prod_{\nu>0} (U_\nu + V_\nu a_\nu^\dagger a_{\bar{\nu}}^\dagger) |0\rangle = \\ &= \prod_{\nu>0} (e^{i\phi} U'_\nu + e^{-i\phi} V'_\nu a_\nu^\dagger a_{\bar{\nu}}^\dagger) |0\rangle = e^{i\Omega\phi} \prod_{\nu>0} (U'_\nu + V'_\nu e^{-2i\phi} a_\nu^\dagger a_{\bar{\nu}}^\dagger) |0\rangle. \end{aligned} \quad (\text{A50})$$

Leaving out the overall phase one can write

$$\begin{aligned} |BCS(\phi)\rangle_{\mathcal{K}} &= \prod_{\nu>0} (U'_\nu + V'_\nu e^{-2i\phi} a_\nu^\dagger a_{\bar{\nu}}^\dagger) |0\rangle = \\ &= \prod_{\nu>0} (U'_\nu + V'_\nu a_\nu'^\dagger a_{\bar{\nu}}'^\dagger) |0\rangle = |BCS(\phi=0)\rangle_{\mathcal{K}'}, \end{aligned} \quad (\text{A51})$$

where \mathcal{K} and \mathcal{K}' denote the laboratory and the body-fixed, intrinsic frame in which by definition has $\phi = 0$ (see Fig. B.1).

The creation operator in the intrinsic, body-fixed frame of reference is

$$a_\nu'^\dagger = \mathcal{G} a_\nu^\dagger \mathcal{G}^{-1} = e^{-i\phi} a_\nu^+, \quad (\text{A52})$$

where $\mathcal{G} = e^{-iN\phi}$ is the gauge operator inducing rotations in the two-dimensional gauge space. The quantities U'_ν and V'_ν are real.

In the independent particle limit, that is,

$$\begin{aligned} \lim_{\Delta \rightarrow 0} \prod_{\nu>0} (U_\nu + V_\nu a_\nu^\dagger a_{\bar{\nu}}^\dagger) |0\rangle &= \prod_{\nu>0, \nu < \nu_F} a_\nu^+ a_{\bar{\nu}}^+ |0\rangle = a_{\nu_1}^+ a_{\bar{\nu}_1}^+ a_{\nu_2}^+ a_{\bar{\nu}_2}^+ \dots a_{\nu_N}^+ a_{\bar{\nu}_N}^+ |0\rangle \\ &= \frac{1}{\sqrt{2N!}} \det(1 \bar{1}, 2 \bar{2} \dots N \bar{N}) |0\rangle, \end{aligned} \quad (\text{A53})$$

as expected.

Summing up, the instability of the Fermi surface associated with transverse pairspin polarization is associated with a many-body wavefunction, product of the individual pairspin states,

$$|0\rangle_\nu = U_\nu |s_z(\nu) = -1/2\rangle + V_\nu |s_z(\nu) = +1/2\rangle = U_\nu |2\rangle_\nu + V_\nu |1\rangle_\nu, \quad (\text{A54})$$

superposition of pairspin up and down and therefore non axially symmetric with respect to the gauge axis (z -axis). In other words, a linear combination of pair addition and subtraction modes mixed at the level of individual pairs of time-reversal states $(\nu, \bar{\nu})$ (see Fig. A.2). In the same way

as $|^{208}\text{Pb}(gs)\rangle$ spends part of the time in the state $|^{210}\text{Pb}(gs)\rangle$ and part in $|^{206}\text{Pb}(gs)\rangle, |^{120}\text{Sn}(gs)\rangle$ is a mixture of pair addition and removal states $|1\rangle$ and $|2\rangle$, respectively. The transverse polarization - which inherently breaks gauge symmetry - arises from such a superposition, a phenomenon which is produced by the action of the “external” mean pair field U_p .

The pairspin polarization may rotate collectively about the z -gauge axis. The azimuthal angle is therefore a dynamical variable (pairing rotations). The static pair field constitutes a deformation that defines an orientation. Through this deformation, the system spontaneously breaks away from axial symmetry, and the indeterminacy in the number of particles in a pair correlated state is an inherent feature of this symmetry breaking. The static deformation introduces a collective degree of freedom ϕ and gives the system the ability to rotate as a whole around the gauge axis.

When the mean field solution leads to $\langle \vec{S}_\perp \rangle = 0$, the intrinsic motion has axial symmetry and hence conserves particle number. In these systems, gauge invariance can also be broken dynamically, a phenomenon which gives rise to the pairing vibrational spectrum observed around closed shell nuclei, in terms of highly enhanced, single Cooper pair tunneling processes.

Excited states

The BCS equation in the body-fixed frame,

$$\begin{pmatrix} \epsilon_v & -\Delta' \\ -\Delta' & -\epsilon_v \end{pmatrix} \begin{pmatrix} V'_v \\ U'_v \end{pmatrix} = -E \begin{pmatrix} V'_v \\ U'_v \end{pmatrix}, \quad (\text{A55})$$

leads to the eigenvalue equation

$$(\epsilon_v + E)(\epsilon_v - E) - \Delta'^2 = 0, \quad (\text{A56})$$

with eigenvalues $E_v = \sqrt{\epsilon_v^2 + \Delta'^2}$, corresponding to the ground state previously considered (cf. Eq. (A37)) and $-E_v$, corresponding to excited states. The associated eigenvectors are

$$|gs\rangle = \begin{pmatrix} V'_v \\ U'_v \end{pmatrix}, \quad |exc\rangle = \begin{pmatrix} U'_v \\ -V'_v \end{pmatrix}. \quad (\text{A57})$$

The state $|exc\rangle$ is a two-quasiparticle state. It can be excited acting with $\alpha_v^+ \alpha_v^+$ on $|BCS\rangle_{\mathcal{K}}$. In fact, using $\alpha_v^+ = U'_v a_v'^+ - V'_v a_v'$ one finds (it is of notice that $s'_z(v) = s_z(v)$)

$$\alpha_v^+ \alpha_v^+ = U_v'^2 P_v'^+ - V_v'^2 P_v' + 2U_v' V_v' s_z(v) = \begin{pmatrix} U_v' V_v' & U_v'^2 \\ -V_v'^2 & -U_v' V_v' \end{pmatrix}, \quad (\text{A58})$$

and

$$\alpha_{\bar{\nu}}\alpha_{\nu} = U_{\nu}^{\prime 2}P'_{\nu} - V_{\nu}^{\prime 2}P_{\nu}^{\prime +} + 2U_{\nu}'V_{\nu}'s'_{\bar{z}}(\nu) = \begin{pmatrix} U_{\nu}'V_{\nu}' & -V_{\nu}^{\prime 2} \\ U_{\nu}^{\prime 2} & -U_{\nu}'V_{\nu}' \end{pmatrix}. \quad (\text{A59})$$

Making use of Eqs. (A23-A24), one finds that

$$\alpha_{\nu}^{+}\alpha_{\bar{\nu}}^{+}|\text{gs}\rangle = \alpha_{\nu}^{+}\alpha_{\bar{\nu}}^{+}\begin{pmatrix} V_{\nu}' \\ U_{\nu}' \end{pmatrix} = \begin{pmatrix} U_{\nu}'V_{\nu}' & U_{\nu}^{\prime 2} \\ -V_{\nu}^{\prime 2} & -U_{\nu}'V_{\nu}' \end{pmatrix}\begin{pmatrix} V_{\nu}' \\ U_{\nu}' \end{pmatrix} = \begin{pmatrix} U_{\nu}' \\ -V_{\nu}' \end{pmatrix} = |\text{exc}\rangle, \quad (\text{A60})$$

and

$$\alpha_{\nu}^{+}\alpha_{\bar{\nu}}^{+}|\text{exc}\rangle = \alpha_{\nu}^{+}\alpha_{\bar{\nu}}^{+}\begin{pmatrix} U_{\nu}' \\ -V_{\nu}' \end{pmatrix} = \begin{pmatrix} U_{\nu}'V_{\nu}' & U_{\nu}^{\prime 2} \\ -V_{\nu}^{\prime 2} & -U_{\nu}'V_{\nu}' \end{pmatrix}\begin{pmatrix} U_{\nu}' \\ -V_{\nu}' \end{pmatrix} = 0. \quad (\text{A61})$$

Analogously, one finds

$$\alpha_{\bar{\nu}}\alpha_{\nu}|\text{gs}\rangle = 0, \quad (\text{A62})$$

and

$$\alpha_{\bar{\nu}}\alpha_{\nu}|\text{exc}\rangle = |\text{gs}\rangle. \quad (\text{A63})$$

We also remark that

$$2is'_y(\nu) = P_{\nu}^{\prime +} - P'_{\nu} = \alpha_{\nu}^{+}\alpha_{\bar{\nu}}^{+} - \alpha_{\bar{\nu}}\alpha_{\nu}. \quad (\text{A64})$$

One can then show that the operator $2is_y(\nu)$ acting once on the ground state produces the excited state and, acting twice gives back the ground state, but for a sign change, that is,

$$2is'_y(\nu)|\text{gs}\rangle = |\text{exc}\rangle \quad , \quad 2is'_y(\nu)|\text{exc}\rangle = -|\text{gs}\rangle. \quad (\text{A65})$$

Thus, two-quasiparticle excitation is equivalent to a rotation of the intrinsic system by an angle π around the y -axis. This is in keeping with the fact that $e^{\pi i S_y} = 2iS_y$.

Ground state energy and correlations

The energy of the ground state of the total system at the mean field level is obtained as the sum of the energy of each pair spin, $\epsilon_{\nu} - E_{\nu}$ (cf. eq. (A36)), which is the eigenvalue diagonalizing the terms $\epsilon_{\nu}N_{\nu} - (P^{\dagger}\Delta + P\Delta^*)$ of the mean field hamiltonian, plus the constant term $\frac{\Delta^2}{G}$ (cf. eq. (4)),

$$E_{gs} = \sum_{\nu>0}(\epsilon_{\nu} - E_{\nu}) + \frac{\Delta^2}{G}. \quad (\text{A66})$$

In the case of the non-interacting system ($\Delta \rightarrow 0$) $E_\nu \rightarrow |\epsilon_\nu|$, so that the system's ground state energy reads

$$E_{gs}^0 = \sum_{\nu>0} (\epsilon_\nu - |\epsilon_\nu|). \quad (\text{A67})$$

Consequently, the contributions corresponding to $\epsilon_\nu > 0$ (i.e. $\epsilon_\nu > \lambda$), cancel out, remaining only those of the states below the Fermi energy ($\epsilon_\nu < 0$). Thus,

$$E_{gs}^0 = 2 \sum_{\nu>0; \epsilon_\nu<0} \epsilon_\nu, \quad (\text{A68})$$

in keeping with the fact that in the present case all the pairs below the Fermi energy fully occupied. An important quantity characterizing superfluid systems is the so called correlation energy, E_{corr} . It is defined as the difference between the energy of the interacting system and that of the non-interacting one,

$$E_{corr} = E_{gs} - E_{gs}^0 = \sum_{\nu>0} (\epsilon_\nu - E_\nu) + \frac{\Delta'^2}{G} - 2 \sum_{\nu>0; \epsilon_\nu<0} \epsilon_\nu. \quad (\text{A69})$$

Collecting the contribution arising from levels displaying $\epsilon_\nu > 0$ and $\epsilon_\nu < 0$, the above equation can be written as

$$E_{corr} = \sum_{\nu>0; \epsilon_\nu>0} (\epsilon_\nu - E_\nu) + \sum_{\nu>0; \epsilon_\nu<0} (-\epsilon_\nu - E_\nu) + \frac{\Delta'^2}{G} = \sum_{\nu>0; \epsilon_\nu>0} (\epsilon_\nu - E_\nu) + \sum_{\nu>0; \epsilon_\nu<0} (|\epsilon_\nu| - E_\nu) + \frac{\Delta'^2}{G}. \quad (\text{A70})$$

Assuming a symmetric distribution of levels around the Fermi energy, the above expression becomes

$$E_{corr} = 2 \sum_{\nu>0; \epsilon_\nu>0} (\epsilon_\nu - E_\nu) + \frac{\Delta'^2}{G}. \quad (\text{A71})$$

It proofs useful to express the ground state energy in the term of occupation probabilities and potential interaction energy, namely as (see term U eq. (G.11) of ref. [10])

$$E_{gs} = \sum_{\nu>0} 2\epsilon_\nu V_\nu'^2 - \frac{\Delta'^2}{G}. \quad (\text{A72})$$

Using the expression for $V_\nu'^2$

$$E_{gs} = \sum_{\nu>0} \epsilon_\nu \left(1 - \frac{\epsilon_\nu}{E_\nu} \right) - \frac{\Delta'^2}{G}, \quad (\text{A73})$$

which may be rewritten as

$$\begin{aligned} E_{gs} &= \sum_{\nu>0} \epsilon_\nu \left(1 - \frac{\epsilon_\nu}{E_\nu} - \frac{E_\nu}{\epsilon_\nu} + \frac{E_\nu}{\epsilon_\nu} \right) - \frac{\Delta'^2}{G} = \sum_{\nu>0} (\epsilon_\nu - E_\nu) + \sum_{\nu>0} \left(E_\nu - \frac{\epsilon_\nu^2}{E_\nu} \right) - \frac{\Delta'^2}{G} \\ &= \sum_{\nu>0} (\epsilon_\nu - E_\nu) + \sum_{\nu>0} \frac{\Delta'^2}{E_\nu} - \frac{\Delta'^2}{G} = \sum_{\nu>0} (\epsilon_\nu - E_\nu) + 2 \frac{\Delta'^2}{G} - \frac{\Delta'^2}{G} \\ &= \sum_{\nu>0} (\epsilon_\nu - E_\nu) + \frac{\Delta'^2}{G}, \end{aligned} \quad (\text{A74})$$

which coincides with (A66).

Appendix B: Pairing rotational band wavefunction

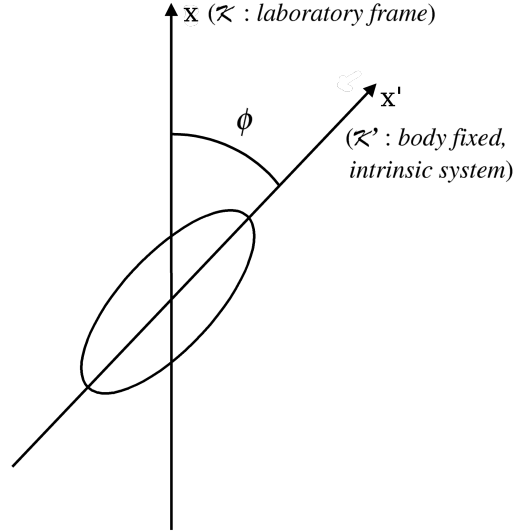


FIG. B.1: Schematic representation of the deformation in gauge space associated with a superfluid nucleus leading to pairspin alignment (see also Fig. A.1)

Let us start by defining the operator inducing a gauge transformation. In keeping with the fact that the generator of such a transformation is the particle number operator, we will be dealing with rotations in a two-dimensional space.

The operator inducing rotation in pairspin space about the gauge z -axis is given $e^{-2is_z(\nu)\phi}$. The representation of this operator in pairspin space is

$$\begin{pmatrix} e^{-i\phi} & 0 \\ 0 & e^{i\phi} \end{pmatrix}. \quad (\text{B1})$$

This operator converts the state $|\phi = 0\rangle_\nu = \begin{pmatrix} V'_\nu \\ U'_\nu \end{pmatrix}$, into the state rotated by an angle ϕ (cf. Eqs. (A40),(A41)):

$$\begin{pmatrix} e^{-i\phi} & 0 \\ 0 & e^{i\phi} \end{pmatrix} \begin{pmatrix} V'_\nu \\ U'_\nu \end{pmatrix} = \begin{pmatrix} e^{-i\phi} V'_\nu \\ e^{i\phi} U'_\nu \end{pmatrix} \quad (\text{B2})$$

In the following we shall use the operator $\mathcal{G}_v(\phi) = e^{-i\phi N_v}$ which differs from $e^{-2is_z(v)}$ only by an overall phase $e^{i\phi}$. Its representation in pairspin space is given by

$$\begin{pmatrix} e^{-2i\phi} & 0 \\ 0 & 1 \end{pmatrix}, \quad (\text{B3})$$

and its action on $|\phi = 0\rangle_v = \begin{pmatrix} V'_v \\ U'_v \end{pmatrix}$ is given by

$$\begin{pmatrix} e^{-2i\phi} & 0 \\ 0 & 1 \end{pmatrix} \begin{pmatrix} V'_v \\ U'_v \end{pmatrix} = \begin{pmatrix} e^{-2i\phi} V'_v \\ U'_v \end{pmatrix}, \quad (\text{B4})$$

producing the phase difference characterizing the rotated, $|BCS(\phi)\rangle$ state (cf. Eq. (A.51)). Calculating the average value of P in the (rotated) state $\mathcal{G}(\phi)|\phi = 0\rangle_v$, that is $\alpha_0(v) = {}_v\langle\phi = 0|\mathcal{G}^{-1}(\phi)P\mathcal{G}(\phi)|\phi = 0\rangle_v$, one finds

$$(e^{2i\phi} V'_v \quad U'_v) \begin{pmatrix} 0 & 0 \\ 1 & 0 \end{pmatrix} \begin{pmatrix} e^{-2i\phi} V'_v \\ U'_v \end{pmatrix} = e^{-2i\phi} U'_v V'_v. \quad (\text{B5})$$

We can also calculate the same average value by rotating the operator (Heisenberg representation), rather than acting on the state. The rotated operator is given by $\mathcal{G}_v^\dagger(\phi)P_v(\phi = 0)\mathcal{G}_v(\phi)$. The action of $\mathcal{G}_v^\dagger(\phi)P_v(\phi = 0)\mathcal{G}_v(\phi)$ transforms the initial operator in the intrinsic frame $P_v(\phi = 0)$, in which it has the average value $\alpha'_0(v) = U'_v V'_v$ into the laboratory frame, in which its average value is $\alpha_0(v) = \alpha'_0(v)e^{-2i\phi}$. The inverse transformation, from the laboratory into the intrinsic frame, is effected by the operator $(\mathcal{G}_v^\dagger(\phi)P_v(\phi)\mathcal{G}_v(\phi))^{-1} = \mathcal{G}_v(\phi)P_v(\phi)\mathcal{G}_v^\dagger(\phi)$. In what follows, we shall use $P'_v \equiv P_v(\phi = 0)$, and $P_v \equiv P_v(\phi)$.

Similar considerations can be applied to the many-body wavefunctions. Let us consider a wavefunction

$$\Psi_{\mathcal{K}} = a_1^\dagger a_2^\dagger \dots a_{N_0}^\dagger |0\rangle, \quad (\text{B6})$$

with a fixed number of particles. Let us now apply $\mathcal{G}(\phi)$ to the creation operator

$$a_v'^\dagger = \mathcal{G}(\phi)a_v^\dagger\mathcal{G}^{-1}(\phi) = e^{-i\phi}a_v^\dagger, \quad (\text{B7})$$

a'^\dagger being referred to the intrinsic, body-fixed reference system (see Fig. B.1). Thus

$$\Psi_{\mathcal{K}}(\phi) = e^{iN_0\phi} a_1'^\dagger a_2'^\dagger \dots a_{N_0}'^\dagger |0\rangle = e^{iN_0\phi} \Psi_{\mathcal{K}'}(\phi = 0), \quad (\text{B8})$$

$$\Psi_{\mathcal{K}'}(\phi = 0) = a_1'^{\dagger} a_2'^{\dagger} \dots a_{N_0}'^{\dagger} |0\rangle. \quad (\text{B9})$$

In keeping with the fact that

$$-i \frac{\partial \Psi_{\mathcal{K}}(\phi)}{\partial \phi} = -i \times i N_0 e^{iN\phi} \Psi_{\mathcal{K}'}(\phi = 0) = N_0 \Psi_{\mathcal{K}}(\phi), \quad (\text{B10})$$

$$N = -i \frac{\partial}{\partial \phi}, \quad N \Psi_{\mathcal{K}}(\phi) = N_0 \Psi_{\mathcal{K}}(\phi). \quad (\text{B11})$$

This is equivalent to saying that

$$[\phi, N]\psi = (\phi N - N\phi)\psi = \Phi \left(-i \frac{\partial}{\partial \phi} \psi \right) + i \frac{\partial}{\partial \phi} (\phi \psi) = +i\psi - i\phi \frac{\partial \psi}{\partial \phi} - i\phi \frac{\partial \psi}{\partial \phi} = i\psi, \quad (\text{B12})$$

i.e. $[\phi, N] = i$. The BCS wavefunction can then be written, in the intrinsic body-fixed frame, as

$$|BCS(\phi = 0)\rangle_{\mathcal{K}'} \sim \prod_{\nu} \alpha_{\nu} |0\rangle \sim \prod_{\nu>0} \alpha_{\nu} \alpha_{\bar{\nu}} |0\rangle. \quad (\text{B13})$$

The corresponding normalized wavefunction is then

$$\begin{aligned} |BCS(\phi = 0)\rangle_{\mathcal{K}'} &= \prod_{\nu>0} (U'_{\nu} + V'_{\nu} a_{\nu}^{\dagger} a_{\bar{\nu}}^{\dagger}) |0\rangle = \prod_{\nu} (U'_{\nu} + e^{-2i\phi} V'_{\nu} a_{\nu}^{\dagger} a_{\bar{\nu}}^{\dagger}) |0\rangle \\ &= |BCS(\phi)\rangle_{\mathcal{K}} = \left(\prod_{\nu>0} U'_{\nu} \right) \left(1 + \frac{e^{-2i\phi}}{1!} \sum_{\nu>0} c_{\nu} a_{\nu}^{\dagger} a_{\bar{\nu}}^{\dagger} + \frac{e^{-4i\phi}}{2!} \left(\sum_{\nu>0} c_{\nu} a_{\nu}^{\dagger} a_{\bar{\nu}}^{\dagger} \right)^2 + \dots \right), \end{aligned} \quad (\text{B14})$$

where $c_{\nu} = V'_{\nu}/U'_{\nu}$. Thus,

$$\begin{aligned} |N_0\rangle &= \int d\phi e^{iN_0\phi} |BCS(\phi = 0)\rangle_{\mathcal{K}'} = \int d\phi e^{iN_0\phi} |BCS(\phi)\rangle_{\mathcal{K}} \\ &= (\prod_{\nu>0} U'_{\nu}) \int d\phi e^{iN_0\phi} \left(1 + \dots + \frac{e^{-iN\phi}}{(N/2)!} \left(\sum_{\nu>0} c_{\nu} a_{\nu}^{\dagger} a_{\bar{\nu}}^{\dagger} \right)^{N/2} + \dots \right) |0\rangle \\ &\sim \left(\sum_{\nu>0} c_{\nu} a_{\nu}^{\dagger} a_{\bar{\nu}}^{\dagger} \right)^{N_0/2} |0\rangle. \end{aligned} \quad (\text{B15})$$

It is of notice that the factor $e^{iN_0\phi}$ above is equivalent to the transformation coefficient e^{ipq} between p and q representations. Finally, the members of a pairing rotational band are described by the states,

$$|N_0\rangle \sim \left(\sum_{\nu>0} c_{\nu} a_{\nu}^{\dagger} a_{\bar{\nu}}^{\dagger} \right)^{N_0/2} |0\rangle. \quad (\text{B16})$$

Now, from this relation it becomes clear that the Cooper pair wavefunction

$$|\tilde{0}\rangle = \sum_{\nu>0} c_{\nu} a_{\nu}^{\dagger} a_{\bar{\nu}}^{\dagger} |0\rangle, \quad (\text{B17})$$

is to be interpreted to be valid for values of ε_ν close to ε_F , otherwise one risks not to be able to normalize it ($U_\nu \rightarrow 0$ for $\varepsilon_\nu \ll \varepsilon_F < 0$ for deeply bound occupied states). This is in keeping with the fact that pair condensation in general, and nuclear superfluidity in particular, are associated with a modification of the Fermi surface within a narrow band around it ($\varepsilon_F \pm \Delta$). In other words, pairspin alignment as described by BCS implies that something unique takes place in the long wavelength limit of the spectrum, namely the appearance of a coherent state with almost (aside from the weak ($\varepsilon_\nu \approx \varepsilon_F$) dealignment introduced by H_{sp}), perfect phase coherence. This state behaves essentially semiclassically, and its properties can hardly depend on the ultraviolet behavior of the system. In other words, E_{cutoff} can be set to include only the valence single-particle shells, adjusting G to reproduce the value of the pairing gap. Within this context see also the discussion in Sect. 4 in connection with Fig. 8 and Tables I and II.

In the case of a single j -shell (see e.g. [10] App. I),

$$V' = \sqrt{\frac{N}{2\Omega}} \quad , \quad U = \sqrt{1 - \frac{N}{2\Omega}}, \quad (\text{B18})$$

thus

$$U'V' = \sqrt{\frac{N}{2\Omega} \left(1 - \frac{N}{2\Omega}\right)}, \quad (\text{B19})$$

while

$$\frac{V'}{U'} = \frac{\sqrt{\frac{N}{2\Omega}}}{\sqrt{1 - \frac{N}{2\Omega}}} = \sqrt{\frac{N}{2\Omega - N}}. \quad (\text{B20})$$

For a number of particles considerably smaller than the full degeneracy of the single-particle subspace in which nucleons can correlate, that is for $N \ll 2\Omega$, one can write

$$U'V' = \sqrt{\frac{N}{2\Omega} \left(1 - \frac{N}{4\Omega}\right)} \approx \sqrt{\frac{N}{2\Omega}}, \quad (\text{B21})$$

and

$$\frac{V'}{U'} = \sqrt{\frac{N}{2\Omega} \frac{1}{\left(1 - \frac{N}{2\Omega}\right)}} \approx \sqrt{\frac{N}{2\Omega}} \left(1 + \frac{N}{4\Omega}\right) \approx \sqrt{\frac{N}{2\Omega}} \approx U'V'. \quad (\text{B22})$$

Consequently

$$|\tilde{0}\rangle \approx \sum_{\nu>0} U_\nu V_\nu a_\nu^\dagger a_\nu^\dagger |0\rangle, \quad (\text{B23})$$

in keeping with Eqs. (15b) and (28).

In what follows we work out some relations which are useful to calculate expectation values in the $|BCS\rangle$ state.

Making use of (B7) (i.e. $a'_\mu{}^\dagger = \mathcal{G}a_\mu^\dagger\mathcal{G}^{-1} = e^{-i\phi}a_\mu^\dagger$) one can write

$$a'_\mu{}^\dagger = e^{i\phi}a'_\mu{}^\dagger = e^{i\phi} \begin{cases} a'_\nu{}^\dagger & (\mu = \nu), \\ a'_{\bar{\nu}}{}^\dagger & (\mu = \bar{\nu}), \end{cases} \quad (\text{B24})$$

thus

$$a_\mu = e^{-i\phi}a'_\mu = e^{-i\phi} \begin{cases} a'_\nu & (\mu = \nu), \\ a'_{\bar{\nu}} & (\mu = \bar{\nu}). \end{cases} \quad (\text{B25})$$

Making use of (1b) and (2) one can write

$$\alpha_\mu^\dagger = \begin{cases} U'_\nu a'_\nu{}^\dagger - V'_\nu a'_{\bar{\nu}} & (\mu = \nu), \\ U'_\nu a'_{\bar{\nu}}{}^\dagger + V'_\nu a'_\nu & (\mu = \bar{\nu}), \end{cases} \quad (\text{B26})$$

in keeping with the fact that U'_μ and V'_μ are real c-numbers, and thus $U'_\mu = U'_{\bar{\mu}}$ and $V'_\mu = V'_{\bar{\mu}}$, and consequently $U_{\bar{\nu}} = U_\nu$ and $V_{\bar{\nu}} = V_\nu$, as well as the fact that $a_{\bar{\nu}} = -a_\nu$, a consequence of the anti-unitary character of the time reversal operator. Within this context it is of notice that the intrinsic property of a nucleon of being in a state with quantum numbers (j, m) or $(j, -m)$ does not of course affect the gauge angle of rotation (2ϕ , see also Fig. A.1) defining the intrinsic (body-fixed) frame of reference with respect to the laboratory system. Taking the hermitian conjugate of the second case of eq. (B26) one obtains

$$\alpha_{\bar{\nu}} = U'_\nu a'_\nu + V'_\nu a'_\nu{}^\dagger. \quad (\text{B27})$$

Multiplying the first entry of Eq. (B26) by U'_ν and (B27) by V'_ν one obtains,

$$\begin{aligned} U'_\nu \alpha_\nu^\dagger &= U'^2_\nu a'_\nu{}^\dagger - V'_\nu U'_\nu a'_{\bar{\nu}}, \\ V'_\nu \alpha_{\bar{\nu}} &= V'_\nu U'_\nu a'_\nu + V'^2_\nu a'_\nu{}^\dagger. \end{aligned}$$

Summing these two expressions and making use of (3) one obtains

$$a'_\nu{}^\dagger = U'_\nu \alpha_\nu^\dagger + V'_\nu \alpha_{\bar{\nu}}, \quad (\text{B28a})$$

which is equivalent to

$$a'_\nu{}^\dagger = U_\nu \alpha_\nu^\dagger + V_\nu^* \alpha_{\bar{\nu}}. \quad (\text{B28b})$$

Similarly, multiplying the hermitian conjugate of the first entry of Eq. (B26) by V'_ν and the second entry by U'_ν and subtracting the resulting expressions leads to

$$a'_{\bar{\nu}}{}^\dagger = U'_\nu \alpha_{\bar{\nu}}^\dagger - V'_\nu \alpha_\nu, \quad (\text{B29a})$$

which is equivalent to

$$a_{\bar{\nu}}^{\dagger} = U_{\nu} \alpha_{\bar{\nu}}^{\dagger} - V_{\nu}^* \alpha_{\nu}. \quad (\text{B29b})$$

One then obtains

$$P^{\dagger} = \sum_{\nu>0} a_{\nu}^{\dagger} a_{\bar{\nu}}^{\dagger} = \sum_{\nu>0} \left\{ U_{\nu}^2 \alpha_{\nu}^{\dagger} \alpha_{\bar{\nu}}^{\dagger} - (V_{\nu}^*)^2 \alpha_{\bar{\nu}} \alpha_{\nu} - U_{\nu} V_{\nu}^* (\alpha_{\nu}^{\dagger} \alpha_{\nu} + \alpha_{\bar{\nu}}^{\dagger} \alpha_{\bar{\nu}}) + U_{\nu} V_{\nu}^* \right\}, \quad (\text{B30a})$$

$$P = \sum_{\nu>0} a_{\bar{\nu}} a_{\nu} = \sum_{\nu>0} \left\{ (U_{\nu}^*)^2 \alpha_{\bar{\nu}} \alpha_{\nu} - V_{\nu}^2 \alpha_{\nu}^{\dagger} \alpha_{\bar{\nu}}^{\dagger} - U_{\nu}^* V_{\nu} (\alpha_{\nu}^{\dagger} \alpha_{\nu} + \alpha_{\bar{\nu}}^{\dagger} \alpha_{\bar{\nu}}) + U_{\nu}^* V_{\nu} \right\}, \quad (\text{B30b})$$

thus

$$\begin{aligned} \alpha_0 &= \langle BCS | P | BCS \rangle = \sum_{\nu>0} U_{\nu}^* V_{\nu} = e^{-2i\phi} \sum_{\nu>0} U'_{\nu} V'_{\nu} = e^{-2i\phi} \alpha'_0 \\ &= \left(\sum_{\nu>0} U_{\nu} V_{\nu}^* \right)^* = \langle BCS | P^{\dagger} | BCS \rangle^*. \end{aligned} \quad (\text{B31})$$

Summing up

$$\alpha_0 = \sum_{\nu>0} U_{\nu}^* V_{\nu}, \quad (\text{B32})$$

and

$$\alpha'_0 = \sum_{\nu>0} U'_{\nu} V'_{\nu}, \quad (\text{B33})$$

leading to

$$\Delta = G \alpha_0 = e^{-2i\phi} G \alpha'_0 = e^{-2i\phi} \Delta'. \quad (\text{B34})$$

An alternative derivation of the above relations can be obtained by inserting the expressions of a_{ν}^{\dagger} and $a_{\bar{\nu}}^{\dagger}$ obtained from (B28a) and (B29a) into

$$P = \sum_{\nu>0} a_{\bar{\nu}} a_{\nu} = e^{-2i\phi} \sum_{\nu>0} a'_{\bar{\nu}} a'_{\nu} = e^{-2i\phi} P', \quad (\text{B35})$$

which leads to

$$\begin{aligned} P &= e^{-2i\phi} \sum_{\nu>0} (U'_{\nu} \alpha_{\bar{\nu}} - V'_{\nu} \alpha_{\nu}^{\dagger}) (U'_{\nu} \alpha_{\nu} + V'_{\nu} \alpha_{\bar{\nu}}^{\dagger}) \\ &= e^{-2i\phi} \sum_{\nu>0} \left\{ U_{\nu}'^2 \alpha_{\bar{\nu}} \alpha_{\nu} - V_{\nu}'^2 \alpha_{\nu}^{\dagger} \alpha_{\bar{\nu}}^{\dagger} - U'_{\nu} V'_{\nu} (\alpha_{\nu}^{\dagger} \alpha_{\nu} + \alpha_{\bar{\nu}}^{\dagger} \alpha_{\bar{\nu}}) + U'_{\nu} V'_{\nu} \right\}. \end{aligned} \quad (\text{B36})$$

Appendix C: Commutation relations

Making use of the relations

$$[AB, C] = A[B, C] + [A, C]B, \quad (C1)$$

$$[C, AB] = A[C, B] + [C, A]B, \quad (C2)$$

$$[AB, C] = A\{B, C\} - \{A, C\}B, \quad (C3)$$

and of the definitions

$$P_\nu^+ = a_\nu^+ a_{\bar{\nu}}^+ \quad ; \quad P_\nu = a_{\bar{\nu}} a_\nu, \quad (C4)$$

one can calculate the commutator

$$[P_\nu, P_\nu^+] = [a_{\bar{\nu}} a_\nu, a_\nu^+ a_{\bar{\nu}}^+] = a_\nu^+ [a_{\bar{\nu}} a_\nu, a_{\bar{\nu}}^+] + [a_{\bar{\nu}} a_\nu, a_\nu^+] a_{\bar{\nu}}^+ \quad (C5)$$

$$= a_\nu^+ (-\{a_{\bar{\nu}}, a_{\bar{\nu}}^+\} a_\nu) + (a_{\bar{\nu}} \{a_\nu, a_\nu^+\}) a_{\bar{\nu}}^+ \quad (C6)$$

$$= -a_\nu^+ a_\nu + a_{\bar{\nu}} a_{\bar{\nu}}^+ = 1 - (a_\nu^+ a_\nu + a_{\bar{\nu}}^+ a_{\bar{\nu}}) = 1 - N_\nu, \quad (C7)$$

where

$$N_\nu = a_\nu^+ a_\nu + a_{\bar{\nu}}^+ a_{\bar{\nu}}. \quad (C8)$$

Similarly,

$$[a_\nu^+ a_\nu, P_\nu^+] = [a_\nu^+ a_\nu, a_\nu^+ a_{\bar{\nu}}^+] = a_\nu^+ [a_\nu^+ a_\nu, a_{\bar{\nu}}^+] + [a_\nu^+ a_\nu, a_\nu^+] a_{\bar{\nu}}^+ = \quad (C9)$$

$$a_\nu^+ \{a_\nu, a_\nu^+\} a_{\bar{\nu}}^+ = a_\nu^+ a_{\bar{\nu}}^+ \quad (C10)$$

and

$$[a_{\bar{\nu}}^+ a_{\bar{\nu}}, P_\nu^+] = [a_{\bar{\nu}}^+ a_{\bar{\nu}}, a_\nu^+ a_{\bar{\nu}}^+] = a_\nu^+ [a_{\bar{\nu}}^+ a_{\bar{\nu}}, a_{\bar{\nu}}^+] + [a_{\bar{\nu}}^+ a_{\bar{\nu}}, a_\nu^+] a_{\bar{\nu}}^+ \quad (C11)$$

$$= a_\nu^+ (a_{\bar{\nu}}^+ \{a_{\bar{\nu}}, a_{\bar{\nu}}^+\}) = a_\nu^+ a_{\bar{\nu}}^+ . \quad (C12)$$

Thus

$$[N_\nu, P_\nu^+] = 2P_\nu^+. \quad (C13)$$

Consequently,

$$[N_\nu, P_\nu] = -2P_\nu. \quad (C14)$$

Summing up,

$$[P_\nu^+, P_\nu] = N_\nu - 1 \quad (C15)$$

$$[N_\nu - 1, P_\nu^+] = 2P_\nu^+ \quad (\text{C16})$$

and

$$[N_\nu - 1, P_\nu] = -2P_\nu. \quad (\text{C17})$$

Making use of these relations and of the definitions

$$s_x(\nu) = \frac{1}{2}(P_\nu^+ + P_\nu) \quad , \quad s_y(\nu) = \frac{1}{2i}(P_\nu^+ - P_\nu), \quad (\text{C18})$$

and

$$s_z(\nu) = \frac{1}{2}(N_\nu - 1), \quad (\text{C19})$$

one obtains

$$\begin{aligned} [s_x(\nu), s_y(\nu)] &= \left[\frac{1}{2}(P_\nu^+ + P_\nu), \frac{1}{2i}(P_\nu^+ - P_\nu) \right] = \frac{1}{4i}(-[P_\nu^+, P_\nu] + [P_\nu, P_\nu^+]) \\ &= \frac{1}{2i}[P_\nu, P_\nu^+] = \frac{1}{2i}(1 - N_\nu) = is_z(\nu), \end{aligned} \quad (\text{C20})$$

$$\begin{aligned} [s_y(\nu), s_z(\nu)] &= \frac{1}{4i}([P_\nu^+, (N_\nu - 1)] - [P_\nu, (N_\nu - 1)]) = -\frac{1}{4i}(2P_\nu^+ + 2P_\nu) \\ &= -\frac{1}{2i}(P_\nu^+ + P_\nu) = is_x(\nu), \end{aligned} \quad (\text{C21})$$

$$\begin{aligned} [s_z(\nu), s_x(\nu)] &= \frac{1}{4}[(N_\nu - 1), P_\nu^+ + P_\nu] = \frac{1}{4}((N_\nu - 1), P_\nu^+) + [(N_\nu - 1), P_\nu] \\ &= -\frac{1}{2}(P_\nu - P_\nu^+) = +is_y(\nu). \end{aligned} \quad (\text{C22})$$

Appendix D: Generalized Rigidity in Gauge Space

Generalized rigidity in gauge space implies that if one pushes, with the help of a field that changes the number of particles in two, one of the poles of a deformed system in gauge space (see e.g. Fig. B.1), system which can be viewed as a wavepacket in particle number, the other pole reacts rigidly to the push, and the system starts rotating as a whole (pairing rotational band). Similarly, if it was already in rotation it changes its rotational frequency from $\omega = \lambda(N_0)/\hbar$ to $\omega' = \lambda(N_0 \pm 2)/\hbar$, λ being the Lagrange multiplier which, in BCS theory, is closely connected with the particle number equation.

If the gauge space image is not sufficiently concrete to create a physical picture of the process, let us think of a quadrupole deformed nucleus whose intrinsic state is described in terms of the

Nilsson intrinsic state. Making use of a proton beam which acts upon one of the poles, the system reacts as a whole and starts rotating with a frequency associated with one of the allowed values of the angular momentum, the transfer quantum corresponding to an energy inversely proportional to the moment of inertia.

One may argue that the reaction of the pole not acted upon by the external field is not instantaneous but takes place only after an interval of time, compatible with the propagation of information in the nuclear medium, has elapsed. This parlance is not even wrong, as a wavefunction, in particular that describing the intrinsic ground state of a superfluid nucleus (see Eq. (12)), is not a matter function but a probability amplitude function [62] with perfect phase coherence throughout. Within the quadrupole deformed nucleus analogy, generalized rigidity implies that the nucleus reacts rigidly as a whole to the action of the proton field acting on a pole[63], even if the moment of inertia of the associated rotational band is that of superfluid nuclear matter, and thus considerably smaller than the rigid moment of inertia.

The specific experiment to study the consequences (emergent properties) resulting from a spontaneous breaking of symmetry (e.g. of rotational invariance) is a probe which itself violates the symmetry in question. Now, while most of the devices we find in a well equipped nuclear laboratory violate rotational invariance – think for example of a proton beam line defining a privileged orientation in 3D-space – one does not find many which violate gauge invariance. In other words, while rulers and goniometers defy empty space isotropy and homogeneity, one does not usually walk around with instruments which do not have a fixed number of particles.

This was the real importance of the Josephson effect (see Fig. D.1), which provided a simple, and quantitative accurate answer to the question: how does one measures the gauge phase of a superconductor? The answer is, with the help of another superconductor displaying also an unknown but nonetheless well defined gauge phase. Establishing a weak coupling (oxide layer) so that electrons can tunnel, one at a time, between the junction. If the first system can be viewed as a rotor in gauge space, the second one can equally well be represented in this way. Biasing the junction with a constant potential difference, will lead to a two-rotor-coupled system (through pair transfer across the junction), rotating with frequencies which differ by $e\Delta V/\hbar = (\lambda_1 - \lambda_2)/\hbar$. Such a system will display a resonant behavior (alternating current with frequency $e\Delta V t/\hbar$) provided the rotor, deformed system picture in gauge space, is applicable. The fact that this effect provides the most accurate measure of (e/\hbar) available, testifies to the validity of the deformed rotor picture in gauge space associated with the *BCS* wavefunction (12).

It is sobering that this is so, in keeping with the fact that it was Bardeen the most strenuous opponent to Josephson's ideas, even more so if one is reminded that the choice argument of such opposition was based on the fact that the pairing gap $\Delta = G\alpha_0$ vanishes at the junction. Now, the order parameter of BCS theory (as well as the justification of Cooper pair model) is $\alpha_0 = \langle P^+ \rangle = \langle P \rangle^*$, namely the condensed pair field. Electrons may tunnel one at a time, without obliterating the validity of pair transfer, as the coherence length ($\xi = \hbar v_F / 2\Delta$) is much larger than typical junction dimensions, diverging at the junction (kind of extreme ^{11}Li -halo-like phenomenon (see e.g. [64], [65]) within the condensed matter framework).

Within this scenario one can posit that, in the nuclear case, the equivalent of the Josephson junction device or better, the setup of an experiment which can measure differences in gauge phases, allows for embodiments which are not possible within the field of condensed matter physics. This is related to the fact that fluctuations in finite many-body systems, in general and pairing vibrations in normal nuclei in particular, are not only quantitatively but also qualitatively stronger than in condensed matter.

Consequently, not only a collision between two superfluid nuclei (see Fig. D.1(b)) can be viewed as a time dependent generalization of a Josephson junction (see Fig. D.1(a)). Also a normal-superfluid nuclear reaction can provide similar information, as a closed shell system displays a very collective pairing vibrational spectrum which can be viewed as large amplitude dynamical gauge symmetry violating mode (see Fig. D.1(c)).

Let us consider the ground state of a (light) closed shell system. Within the present discussion, it can be written as

$$|\widetilde{a(gs)}\rangle = \alpha|a(gs)\rangle + \beta|(a-2)(gs) \otimes (a+2)(gs)\rangle \quad (\text{D1})$$

where $|(a-2)(gs)\rangle$ and $|(a+2)(gs)\rangle$, are the pair removal and pair addition modes, while $\alpha^2 + \beta^2 = 1$ is the normalization condition. In other words, the closed-shell system is part of the time in states with two more (see (I) inset Fig. D.1), or two less correlated nucleons (see (II) inset Fig. D.1). The two-hole uncorrelated states which, arguably, ensure particle number correlation, in fact describes the ground state correlations (backwardgoing amplitudes, see e.g. Table III Y-amplitudes as well as insets in Fig. 3) associated with the pair addition mode which, dynamically, deforms the nucleus in gauge space defining a transient, privileged orientation. The same can be said concerning the two-particle uncorrelated system shown in the inset (II) of Fig. D.1(c).

Let us now return to the analogy with quadrupole rotational and vibrational bands. Going away from closed shell nuclei in medium heavy systems the energy of the first 2^+ state lowers in energy,

the corresponding period becoming longer, the associated amplitudes larger (see e.g. [10] Ch.7). Eventually, after the quantal phase transition has taken place, the rotation of the system as a whole can be viewed as a very low frequency quadrupole vibrational mode (for which the restoring force vanishes while inertia remains finite), which dynamically defines a privileged quadrupole deformation symmetry axis (and thus an associated set of Euler angles), orientation which after each period changes orientation, with a frequency inversely proportional to the inertia of the mode.

In a similar way the state (D1) defines dynamically, a privileged orientation in gauge space which specifically can probe the corresponding static quantity of a superfluid target nucleus A (see Fig. D.1(c)), that is,

$$a + A \rightarrow \left\{ a((a+2) \otimes (a-2)(gs)) + A \left(\sum_N c_N |N \right) \right\} \rightarrow \begin{cases} (a-2)(gs) + (A+2)(gs), \\ (a+2)(gs) + (A-2)(gs), \end{cases} \quad (D2)$$

where $A(\sum_N c_N |N)$ labels the ground state of a superfluid nucleus, e.g. of ^{120}Sn which can be viewed as a wavepacket in neutron number, the scattering state within curly brackets being a virtual set of states each displaying a dynamical or a static privileged orientation in gauge space and thus a gauge phase. A particular embodiment of such a reaction can be

$${}^9_3\text{Li}_6 + {}^{120}_{50}\text{Sn}_{70} \rightarrow \begin{cases} {}^7_3\text{Li}_4 + {}^{122}_{50}\text{Sn}_{72}, \\ {}^{11}_3\text{Li}_8 + {}^{118}_{50}\text{Sn}_{68}, \end{cases} \quad (D3)$$

in keeping with the fact that $N = 6$ corresponds to a (parity inversion) magic number, $|^9\text{Li}(gs)\rangle$ and $|^{11}\text{Li}(gs)\rangle$ being the pair removal and pair addition modes of ^9Li (see [66, 67]).

Appendix E: Kramers-Kronig dispersion relation

The nuclear superfluid phase, and associated pairing rotational band behaves, because of its ODLRO essentially as a classical (coherent) state. This is the basic reason which is at the basis of the results displayed in Fig. 7 and Table IV, that is the remarkable quantitative accuracy with which theory provide an overall account of the absolute value of the experimental findings.

There is, however, a second reason for the higher accuracy with which one can, in principle, predict absolute two-nucleon transfer cross sections, as compared with one-nucleon transfer cross sections, or, simply, (although, arguably, less well defined see e.g. [5, 68, 69]) absolute values of the single-particle spectroscopic factors. This is connected with the ambiguity and eventual lack

of consistency of empirically determined optical parameters. Typical of the first type of limitations, is connected with the fact that the depth of the real part of the optical potential can have different, commensurable values, all leading to the same phase shift (e.g. so-called Igo's ambiguity [70]). Concerning the second point (consistency), one is reminded of the fact that the real and the imaginary part of the optical potentials ($U + iW$) controlling off- and on -the energy shell processes, are the real and imaginary part of the nuclear mass operator (sum of polarization and correlation contributions), referred to, also, as the nuclear dielectric function [5]. Consequently U and W must fulfill the Kramers-Kronig dispersion relation (cf. refs. [71, 72], see also [5]). This is a bidirectional mathematical relation, connecting the real and imaginary parts of any complex function that is analytic in the upper half of the complex plane. The Kramers-Kronig is a rather fundamental relation, in that it is strictly related to causality. Summing up, the real and imaginary parts of the optical potentials empirically determined from a global elastic scattering fitting, should respect the above mentioned dispersion relation. This condition is only marginally fulfilled in a number of cases, thus introducing uncertainties difficult to control. In keeping with the fact that, theoretically, $U(r)$ results from the convolution of the nucleon-nucleon interaction with the nuclear density $\rho(r)$, and that this quantity is best known around the nuclear surface, in a similar way in which $W(r)$ receives important contributions from the interweaving of single-particle motion and collective surface vibrations, one can posit that the lack of consistency between U and W are likely to be more serious for values of r larger and smaller than the nuclear radius (i.e. $r > R_0$ and $r < R_0$). The phase coherence of the nuclear condensate implies that Cooper pair wavefunctions, closely related to the effective two-particle transfer nuclear formfactors, are rather compact objects, essentially concentrated on the nuclear surface (see e.g. Fig. 8). Consequently, the main contribution to the absolute two-particle differential cross section arises from values of $r \approx R_0$ (nuclear surface), region in which the optical potential is best known. On the other hand, the formfactor associated with single-particle transfer is a standard mean field wavefunction (in any case as far as the main peak of the single-particle strength function – one-pole approximation – is concerned). Consequently, the absolute one-nucleon transfer differential cross section can depend, in an important way, on the knowledge of the optical potential inside the nuclear volume.

The above discussion can also be related to the fluctuation-dissipation theorem (cf. eg. refs. [73, 74]), closely related to the Kramers-Kronig dispersion relation. While it is true that single-particle motion emerges from the same features leading to collective nuclear vibrations [61] - the independent particle shell structure being a result of a collective and concerted motion of all the

nucleons allowing free motion to each single of them, and letting themselves felt through the pushing and pulling only when a particle tries to leave the system, forcing it to bounce elastically off the nuclear surface - the picture becomes less stable as soon as the particle-vibration coupling strength is switched on, leading to real, dressed particles (mechanism also contributing to the imaginary part of the optical potential). Within this context one can posit that the associated single-particle strength function in general and thus its centroid and width in particular, depend on a delicate interplay of spin- and non spin- flip matrix elements, large and small energy denominators, and the like. On the other hand the strength function associated with a Cooper pair, being a coherent object behaving almost semiclassically, resents much less of the above mentioned inhomogeneous damping phenomena.

Summing up, even without totally consistent optical potentials in the Kramers-Kronig sense, it is likely that one can calculate the absolute value of the two-particle transfer cross section between members of pairing rotational (vibrational) bands with high accuracy. On the other hand, in the case of one-nucleon transfer processes, this possibility is likely to be restricted to the centroid and width of the (main peak) single-particle strength function, the integrated area being affected, as a rule, by little controllable, non-specific background effects, difficult to estimate and/or remove. Such limitations will likely be more important in the case of strongly fragmented single-particle states.

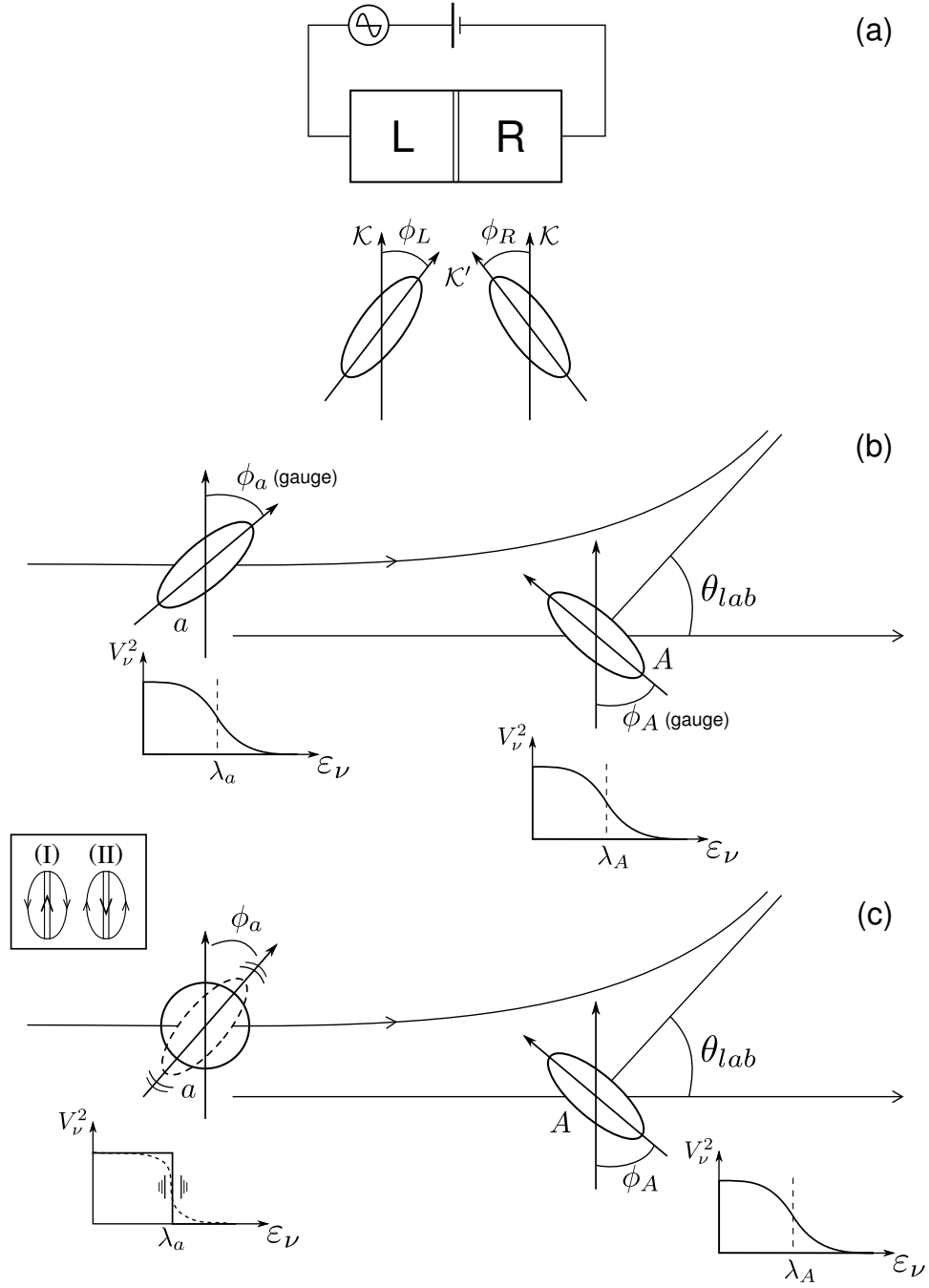


FIG. D.1: Josephson junction between left (L) and right (R) superconductors weakly coupled through a thin (DC biased) oxide layer; (b) time dependent nuclear Josephson junction established at about the distance of closest approach by the superfluid nuclei a and A in the reaction $a + A \rightarrow (a \pm n) + A(- + n)$, where $n = 0, 1, 2, \dots$ is the number of Cooper pairs transferred in the process; (c) dynamical time dependent Josephson junction between a closed shell system a displaying strong pairing vibrations (pair addition and pair removal mode) and a superfluid nucleus A . In the inset (left) the ground zero point fluctuations of the system a associated with the pair addition (arrowed double line pointing up) and pair removal mode (arrowed double line pointing down) are shown.

REFERENCES

-
- [1] M. Mayer and J. Jensen, *Elementary Theory of Nuclear Shell Structure*. Wiley, New York, NY, 1955.
- [2] P. Cottle, “Doubly Magic Tin,” *Nature*, vol. 465, p. 430, 2010.
- [3] K. L. Jones, A. S. Adekola, D. W. Bardayan, J. C. Blackmon, K. Y. Chae, K. A. Chipps, J. A. Cizewski, L. Erikson, C. Harlin, R. Hatarik, R. Kapler, R. L. Kozub, J. F. Liang, R. Livesay, Z. Ma, B. H. Moazen, C. D. Nesaraja, F. M. Nunes, S. D. Pain, N. P. Patterson, D. Shapira, J. F. Shriner, M. S. Smith, T. P. Swan, and J. S. Thomas, “The magic structure of ^{132}Sn explored through the single-particle states of ^{133}Sn ,” *Nature*, vol. 465, p. 454, 2010.
- [4] R. Haufler, L.-S. Wang, L. Chibante, C. Jin, J. Conceicao, Y. Chai, and R. Smalley, “Fullerene triplet state production and decay: R2PI probes of C_{60} and C_{70} in a supersonic beam,” *Chemical Physics Letters*, vol. 179, no. 56, p. 449, 1991.
- [5] C. Mahaux, P. F. Bortignon, R. A. Broglia, and C. H. Dasso, “Dynamics of the shell model,” *Phys. Rep.*, vol. 120, p. 1, 1985.
- [6] N. Bogoljubov, “On a new method in the theory of superconductivity,” *Il Nuovo Cimento (1955-1965)*, vol. 7, 1958.
- [7] J. Valatin, “Comments on the theory of superconductivity,” *Il Nuovo Cimento (1955-1965)*, vol. 7, 1958.
- [8] P. W. Anderson, “Random-Phase Approximation in the theory of superconductivity,” *Phys. Rev.*, vol. 112, p. 1900, 1958.
- [9] A. Bohr and O. Ulfbeck, “Quantal structure of superconductivity. Gauge angle,” *1st Topsøe Summer School, AEK Risø, Denmark (unpublished)*, 1988. http://www.risoe.dtu.dk/rispubl/reports_INIS/RISOM2756.pdf.
- [10] D. Brink and R. A. Broglia, *Nuclear Superfluidity*. Cambridge: Cambridge University Press, 2005.
- [11] D. R. Bès and R. A. Broglia, “Pairing vibrations,” *Nucl. Phys.*, vol. 80, p. 289, 1966.
- [12] R. A. Broglia, O. Hansen, and C. Riedel, “Two-neutron transfer reactions and the pairing model,” *Adv. Nucl. Phys.*, vol. 6, p. 287, 1973. <http://merlino.mi.infn.it/repository/BrogliaHansenRiedel.pdf>.
- [13] R. S. Nikam and P. Ring, “Manifestation of the Berry phase in diabolic pair transfer in rotating nuclei,” *Phys. Rev. Lett.*, vol. 58, p. 980, 1987.

- [14] R. Nikam, P. Ring, and L. Canto, "A nuclear squid: Diaboloic pair transfer in rotating nuclei," *Phys. Lett. B*, vol. 185, no. 3, p. 269, 1987.
- [15] Y. R. Shimizu, J. D. Garrett, R. A. Broglia, M. Gallardo, and E. Vigezzi, "Pairing fluctuations in rapidly rotating nuclei," *Rev. Mod. Phys.*, vol. 61, p. 131, 1989.
- [16] Within this context one can also mention a different (although not directly pertinent to the Sn-isotopes studied in the present paper) analogy between nuclear and metallic normal state properties which has important consequences on Cooper pair stability. Bad conductors, that is bad single-particle electronic metals (like e.g. Pb, Sn and Hg), display stable Cooper pair condensation at low temperatures, becoming superconductors, while good conductors, independent electron motion metals, (e.g. Au, Ar, Cu) do not. In the nuclear case, arguably, one of the best nuclear embodiments of Cooper's model is the $|gs(^{11}\text{Li}) >$ state, pair addition mode of ^9Li . The associated.
- [17] R. A. Broglia, C. Riedel, and T. Udagawa, "Coherence properties of two-neutron transfer reactions and their relation to inelastic scattering," *Nucl. Phys. A*, vol. 169, p. 225, 1971.
- [18] R. A. Broglia, C. Riedel, and T. Udagawa, "Sum rules and two-particle units in the analysis of two-neutron transfer reactions," *Nucl. Phys. A*, vol. 184, p. 23, 1972.
- [19] Within this context one can mention the fact that if instead of pairspins with two projections, one studies the properties of finite systems which depend on the alignment of a pairspin with twenty components, like protein evolution and structure in which each projection corresponds to one of the twenty naturally occurring aminoacids, the fluctuations of pair spin and thus of emergent properties, become even richer and subtler than in the case shown in Fig. 5 (see e.g. ref. [66] and refs. therein). From a technical point of view, but not only, the situation may be analogous to that resulting moving from tinkering with the Ising model, to confront oneself with Potts model.
- [20] R. A. Broglia and A. Winther, *Heavy Ion Reactions, 2nd ed.* Boulder: Westview Press, Perseus Books, 2005.
- [21] B. D. Josephson, "Possible new effects in superconductive tunnelling," *Phys. Lett.*, vol. 1, p. 251, 1962.
- [22] J. Bardeen, "Tunneling into superconductors," *Phys. Rev.*, vol. 9, p. 147, 1962.
- [23] M. H. Cohen, L. M. Falicov, and J. C. Phillips, "Superconductive tunneling," *Phys. Rev. Lett.*, vol. 8, p. 316, 1962.
- [24] T. Udagawa and D. Olsen, "Note on the forbidden (p, t) excitation of unnatural parity final states from $0+$ targets via multistep processes," *Physics Letters B*, vol. 46, p. 285, 1973.

- [25] W. S. Chien, C. H. King, J. A. Nolen, and M. A. M. Shahabuddin, “Unnatural parity transitions in $^{22}\text{Ne}(p, t)^{20}\text{Ne}$,” *Phys. Rev. C*, vol. 12, p. 332, 1975.
- [26] H. Segawa, K. I. Kubo, and A. Arima, “Two-step analysis of the $^{18}\text{O}(p, t)^{16}\text{O} 2^-$ excitation and phase relations in the nonorthogonal term,” *Phys. Rev. Lett.*, vol. 35, p. 357, Aug 1975.
- [27] M. Schneider, J. Burch, and P. Kunz, “Competition of two-step processes in the reactions $^{60,62}\text{Ni}(p, t)$ leading to unnatural parity states,” *Physics Letters B*, vol. 63, p. 129, 1976.
- [28] N. B. de Takacsy, “Two-step mechanism in the reaction $^{208}\text{Pb}(p, t)$,” *Phys. Rev. Lett.*, vol. 31, p. 1007, 1973.
- [29] N. D. Takacsy, “On the contribution from a two-step mechanism, involving the sequential transfer of two neutrons, to the calculation of (p, t) reaction cross sections,” *Nuclear Physics A*, vol. 231, p. 243, 1974.
- [30] N. Hashimoto and M. Kawai, “The (p, d) (d, t) process in strong (p, t) reactions,” *Prog. Theor. Phys.*, vol. 59, p. 1245, 1978.
- [31] K. Kubo and H. Amakawa, “Energy dependence of two-step (p, t) cross sections,” *Phys. Rev. C*, vol. 17, p. 1271, 1978.
- [32] B. F. Bayman and J. Chen, “One-step and two-step contributions to two-nucleon transfer reactions,” *Phys. Rev. C*, vol. 26, p. 1509, 1982.
- [33] K. Yagi, S. Kunori, Y. Aoki, K. Nagano, Y. Toba, and K. I. Kubo, “Anomalous analyzing powers for strong (p_{pol}, t) ground-state transitions and interference between direct and (p, d) (d, t) sequential process,” *Phys. Rev. Lett.*, vol. 43, p. 1087, 1979.
- [34] M. Igarashi, K. ichi Kubo, and K. Yagi, “Two-nucleon transfer reaction mechanisms,” *Physics Reports*, vol. 199, no. 1, 1991.
- [35] M. B. Becha, C. O. Blyth, C. N. Pinder, N. M. Clarke, R. P. Ward, P. R. Hayes, K. I. Pearce, D. L. Watson, A. Ghazarian, M. D. Cohler, I. J. Thompson, and M. A. Nagarajan, “The $^{40}\text{Ca}(t, p)^{42}\text{Ca}$ reaction at triton energies near 10 MeV per nucleon,” *Phys. Rev. C*, vol. 56, p. 1960, Oct 1997.
- [36] Within this context it is of notice that the incoming proton (distorted) wave, in e.g. a $^{A+2}\text{Sn}(p, t)$ reaction, is diffused by the scattering center, i.e. by the ^{A+2}Sn target, into emergent distorted waves, in particular the one corresponding to the relative motion of a deuteron and of the ^{A+1}Sn system after the interaction v_{np} has acted for the first time. Even when these two systems are at relative distances $r = |\vec{r}_{A+1\text{Sn}} - \vec{r}_d|$ much larger than the target radius, the Cooper pair wavefunction describing the pair correlation of the picked up neutron and of its partner in the ^{A+1}Sn system, has a finite probability

amplitude centered on the outgoing deuteron, and this is so not only in the case of superfluid nuclei (like e.g. ^{120}Sn) but also of normal nuclei (like e.g. ^{132}Sn). This is in keeping with the fact that the stability, collectivity and associated correlation length associated with superfluid Cooper pairs and with pair addition and removal Cooper pairs are very similar, as discussed above. Making use of this finite amplitude, the interaction v_{np} acting a second time (see (35b) below) can trigger the ^{A+1}Sn Cooper pair partner to move into the deuteron leading to the triton, and completing in this way the successive transfer process. From this narrative, it is not surprising that the paper in which the probabilistic interpretation of Schrödinger wavefunction was forcefully proposed, written by Born, describes a collisional process [?].

- [37] Y. C. Tang and R. C. Herndon, “Form factors of ^3H and ^4He with repulsive–core potentials,” *Phys. Lett.*, vol. 18, p. 42, 1965.
- [38] Within this context one can mention the fact that, was it not for H_{sp} , all pairspins would line up in the (x, y) -plane transverse to the gauge axis z (see Appendix A), the pairspin alignment picture essentially becoming “exact” under such condition.
- [39] P. Guazzoni, M. Jaskola, L. Zetta, A. Covello, A. Gargano, Y. Eisermann, G. Graw, R. Hertenberger, A. Metz, F. Nuoffer, and G. Staudt, “Level structure of ^{120}Sn : High resolution (p, t) reaction and shell model description,” *Phys. Rev. C*, vol. 60, p. 054603, 1999.
- [40] P. Guazzoni, L. Zetta, A. Covello, A. Gargano, G. Graw, R. Hertenberger, H.-F. Wirth, and M. Jaskola, “High-resolution study of the $^{116}\text{Sn}(p, t)$ reaction and shell model structure of ^{114}Sn ,” *Phys. Rev. C*, vol. 69, no. 2, p. 024619, 2004.
- [41] P. Guazzoni, L. Zetta, A. Covello, A. Gargano, B. F. Bayman, G. Graw, R. Hertenberger, H.-F. Wirth, and M. Jaskola, “Spectroscopy of ^{110}Sn via the high-resolution $^{112}\text{Sn}(p, t)$ ^{110}Sn reaction,” *Phys. Rev. C*, vol. 74, p. 054605, 2006.
- [42] P. Guazzoni, L. Zetta, A. Covello, A. Gargano, B. F. Bayman, T. Faestermann, G. Graw, R. Hertenberger, H.-F. Wirth, and M. Jaskola, “ ^{118}Sn levels studied by the $^{120}\text{Sn}(p, t)$ reaction: High-resolution measurements, shell model, and distorted-wave born approximation calculations,” *Phys. Rev. C*, vol. 78, p. 064608, 2008.
- [43] P. Guazzoni, L. Zetta, A. Covello, A. Gargano, B. F. Bayman, T. Faestermann, G. Graw, R. Hertenberger, H.-F. Wirth, and M. Jaskola, “High-resolution measurement of the $^{118,124}\text{Sn}(p, t)$ $^{116,122}\text{Sn}$ reactions: Shell-model and microscopic distorted-wave Born approximation calculations,” *Phys. Rev. C*, vol. 83, no. 4, p. 044614, 2011.

- [44] P. Guazzoni, L. Zetta, A. Covello, A. Gargano, B. F. Bayman, G. Graw, R. Hertenberger, H.-F. Wirth, T. Faestermann, and M. Jaskóla, “High resolution spectroscopy of ^{112}Sn through the $^{114}\text{Sn}(p,t)^{112}\text{Sn}$ reaction,” *Phys. Rev. C*, vol. 85, p. 054609, 2012.
- [45] G. Bassani, N. M. Hintz, C. D. Kavaloski, J. R. Maxwell, and G. M. Reynolds, “ (p, t) ground-state $L = 0$ transitions in the even isotopes of Sn and Cd at 40 MeV, $N = 62$ to 74,” *Phys. Rev.*, vol. 139, p. B830, 1965.
- [46] G. Potel, F. Barranco, F. Marini, A. Idini, E. Vigezzi, and R. A. Broglia, “Calculation of the transition from pairing vibrational to pairing rotational regimes between magic nuclei ^{100}Sn and ^{132}Sn via two-nucleon transfer reactions,” *Phys. Rev. Lett.*, vol. 107, p. 092501, 2011.
- [47] G. Potel, F. Barranco, F. Marini, A. Idini, E. Vigezzi, and R. A. Broglia, “Erratum: Calculation of the transition from pairing vibrational to pairing rotational regimes between magic nuclei ^{100}Sn and ^{132}Sn via two-nucleon transfer reactions [phys. rev. lett. 107, 092501 (2011)],” *Phys. Rev. Lett.*, vol. 108, p. 069904, 2012.
- [48] H. An and C. Cai, “Global deuteron optical model potential for the energy range up to 183 MeV,” *Phys. Rev. C*, vol. 73, p. 054605, 2006.
- [49] S. Yoshida, “Note on the two-nucleon stripping reaction,” *Nucl. Phys.*, vol. 33, p. 685, 1962.
- [50] C. N. Yang, “Concept of off-diagonal long-range order and the quantum phases of liquid He and of superconductors,” *Rev. Mod. Phys.*, vol. 34, p. 694, 1962.
- [51] S. Galès, “Study of BCS occupation numbers and spectroscopic factors from one nucleon transfer reactions,” in *Fifty Years of Nuclear BCS* (R. A. Broglia and V. Zelevinsky, eds.), World Scientific Publishing Company, 2012. to be published.
- [52] A. Idini, F. Barranco, and E. Vigezzi, “Quasiparticle renormalization and pairing correlations in spherical superfluid nuclei,” *Phys. Rev. C*, vol. 85, p. 014331, 2012.
- [53] E. R. Flynn, G. J. Igo, and R. A. Broglia, “Three-phonon monopole and quadrupole pairing vibrational states in ^{206}Pb ,” *Phys. Lett. B*, vol. 41, p. 397, 1972.
- [54] P. Bortignon, R. Broglia, and D. Bes, “On the convergence of the nuclear field theory perturbation expansion for strongly anharmonic systems,” *Phys. Lett. B*, vol. 76, p. 153, 1978.
- [55] F. Döna, K. Hehl, C. Riedel, R. Broglia, and P. Federman, “Two-nucleon transfer reaction on oxygen and the nuclear coexistence model,” *Nuclear Physics A*, vol. 101, no. 3, pp. 495 – 512, 1967.
- [56] H. Barz, K. Hehl, C. Riedel, and R. Broglia, “The structure of ^{42}Ca and ^{42}Sc investigated by two-nucleon transfer reactions,” *Nuclear Physics A*, vol. 126, p. 577, 1969.

- [57] K. Wimmer, T. Kröll, R. Krücken, V. Bildstein, R. Gernhäuser, B. Bastin, N. Bree, J. Diriken, P. Van Duppen, M. Huyse, N. Patronis, P. Vermaelen, D. Voulot, J. Van de Walle, F. Wenander, L. M. Fraile, R. Chapman, B. Hadinia, R. Orlandi, J. F. Smith, R. Lutter, P. G. Thirolf, M. Labiche, A. Blazhev, M. Kalkühler, P. Reiter, M. Seidlitz, N. Warr, A. O. Macchiavelli, H. B. Jeppesen, E. Fiori, G. Georgiev, G. Schrieder, S. Das Gupta, G. Lo Bianco, S. Nardelli, J. Butterworth, J. Johansen, and K. Riisager, “Discovery of the shape coexisting 0^+ state in ^{32}Mg by a two neutron transfer reaction,” *Phys. Rev. Lett.*, vol. 105, p. 252501, Dec 2010.
- [58] R. A. Broglia, C. Riedel, and T. Udagawa, “Nuclear spectroscopy on deformed nuclei with two-neutron transfer reactions,” *Nucl. Phys. A*, vol. 135, p. 561, 1969.
- [59] D. R. Bès, R. A. Broglia, G. G. Dussel, R. J. Liotta, and H. M. Sofía, “The nuclear field treatment of some exactly soluble models,” *Nucl. Phys. A*, vol. 260, p. 1, 1976.
- [60] D. R. Bès, R. A. Broglia, G. G. Dussel, R. J. Liotta, and H. M. Sofía, “Application of the nuclear field theory to monopole interactions which include all the vertices of a general force,” *Nucl. Phys. A*, vol. 260, p. 27, 1976.
- [61] B. R. Mottelson, “Selected topics in the theory of collective phenomena in nuclei,” in *International School of Physics “Enrico Fermi” Course XV, Nuclear Spectroscopy* (G. Racah, ed.), (New York), p. 44, Academic Press, 1962.
- [62] It is of notice that similar arguments are at the basis of the discussion of Bohr with Schrödinger and De Broglie (matter waves), let alone with Einstein (instantaneous).
- [63] To avoid arguments such that the wavelength of the external hadronic field (beam) allows it to act on both poles, one can work in terms of a Gedanken experiment, in which the proton bombarding energy is about 1.6 GeV ($\lambda \approx 1 \text{ fm} \ll R$).
- [64] G. Potel, F. Barranco, E. Viguzzi, and R. A. Broglia, “Evidence for phonon mediated pairing interaction in the halo of the nucleus ^{11}Li ,” *Phys. Rev. Lett.*, vol. 105, p. 172502, 2010.
- [65] G. Potel and R. A. Broglia, “Pairing correlations with single Cooper pair transfer to individual quantal states,” in *Fifty Years of Nuclear BCS* (R. A. Broglia and V. Zelevinsky, eds.), World Scientific Publishing Company, 2012. in print, arXiv:1206.1640v1.
- [66] R. A. Broglia, “More is different: 50 years of nuclear BCS,” in *Fifty Years of Nuclear BCS* (R. A. Broglia and V. Zelevinsky, eds.), World Scientific Publishing Company, 2012. in print, arXiv:1206.1523v1.
- [67] G. Potel, A. Idini, F. Barranco, E. Viguzzi, and R. Broglia, “Single Cooper pair transfer in stable and

- in exotic nuclei,” *ArXiv e-prints*, June 2011. [nucl-th] 0906.4298.
- [68] W. Dickhoff and D. Van Neck, *Many-Body Theory Exposed!: Propagator Description of Quantum Mechanics in Many-Body Systems*. World Scientific, 2005.
- [69] B. Jennings, “Non-observability of spectroscopic factors,” *arXiv:1102.3721v1*.
- [70] G. Igo, “Optical-model analysis of excitation function data and theoretical reaction cross sections for alpha particles,” *Phys. Rev.*, vol. 115, p. 1665, 1959.
- [71] R. Kronig, “On the theory of dispersion of X-rays,” *J. Opt. Soc. Am.*, vol. 12, pp. 547–557, 1926.
- [72] H. Kramers, “La diffusion de la lumière par les atomes,” *Atti Cong. Intern. Fisica (Transactions of Volta Centennial Congress) Com.*, vol. 2, pp. 545–559, 1927.
- [73] H. Nyquist, “Thermal agitation of electric charge in conductors,” *Phys. rev.*, vol. 32, pp. 110–113, 1928.
- [74] H. Callen and T. Welton, “Irreversibility and generalized noise,” *Phys. Rev.*, vol. 83, p. 34, 1951.